Aus dem Fachbereich Medizin
der Johann Wolfgang-Goethe-Universität
Frankfurt am Main

betreut am
Zentrum für Radiologie
Klinik für Strahlentherapie & Onkologie
Direktor: Prof. Dr. Claus Rödel

Dissecting the immune contexture to monitor and predict chemoradiotherapy response in patients with rectal cancer

Dissertation
zur Erlangung des Doktorgrades der Medizin
des Fachbereichs Medizin
der Johann Wolfgang-Goethe-Universität
Frankfurt am Main

vorgelegt von

Sabrina Joanna Susanne Lautner

aus Schweinfurt

Frankfurt am Main, 2021

Dekan	Prof. Dr. Stefan Zeuzem
Referent	Prof. Dr. Dr. Emmanouil Fokas
Korreferent/in	Prof. Dr. Klaus Strebhardt
Tag der mündlichen Prüfung:	24.02.2022

Content

1 Tables

1.1 Table of charts

Appendix 1 – Reagents used

Appendix 2 – Antibodies

Appendix 3 – Isotype controls

1.2 Table of figures

1.3 Table of Abbreviations

5FU	5-Fluorouracil
ASCC	anal squamous cell carcinoma
CRT	chemoradiotherapy
CT	computer tomography
CTL	cytotoxic lymphocytes
DAMP	damage-associated molecular pattern
DFS	disease free survival
DKTK	Deutsches Konsortium für translationale Krebsforschung
DMSO	dimethyl sulfoxide
FACS	fluorescence activated cell sorting
FCI	Frankfurt Cancer Institute
FMO	full stained minus one
FSC	forward scattered light
fx	fractions
GranzB	GranzymeB
Gy	Gray
HLA	human leukocyte antigen
IHC	immunohistochemical detection
MDSCs	myeloid-derived suppressor cells
MHC	major histocompatibility complex
MRI	magnetic resonance imaging
nCRT	neoadjuvant chemoradiotherapy
nCRT/CT	neoadjuvant chemoradiotherapy/chemotherapy
NK cell	natural killer cell

NKT cells	natural killer T cells
OS	overall survival
PBMCs	peripheral blood mononuclear cells
PBS	phosphate-buffered saline
pCR	pathological complete response
PD1	programmed death 1
PDL1	programmed death receptor ligand 1
PFS	progression-free survival
RB	retinoblastoma
SSC	side scattered light
TILs	tumor infiltrating lymphocytes
TAMs	tumor-associated macrophages
TANs	tumor-associated neutrophils
TME	total mesorectal excision
TP53	tumor protein 53
Tregs	regulatory T cells
TRG	tumor regression grading
UICC	union internationale contre le cancer

2 Introduction

2.1 Rectal cancer: epidemiology, classification and treatment

Considering the epidemiology of cancer subtypes, with an incidence of 10,2 %, colorectal cancer is the third most common cancer entity worldwide. It also covers the second highest mortality rate in cancers. When looking at the total numbers, rectal cancer contributes to one third of the colorectal cancer cases and hence belongs to the ten most common cancer entities resulting in 3,2 % of the cancer related deaths worldwide.[1]

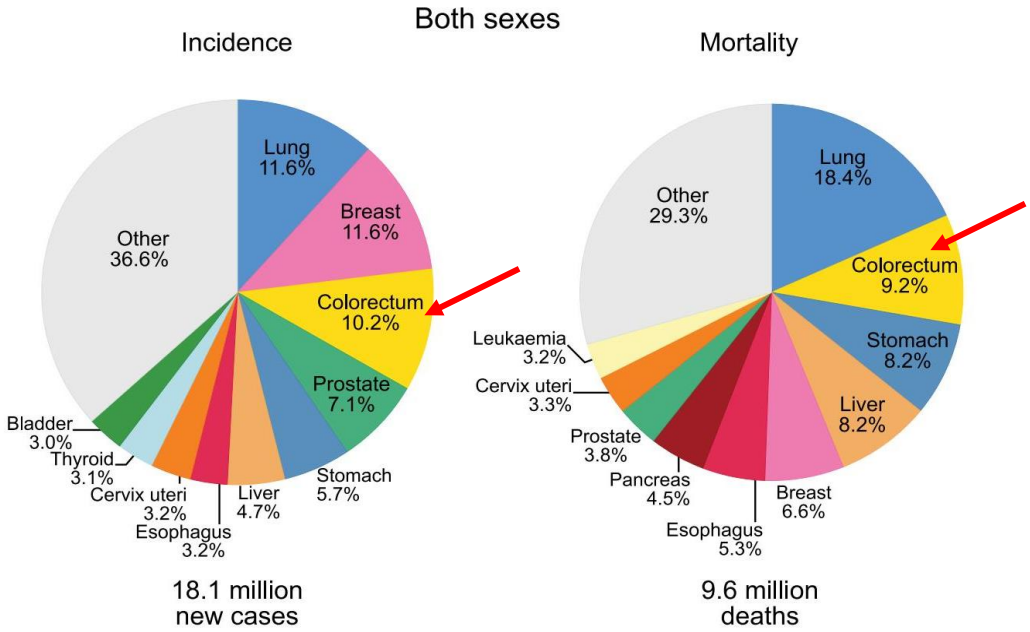

Figure 1 – Worldwide distribution of cancer cases and deaths in both sexes in the year 2018. Figure adapted from Global cancer statistics 2018.[1]

There are several risk factors reported for the development of colorectal cancer, including a genetic disposition, age, incidence of polyps, adiposis and an increased consumption of red or processed meat or alcohol.[2,3] Notably, these life style risk factors do only apply to colon cancer but not to rectal carcinoma.[2] Rectum tumors basically cover adenocarcinomas arising from adenomas (adenoma-carcinoma sequence). The risk of malignancy is highest with villous adenoma (broad-based polyps with mucus formation) with a size >1cm.[3]

The symptoms for rectal cancer are non-characteristic, with the most common to be blood in the stool and a change of bowl movements. For diagnostic

purposes in rectal cancer, an endoscopy (colonoscopy) with biopsies for histological confirmation is necessary. Also, rectal endosonography, a pelvic magnetic resonance imaging (MRI) and computer tomography (CT) of the thorax are required for tumor staging and for search of local and distant metastasis.[3]

Based on tumor size, cancer spread into lymph nodes or metastases to distant organs, the TNM classification of malignant tumors is a globally recognized standard for classifying rectal cancer as given successive (Table 1).[4]

T – primary tumor	
T1	Tumor infiltrates submucosa
T2	Tumor infiltrates Muscularis propria
T3	Tumor infiltrates subserosa, non-peritoneal perirectal fat tissue
T4	Tumor T4a perforates the visceral peritoneum T4b directly infiltrates other organs
N – locoregional lymph nodes (examination of at least 12 lymph nodes)	
N0	no infiltrated lymph nodes
N1	Infiltration of 1-3 lymph nodes N1a 1 lymph node N1b 2-3 lymph nodes N1c tumor deposits in fat tissue of subserosa or perirectal tissue without locoregional lymph node infiltration
N2	Infiltration of 4 or more lymph nodes N2a 4-6 lymph nodes N2b 7 or more lymph nodes
M – distant metastasis	
M0	no distant metastasis
M1	distant metastasis M1a in one organ M1b in more than one organ or peritoneal metastasis

Table 1 - TNM classification of rectal cancer according to Wittekind, Meyer 2012[4]

Further, tumors are characterized by a combination of the TNM criteria shown above resulting in Union Internationale Contre le Cancer (UICC) clinical staging categories (Table 2).[5]

UICC 0	pTis pN0 M0
UICC I	pT1-2 pN0 M0
UICC II	pT3-4 pN0 M0
UICC III	pT1-4 N1-2 M0
UICC IV	pT1-4 pN0-2 M1

Table 2 - UICC stages for rectal cancer (according to European Society for Medical Oncology)

The treatment regimen for rectal cancer was considerably improved over the past decades. By this, the German Rectal Cancer Study Group, covering working groups from surgical oncology (CAO), radiation oncology (ARO) and medical oncology (AIO), has made significant progress in the treatment of rectal cancer with multicenter clinical studies. For instance, a long term evaluation (10 years) of a phase III multicenter, randomized CAO/ARO/AIO-94 trial revealed, that introducing preoperative chemoradiotherapy (CRT) significantly improved the local tumor control, although it did not impact overall survival.[6] Moreover, a subsequent CAO/ARO/AIO-04 study aiming to improve patients' survival revealed a significantly improved disease-free survival (DFS) when adding oxaliplatin to the fluorouracil-based CRT.[7]

At present, preoperative CRT followed by total mesorectal excision (TME) is considered standard of care, as it showed reduced local recurrence rates in locally advanced rectal cancer. Neoadjuvant CRT (nCRT) helps reducing toxicity rates, addresses micro metastases and reduces the local tumor burden to increase complete resection rates (R0 situation).[8] Still, further investigation on improved therapeutic options to reduce toxicity and increase clinical therapy outcome is required.

Against this background, a more recent randomized phase II clinical trial (CAO-ARO-AIO-12) compared the best sequence of neoadjuvant treatment admitted with induction chemotherapy using three cycles of fluorouracil, 5-FU (5 - floururacil) and oxaliplatin. Patients were either treated with preoperative CRT followed by consolidation chemotherapy or vice versa. In this trial, patients

who received CRT followed by consolidation chemotherapy, showed increased incidences of pathological complete response (pCR; ypT0 ypN0) up to 25% compared to pCR levels (15%) reported within the CAO/ARO/AIO-04 trial.[8]

To unravel the patient's therapy response at an early stage of treatment, a Tumor Regression Grading (TRG) was established. Those Grades were first suggested by Dworak et al. and describe five levels of tumor regression based on residual viable tumor cells and stromal fibrotic reaction (Table 3) which can be assessed in pathological tumor resection specimen.[9] Further, Fokas et al. recently showed TRG to be a valuable prognostic factor for clinical outcome. It can also be used as a surrogate marker for DFS.[10]

TRG 0	no regression
TRG 1	mild regression (≤25% of the tumor)
TRG 2	moderate regression (26-50% of the tumor)
TRG 3	good regression (>50% of the tumor)
TRG 4	complete regression (no viable tumor cells detectable)

Table 3 - Tumor regression grade as described by Dworak et al.[9]

With the use of preoperative treatment, it has become evident that tumor response after CRT varies considerably in rectal cancer patients ranging from complete tumor regression in histopathological processing of the surgical specimens in up to 25 % of patients to no response at all in 10% of patients.[11] Thus, there is a need to gain better understanding on the molecular determinants of tumor response to foster treatment individualization and help select patients for e.g. a non-operative organ preservation approach.

2.2 Characteristics of cancer cells and their microenvironment

There are various biological factors, that are considered to contribute to the response of an individual tumor to the therapy, some are associated with intrinsic hallmarks of malignant cells, while other markers are associated with the tumor microenvironment and the immune system.[12] To better characterize common attributes of cancer cells and their environment, Hanahan and

Weinberg were among the first to introduce the Hallmarks of Cancer. These characteristics cover sustaining proliferative signaling, evading growth suppressors, resisting cell death, enabling replicative immortality, inducing angiogenesis and activating invasion and metastasis which contribute to the progression, survival and spread of cancer cells.[13] In 2011, these hallmarks have been revised to additionally include genome instability and mutation, tumor promoting inflammation and avoiding immune destruction (Figure 2, as extracted from Niesel 2021[14]).[13,15]

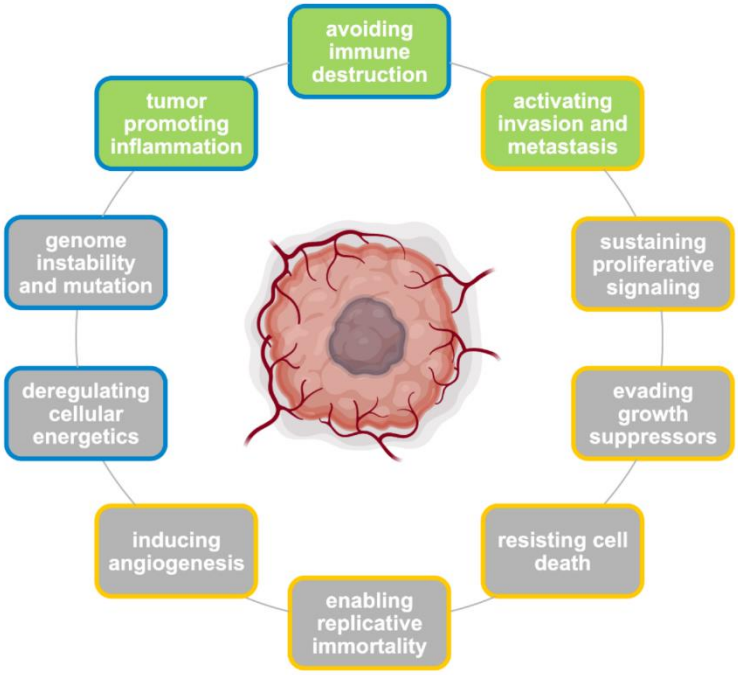

Figure 2 - The hallmarks of cancer as described by Hanahan and Weinberg

This scheme depicts hallmarks (yellow) and emerging hallmarks (blue) of cancer as proposed by Hanahan and Weinberg in 2000 and 2011. Figure derived from Niesel 2021.[14]

Cancer cells are characterized by their ability to proliferate uncontrolled by altering signaling pathways through producing growth ligands and receptors, changing the structure of receptors or constitutive activation of signaling pathways,[16] and through evading growth suppression, primarily via inactivation of tumor suppressor genes such as tumor protein 53 (TP 53) and retinoblastoma (RB) protein.[15] Further, malignant cells can resist cell death by apoptosis, especially in high grade malignancies and therapy resistant tumors.

This is achieved e.g., by the loss of TP53, one of the major modulators of the apoptotic pathway.[17]

In addition, cancer cells enable replicative immortality, e.g. by expressing telomerase, a DNA polymerase which adds repeat segments to the ends of DNA, evading the shortening of DNA[18] and can induce angiogenesis by activation of an angiogenic switch, which leads to the sprouting of new vessels to help sustain the growth of the tumor.[19] Finally, cancer cells have acquired the ability for invasion and metastatic spread, described as a sequence of local invasion, followed by the invasion into blood and lymphatic vessels, the transport with the stream to distant organs and extravasation and formation of micro metastases, leading to macroscopic tumor metastasis over the course of time.[20]

The features described above are enhanced by enabling characteristics: the development of genomic instability and the induction of inflammation. This inflammation – prominent in malignant lesions, - is supported and maintained by the immune system.[15]

2.3 The immune system: an overview

Immune reactions and their cellular players can be divided into two groups, the innate and the adaptive immune system. On a cellular level, key players of the innate immune system cover macrophages, which are basically tissue-based monocytes, as well as granulocytes, mast cells, dendritic cells and natural killer cells. On the other hand, cellular components associated with an adaptive immune response are lymphocytes, most important T cells (with various subtypes), B cells and Natural Killer T cells (NKT cells).[21] When an immune response is triggered by a cascade of signals, the first response is caused by the infiltration of cells belonging to the innate immune system. These cells, especially monocytes and neutrophiles, phagocyte the inflammation causing agents and thereby activate lymphocytes and trigger the adaptive immune response by releasing cytokines.[22]

This concept is transferable to the inflammatory process taking place within the tumor microenvironment. The immune system is activated – by inflammation or by the activation of oncogenes – triggering the release of danger signals, chemokines, cytokines, and prostaglandins. These signals recruit and trigger an immune response, resulting in a cancer related inflammation.[23]

2.4 Interaction between cancer cells and the immune system in the tumor microenvironment

To evade the immune system, cancer cells have to undergo three phases of cancer immunoediting proposed by Dunn et al in 2004. It is described as a dynamic process covering three phases: elimination, equilibrium and escape. Elimination describes the concept of immunosurveillance, equilibrium the phase of latency and escape describes the outgrowth of the tumor.[24] Cancer immunosurveillance is a complex process involving the tumor's cellular origin, transformation mode, stromal response and inherent immunogenicity.[24] In 1986, Dvorak called tumors "wounds that do not heal", referring to the chronic inflammation taking place within the tumor and its surrounding.[25]

Tumor promoting immune cells include mast cells, neutrophils, and macrophages; especially their subtype myeloid-derived suppressor cells (MDSCs). The latter are shown to suppress cytotoxic lymphocytes (CTL) and NK (natural killer) cell activity.[15] Tumor-associated macrophages can produce a variety of cytokines, growth and angiogenic factors and thus may contribute to the stimulation of tumor cell proliferation, invasion and metastatic spread.[26] On the other hand, the concept of the immune surveillance process is shown to eliminate incipient cancer cells. Hence, the immune system acts as an important barrier to tumor formation and progression. Especially cytotoxic T cells (CD8+), T helper cells (CD4+) and NK cells have been recognized to fight upcoming cancer cells in mice models[27] and contribute to tumor elimination and treatment response in patients.[15,28]

T lymphocytes recognize peptides presented in conjunction with major histocompatibility complexes (MHCs) exposed on cancer cells by their T cell receptor. These antigens may cover neoantigens, derived from DNA mutations in the malignant cell, or nonmutated proteins to which T cells have developed

an incomplete tolerance.[29] In order to be recognized as antigens and promote an antitumor reaction, these proteins require presentation by dendritic cells, accompanied by a release of proinflammatory cytokines from the dying cancer cell.[30] These T cells infiltrate the tumor, bind to the cancer cell and kill their target, releasing additional tumor-associated antigens, which maintain and strengthen this process, called the cancer immunity cycle. Common to all cell-cell interaction processes, there are various enhancing and inhibiting factors influencing the cancer immunity cycle (**Fehler! Verweisquelle konnte nicht gefunden werden.**).[12,31] For instance, the killing of the cancer cells is enhanced by the content of T cell granula such as Granzyme B and Perforin, whereas it is inhibited by the expression of checkpoint molecules such as programmed death -1 (PD1) and its ligand PDL1.[31]

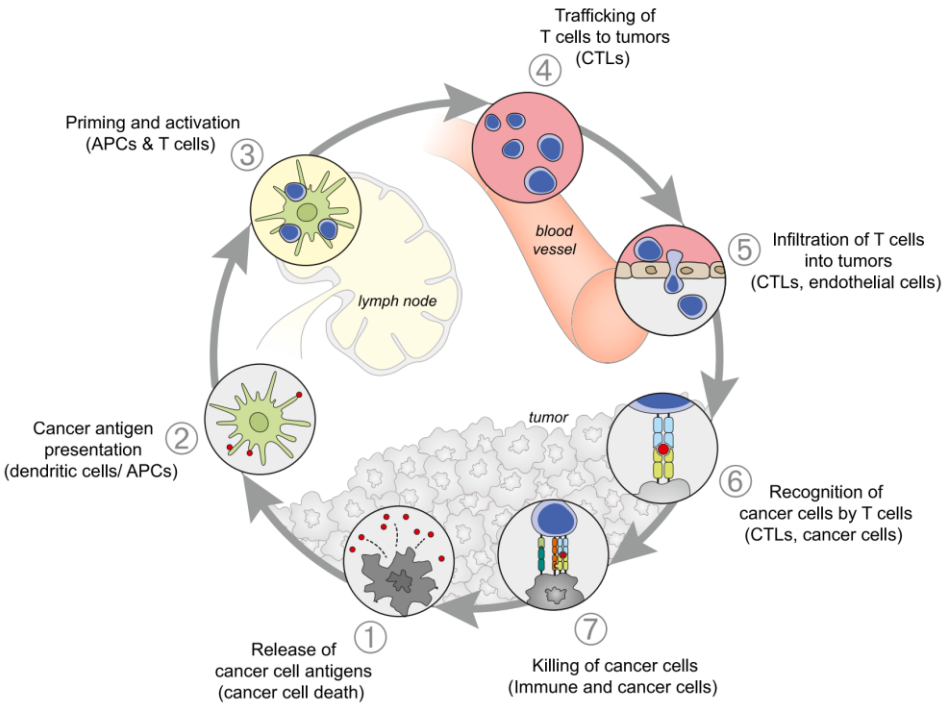

Figure 3 - Cancer immunity cycle: Figure by Chen et.al 2013.[31]

2.5 Prognostic value of tumor infiltrating immune cells

This cancer immunity cycle is dependent on the infiltration of specific immune cells into the tumor and its environment. Various studies have dealt with the prognostic value of these tumor infiltrating immune cells in different cancer entities.

In breast cancer, a low prevalence of CD8+ CTLs and a high number of CD4+ T cells, B cells and macrophages before neoadjuvant chemotherapy was associated with pathological complete response (pCR). Especially CD3, CD4 and B cells and a high CD4/CD8 ratio were an independent prognostic marker for pCR.[32] A prognostic relevance for T cells was further reported in pancreatic cancer, where a high number of infiltrating CD4+ and CD8+ cells is favorable,[33] anal squamous cell carcinoma (ASCC), where a high number of CD8+ cells lead to improved local control,[34,35] and head and neck cancer, where again CD8+ infiltration is auspicious.[36]

In colorectal cancer, a lack of local recurrence has been shown to display higher densities of T cells, CTL (CD8+) and GranzymeB-positive cells as compared to tumors that did recur. Also, these markers, when analyzed in the tumor center and the invasive front, may serve as predictive determinants of DFS and overall survival (OS).[37] Another study by Shinto et al. indicated that the amount of CD8+ T cells in the tumor stroma increased significantly after CRT and that a high post-CRT CD8+ density was associated with a better prognosis.[38]

Notably, an immune score based on the densities of CD45+ and CD8+ infiltrating cells in two different tumor regions, assorting patients in five different groups, was shown to be the best predictor for DFS and OS, even compared to the commonly used TNM characteristics. An inverse correlation between the T stage and the immune cell density was evident as the majority of patients with Tis or T1 T stage revealed a high immune reaction in their tumor site and vice versa.[39]

2.6 Potential prognostic immune markers in peripheral blood

All the findings described above suggest a high impact of the immune system to predict prognosis and treatment response in cancer patients, including adenocarcinoma. Nevertheless, there is only few evidence for a prognostic value of liquid biopsies obtained from patients' blood and the correlation between cancer tissue-located immune cells and blood born cells at present. Huang et al. examined T cells in melanoma patients undergoing anti-PD1-therapy and found a strong correlation between tissue and peripheral blood T

cells. The T cell clones identified in both locations largely display comparable T cell receptor repertoires.[40] In addition, in melanoma patients, there were peripheral blood immune cell markers identified, which differ between the response groups to anti-PD1 immunotherapy. Responders to this regimen showed significantly lower counts of CD4+ and CD8+ T cells but higher counts of HLA-DR+ myeloid cells compared to non-responders. Notably, the frequency and (less relevant) gene expression pattern of circulating CD14 and HLA-DR positive monocytes further predicted responsiveness to anti-PD1 therapy and increased progression-free survival (PFS).[41]

In summary, these data favor the notion on a close connection between immune components in peripheral blood and tumor tissue and a predictive value of liquid biopsies, at least in melanoma patients. Also in other cancer types, peripheral blood immune cell levels differed from healthy controls, such as breast cancer and gastric cancer. In both entities, cancer patients displayed higher levels of circulating Tregs compared to healthy controls.[42,43]

In colorectal cancer, an elevated number of circulating neutrophils and an increased neutrophil-to-lymphocyte ratio has been associated with an impaired long-term survival.[44,45] Further, peripheral blood lymphocytes decreased in the course of CRT, but again increased after CRT. This increase was mainly built on CD8+ T cells and was most pronounced in patients with residual lymph node positivity.[46]

2.7 Aim and purpose of this thesis

In current oncological research, the impact of the immune response is becoming increasingly important in the understanding of the pathogenesis of cancer and in mediating response to anti-cancer therapies. Against this background, the present study aimed to monitor the immune contexture in peripheral blood samples of patients treated within a prospective randomized phase II CAO-ARO-AIO-12 trial on locally advanced rectal cancer and to correlate it with tissue expression and treatment response.

By this, three major questions were addressed.

First, does the peripheral blood and/or primary tumor immune contexture predict for response to nCRT/CT (neoadjuvant chemoradiotherapy/chemotherapy)? Second, does nCRT/CT modulate the peripheral blood and primary tumor immune profile in baseline and preoperative samples?
Third, do the primary tumor and peripheral blood immune profile correlate with each other?

This innovative project was part of the establishment of an immunophenotyping program in Frankfurt am Main under supervision of Prof. Dr. Michael Rieger. Also, this trial took was supported and took place in the context of the DKTK (Deutsches Konsortium für translationale Krebsforschung) and the FCI (Frankfurt Cancer Institute).

3 Methods

3.1 Ethical review

This project covers a translational research project and is part of the randomized phase II clinical trial CAO ARO AIO 12[47]. Ethical review for the entire study was obtained prior to recruiting patients and was approved by the local ethics committee at the University Hospital Frankfurt am Main (Approval number: 406/14).

3.2 Patients

Between February 2017 and July 2018, we recruited 22 prospective patients with histologically confirmed advanced rectal carcinoma (UICC Stadium II and III) treated with a neoadjuvant therapy at the University Hospital Frankfurt am Main. The diagnostic biopsy and the surgery took place at the University Hospital and in the following hospitals: Frankfurt Höchst Hospital, Agaplesion Markus Hospital, Northwest Hospital, Hanau Hospital, Wetzlar Hospital. All patients provided an informed consent.

This study was conducted in the context of the DKTK and FCI in Frankfurt am Main.

3.2.1 Inclusion and exclusion criteria

Inclusion criteria for the multicenter randomized phase II CAO-ARO-AIO-12 clinical trial were as follows:

Tumor localization 0-12 cm from the anocutaneous line, measured with a rigid rectoscope. The tumor had to fulfill the local staging requirements measured in the MRI:

- cT3 tumors with distal extension less than 6 cm from the anocutaneous line
- cT3 tumors localized in the middle third of the rectum (>6 – 12 cm) with evidence of extramural tumor spread into the mesorectal fat
- resectable cT4 tumors
- positive cN+ status in MRI imaging

In case of uncertain MRI staging, transrectal endoscopic ultrasound was used to clarify the tumor situation.

Further, distant metastases were excluded by spiral-CT of the abdomen and thorax. The patients needed to show a WHO/ECOG Performance Status ≤ 1 and unremarkable hematologic, hepatic, renal and metabolic function parameters.

None of the patients received an antineoplastic therapy before or antineoplastic substances during recruitment. Also, the patients have not undergone any major surgery of the pelvic area. Any major concomitant disease, including neurologic, psychiatric and cardiovascular disorders, non-controlled infection or disseminated coagulation disorder needed to be absent, as well as chronic diarrhea and other malignancies less than three years prior to the inclusion in the study.

3.2.2 Schedule of patient's treatment and sample collection

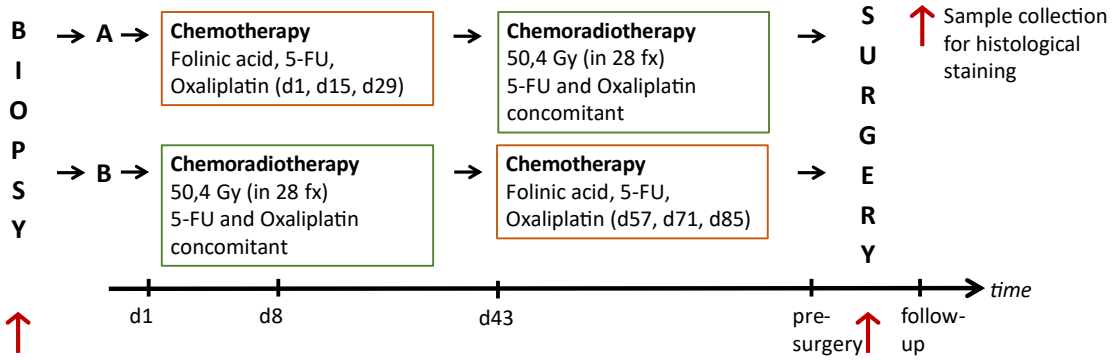

Figure 4 - Therapy regimen overview

Schematic overview showing the two treatment arms (A and B). The days given in the timeline are the timepoints for blood sample collection. Day 43 also marks the change of therapy from CT to CRT arm and vice versa. Tissue samples were collected during diagnostic biopsy and from the surgical specimen.

The patients were randomized in one of the treatment arms as depicted in Figure 4. Treatment arm A starts with three induction chemotherapy cycles, starting on day 1, 15 and 29 with Folinic acid (400mg/m², 2h-civ), Oxaliplatin (100mg/m², 2h-civ) and 5-Floururacil (5-FU, 2400mg/m², 46h-civ), followed by a

break of two weeks and chemoradiotherapy with a radiation dose of 50,4 Gy (Gray) (28 fractions (fx) of 1,8 Gy, five fractions per week), together with 5-FU (250mg/m² per day civ on day 1-14 and day 22-35 of radiotherapy) and Oxaliplatin (50mg/m² at day 1, 8, 22 and 29 of radiotherapy). Arm B differs from the schema as mentioned before by changing the sequence of administration, beginning with the CT block followed by the CRT block.

Surgery was scheduled six weeks after the termination of CT or CRT. Sphincter function and pelvic nerves should be preserved whenever possible, and surgery, by total mesorectal excision as first introduced by R.J. Heald[48] should be performed in an open or laparoscopic manner.

Within the translational study, patients' blood samples were mainly obtained at five time points during the neoadjuvant treatment: before therapy (baseline, d1), on day 8 and 43 of treatment, before surgery and on the first follow-up. At each timepoint, 15 ml of EDTA-blood and 9,5 ml blood for serum analysis was collected.

3.3 Classification of therapy response

The analysis on predicting response to CRT was built on three different, established approaches on classifying response rates in patients.

First, UICC TNM classification was used to distinguish between good, intermediate or partial and poor response to CRT. Good response was considered ypT0 ypN0 (with no residual tumor left in surgical specimens), intermediate or partial response equated to ypT1-4 ypN0 (with reduction of size and lymph node positivity in these patients), and poor response was considered ypT1-4 ypN+ in surgery specimen (considering it as stable or progressive disease despite the course of neoadjuvant CRT).

Second, we focused on lymph node positivity in surgical specimens to address a patient's response to CRT. As all patients showed a lymph node positivity in the primary clinical staging, an ypN0 status in surgery specimen indicated a good response to neoadjuvant CRT and was compared to an ypN+ status in the surgical specimen.

Third, TRG grading was used. It is based on the five-tier classification using TRG 0 – TRG 4 (Table 3).[10] For our analysis, we grouped TRG 0, 1+2 as poor responders and TRG 3+4 as good responders to CRT.

3.4 Processing of patient's EDTA blood

A full list of materials, reagents and kits used is given in Appendix1-3.

Peripheral blood mononuclear cells (PBMCs) from EDTA-blood were collected by a density gradient centrifugation (Biocoll Separating Solution, Biochrom) at 400 x g and 20 min (Mega Star 1.6 centrifuge, VWR, Radnor, USA) after mixing in a 1:1 ratio with phosphate buffered saline (PBS, Gibco). During the centrifugation step, the different cellular blood components were separated by differences in cellular density. The PBMCs are visible as a white ring between the separating solution and the serum. Next, this ring was aspired with a pipette, sparing as much serum and separating solution as possible. By mixing these PBMCs with PBS and centrifugation at 300 x g and 7 min, the cells were cleaned from the leftover separating solution and serum. Next, the cell pellet was resuspended in 1000 µl FACS (Fluorescence activated cell sorting)-buffer (PBS, 10% FCS (Thermo Fischer), 1 mM EDTA) and counted: 50 µl of the cell-mixture was diluted at a 1:10 ratio with PBS, and then 1:1 mixed with Trypan-Blue staining solution (Gibco). This mixture was added to a counting chamber and cells were counted under the microscope (AXIO, Zeiss, Oberkochen) according to the equation, using the mean from four fields to reveal the cell count in the original solution: cell count/ml = mean x 10000 x 2 x 10.

After that, PBMCs were stained for immunophenotyping purposes in three different panels ($1x10^6$ cells in each tube, see 3.5.3), or prepared for further analysis in the future using cryoconservation.

3.4.1 Cryoconservation of PBMCs

Remaining PBMCs that were not used for cytometer measurements, were cryoconserved for further analysis. Accordingly, the number of cells left in suspension were calculated to divide the cells for freezing in equal amounts of cells suspension. PBS was added to a volume of 5 ml to the leftover suspension and cells were pelleted by centrifugation at 300 x g and 7 min. After discarding

the supernatant, the cell pellet was mixed with a medium containing of 40% RPMI (Gibco) + Glutamax (Gibco) + 1 nM Natrium-Pyruvat solution (Gibco), 50% human Serum (Gibco) and 10% dimethyl sulfoxide (DMSO).

Each tube contained 1 ml of cell suspension with a maximum number of $1x10^7$ cells per container. The tubes were then put to the freezer (HERAfreeze, Thermo Scientific, Waltham/UF601, Dometic, Solna) at -80°C for 24 hours and then transferred to the cryo-tank (Arpege110, Air Liquide, Paris) at -170°C and stored until further processing.

3.5 Cytometer measurements

All samples were analyzed by a CytoFlexS Cytometer (Beckman Coulter, Krefeld) equipped with four lasers and 13 detectors. Laser configuration was set with blue (488 nm), red (638 nm), yellow (561 nm) and violet (405 nm).

3.5.1 Background

A flow cytometer measures light signals emitted by particles in suspension marked with an excitable fluorescent tag (Figure 5[49]). Those particles, e.g. antibody coupled PBMCs, are pressurized into a fluid core stream surrounded by sheath fluid. An orthogonally placed laser excites one fluorescent particle at a given time and thus generates photons of a specific wavelength. Those impulses are measured by corresponding detectors.[50] Additionally to the fluorescence signals, the incident laser also generates scattered light signals. Those can be divided in forward scattered light (FSC), proportional to the particle's size, and orthogonal (side) scattered light (SSC), which correlates with intracellular granularity.[50] Data generated from fluorescent as well as scattered light signals are used to characterize a specific subpopulation of cells within the total collection. By using two-dimensional scatter plots, any two of the parameters measured could be plotted to characterize and display different cell populations. By the use of specified thresholds (further referred to as gates), percentages of cell populations can be determined.[50]

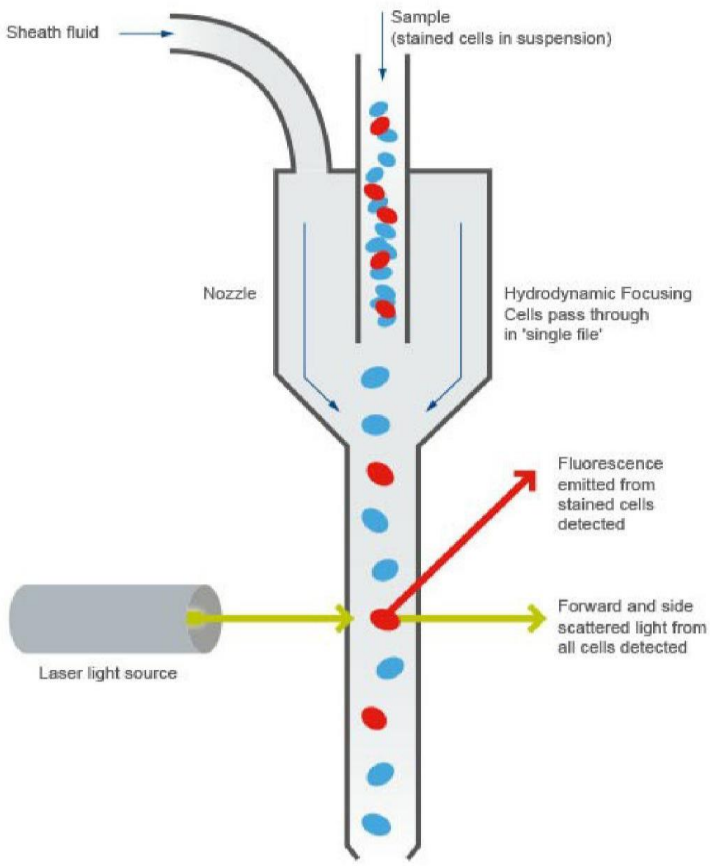

Figure 5 – Principle of flow cytometry [35]

The cells are pressurized in a single cell stream surrounded by sheath fluid. A laser excites the fluorescent tags generating photons of specific wavelenght that can be detected to differentiate the cells.

3.5.2 Quality control and calibration

To ensure validity and reproducibility, a quality control was performed on a daily basis using CytoFlex Daily QC Fluorophores (Beckman Coulter, Krefeld) according to the manufacturer's instruction. Thus, we could verify the performance of the optical alignment and the fluidic system.

Also, when using more than one fluorescent dye at the same time (multiplexing), the dyes generate a spillover in detection channels with similar wavelength. Those spillovers lead to incorrect numbers of detected signals. In order to avoid a miscalculation of cell quantities, a compensation helps removing the spillover from the mis-detecting channel.[51] The appropriate spillover coefficients can be calculated by using compensation controls prepared for each fluorophore, containing a single-stained and an unstained

sample mixed together. The unstained sample helps identifying the autofluorescence whereas the single-stained sample is used to quantify the spillover in other channels. As PBMCs mainly contain only a few percent of the marker-positive cells, antibody capture beads (VersaComp Antibody Capture Bead Kit, Beckman Coulter, Krefeld) were used to generate a sufficient compensation.[51] The compensation matrix was then applied to the measured samples.

Also, in order to separate the cell populations correctly, isotype controls were used. Those isotype controls are antibodies of the same class as the specific antibodies used in the staining procedure but raised against antigens presumably not existing in the examined probes. Thus, undesirable, non-specific binding to fluorochromes or Fc receptors is detected and can be excluded in the analysis.[52]

3.5.3 Immunophenotyping staining procedure

For immunophenotyping purposes, PBMCs were subjected to three staining panels ($1x10^6$ cells in each tube, Table 4), each covering one full stained tube, incubated with antibodies, and one non-stained (unstained) tube without antibody staining, which was processed in a similar manner. In addition, one Viability Dye tube was used for all panels, containing $3x10^6$ cells stained with Viability Dye stain 620 after thermal shock (90°C for 40 sec). Both, the unstained and viability dye tube served as negative controls.

Panel (FACS) from peripheral Blood	**Marker**
Panel 1: myeloid and lymphatic cells	CD45, CD3, CD19, CD14, CD11b, CD15, HLA-DR, CD33
Panel 2: T cells and activation marker	CD45, CD3, CD8, CD4, PD-1, Granzyme B, Perforin
Panel 3: T cells and FoxP3	CD45, CD3, CD8, CD4, FoxP3
Panel 1, Full Blood: myeloid and lymphatic cells	CD45, CD3, CD19, CD14, CD11b, CD15, HLA-DR, CD33, CD56

Table 4 - Panels and markers used

Panel 1 full staining tube was first blocked with Hu FcR Binding Inhibitor and then incubated with surface antibodies specific for the HLA-DR (V450), CD45 (V500), CD33 (APC), CD19 (PeCy7), CD14 (APC-H7), CD15 (FITC), CD11b (PE), CD3 (PerCP-Cy5,5) antigens and with Viability Dye stain 620.

Panel 2 full staining tube was also blocked with Hu FcR Binding Inhibitor and then incubated with antibodies directed against CD4 (V450), CD8 (APC-H7), CD3 (PerCP-Cy5,5), CD25 (BV510) and Programmed Death Receptor-1 (PD1, PeCy7) and with Viability Dye stain 620. Then, the Fix & Perm Kit was used to fixate and permeabilize the cells. By this, 100 µl of Reagent A was added and incubated for 15 min, followed by a washing step with PBS and centrifugation at 300 x g and 7 min. Next, 100 µl of reagent B was added and incubated for 15 min and cells were washed again with PBS and centrifugation at 300 x g and 7 min. Finally, the tube was incubated with antibodies targeting intracellular Granzyme B (PE) and Perforin (FITC).

Panel 3 staining tube was first incubated with antibodies targeting CD4 (V450), CD8 (APC-H7), CD3 (PerCP-Cy5,5), CD25 (BV510) and PD1 (PeCy7) and Viability Dye, then fixed, permeabilized and blocked using the Staining Set for FoxP3 containing concentrates of a solution for fixation and permeabilization, and a corresponding washing buffer. These reagents were used in the same way as the fix & perm kit for panel 2 as described above. Subsequently, cells were incubated with FoxP3 (APC) antibody.

To facilitate the staining procedure for upcoming trials, we further established an additional staining procedure from non-separated peripheral blood samples. As we aimed to use an extra CD56 antibody to quantify natural killer cells, we only applied this technique to the Panel 1 staining. We processed the blood of nine patients (P01-035 – P01-043). We used two times 200 µl of the 1:1 blood and PBS mixture (as described above) for full-stained and an unstained tube. The full stained tube was first incubated with 20 µl of Fc-Blocker (10 min) and then incubated with surface antibodies HLA-DR, CD45, CD33, CD19, CD14, CD15, CD11b, CD3, CD56 as well as Viability Dye stain 620 for 30 min. After incubation, erythrocytes were lysed using BD FACS Lysing Solution. After

centrifugation (300 x g for 7 min), decantation and washing the cells with PBS, the pellet was resuspended in 150µl PBS.

All samples were measured at maximum one hour after staining in FacsTubes (Sarstedt, Nümbrecht).

3.5.4 Gating strategy and validation

For analysis of the data, the CytExpert software (Beckman Coulter, Krefeld) was used. The term “gating” refers to a method of selecting specific cell populations within an experiment using flow cytometry, placing thresholds (gates) around cell populations of interest.[53]

3.5.4.1Establishment of our gating strategy – FMO Panel

To determine the exact range of the negative population, full-stained minus one (FMO) panels were applied. As these panels contain every antibody except one, the negative population can be determined. This clarifies the gating strategy and reduces the error originating in the autofluorescence of the other antibodies.[54] By using the staining protocol as described above, an FMO panel for each antibody used was formed. One full stained, one non-stained and one viability panel were created while one additional panel was employed by omitting the antibody of interest.

By gating the required cell type one time in the full stained panel and one time in the FMO Panel, the thresholds for the population of interest could be determined.

3.5.4.2 Gating strategy

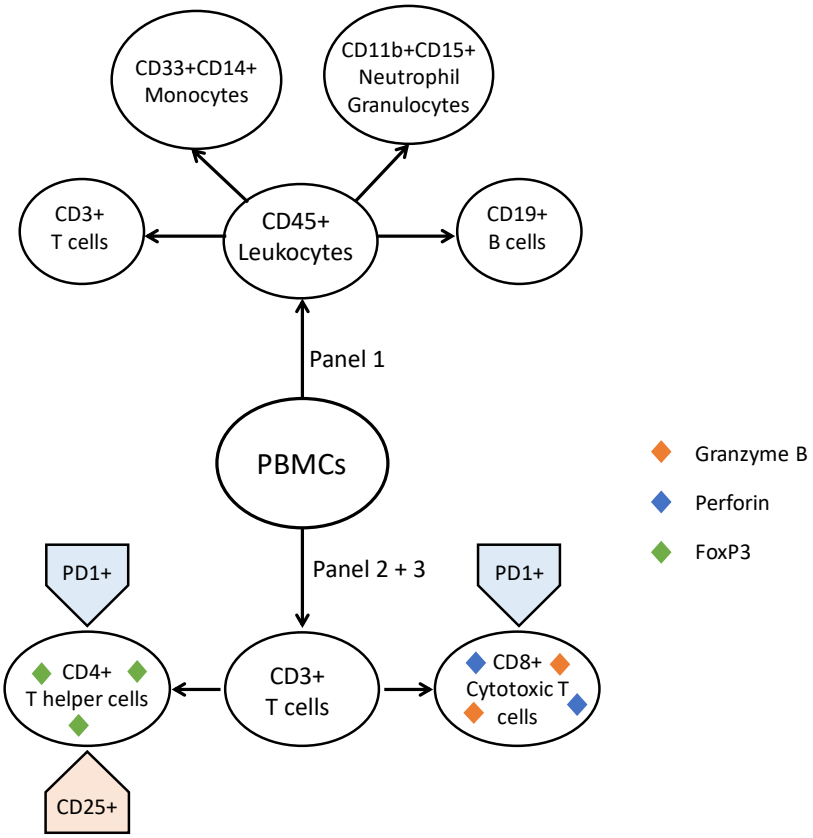

Figure 6 – Gating strategies applied

Panel 1 uses leukocytes (CD45+) as a starting point for further gating. Discriminated are monocytes (CD45+CD33+CD14+), neutrophil granulocytes (CD45+CD33-CD14-CD11b+CD15+), T cells (CD45+CD14-CD33-CD11b-CD15-CD3+) and B cells (CD45+CD33-CD14-CD11b-CD15-CD19+).
Panel 2 and 3 use T cells (CD3+) as a starting point for further gating to discriminate T helper cells (CD3+CD4+CD8-) and cytotoxic T cells (CD3+CD8+CD4-). Additional surface activation markers (PD1 and CD25) as well as intracellular toxicity markers (Granzyme B, Perforin) and FoxP3 as a marker for regulatory T cells (CD3+CD4+CD25+FoxP3) are applied as well.

Evaluation of all three panels as depicted before have a common trunk of gating in the beginning, as they were started with all events, and FSC and SSC signals to determine erythrocytes and debris (Figure 7a). After excluding those cells, the population was further cleared up by isolating all singulets, which means that all cells that generate unequal signals in FSC-A and FSC-H and therefore do not cover a 45° line from the origin of the diagram were excluded (Figure

7b). Then, we discriminated between viable cells and dead cells based on our viability dye assay. The latter interacts with damaged cell membranes and generates a signal in dead cells (Figure 7c).

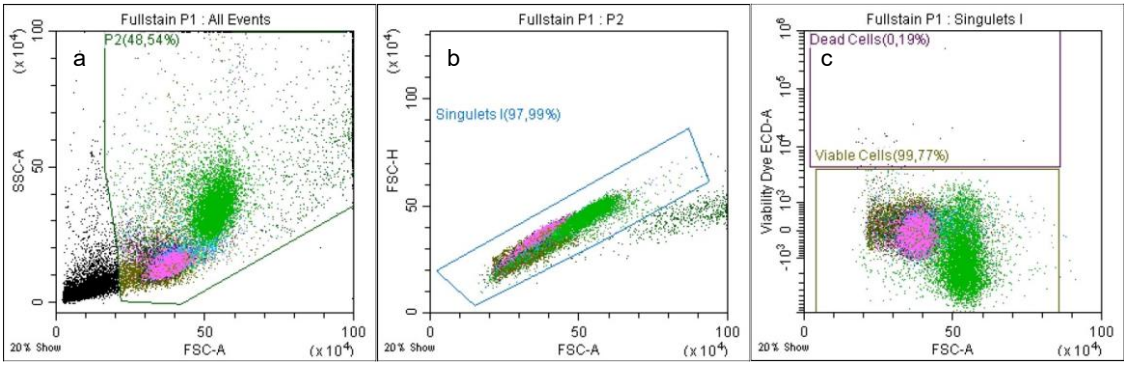

Figure 7 - Exemplary gating strategy: common trunk

a – excluding erythrocytes using SSC-A and FSC-A signal; b – isolating singulets by excluding all cells producing an uneven signal in FSC-H and FSC-A; c – discriminating between viable and dead cells based on the viability dye assay.

3.5.4.2.1 Gating Panel 1

For panel 1 analysis, viable cells were first plotted using SSC and CD45 parameters and the resulting leukocyte population as the starting point for the analysis and as a point of reference for further statistical evaluation (Figure 8).

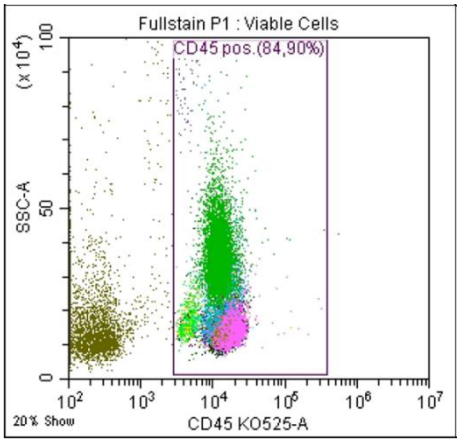

Figure 8 – Exemplary gating strategy: Panel 1, leukocyte gating

Those leukocyte subpopulations were further differentiated. First, the monocytes were identified by their specific markers CD33 and CD14 (Figure 9a). The resulting monocyte population (CD45+CD33+CD14+) was then excluded. The small population of neutrophilic granulocytes

(CD45+CD11b+CD15+CD33-CD14-) was then characterized and excluded (Figure 9b). The resulting cells represent T cells (CD45+CD3+CD14-CD33-CD15-CD11b-) and B cells (CD45+CD19+CD14-CD33-CD15-CD11b-) (Figure 9c). A small population of uncharacterized cells is left, which is most likely comprised of natural killer cells and innate immune cells.

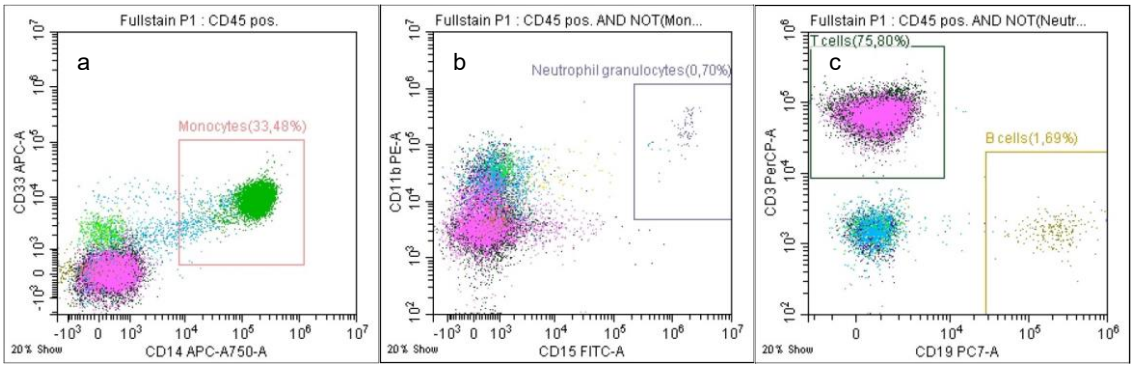

Figure 9 - Exemplary gating strategy: Panel 1

Gating strategy for leukocyte subpopulations: a - monocytes (CD45+CD33+CD14+), b – neutrophil granulocytes (CD45+CD11b+CD15+CD33-CD14-), c – T cells (CD45+CD3+CD14-CD33-CD15-CD11b-) and B cells (CD45+CD19+CD14-CD33-CD15-CD11b-).

3.5.4.2.2 Gating Panel 2

Starting with the viable cells at the end of the common gating for all panels, in Panel 2 CD3 positive lymphocytes were used as reference for further analysis (Figure 10a). This population was further divided into cytotoxic T cells characterized by their CD8 antigen expression (CD3+CD8+CD4-) and T helper cells with a CD4 positive phenotype (CD3+CD4+CD8-) (Figure 10b).

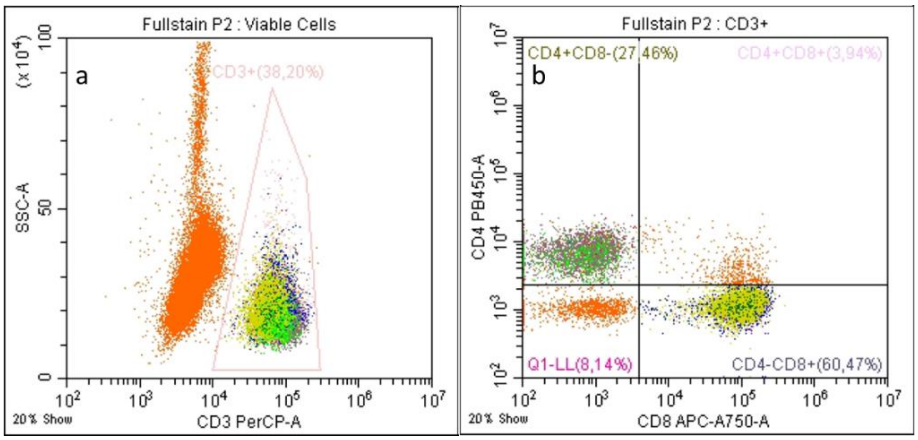

Figure 10 - Exemplary gating strategy: Panel 2 and 3

Beginning of gating in Panel 2. a – CD3+ lymphocytes; b – dividing the lymphocytes in cytotoxic T cells (CD3+CD8+CD4-) and T helper cells (CD3+CD4+CD8-)

Both subpopulations were next analyzed by additional surface and intracellular markers to access activation status of the cells. These markers include Programmed Cell Death Protein 1 (PD1), Perforin and GranzymeB (GranzB) and the interleukin-2 receptor (CD25, Figure 11).

To depict the cytotoxic potential of these lymphocyte subsets, we also plotted T helper cells and cytotoxic T cells carrying Perforin and GranzB simultaneously (Figure 12).

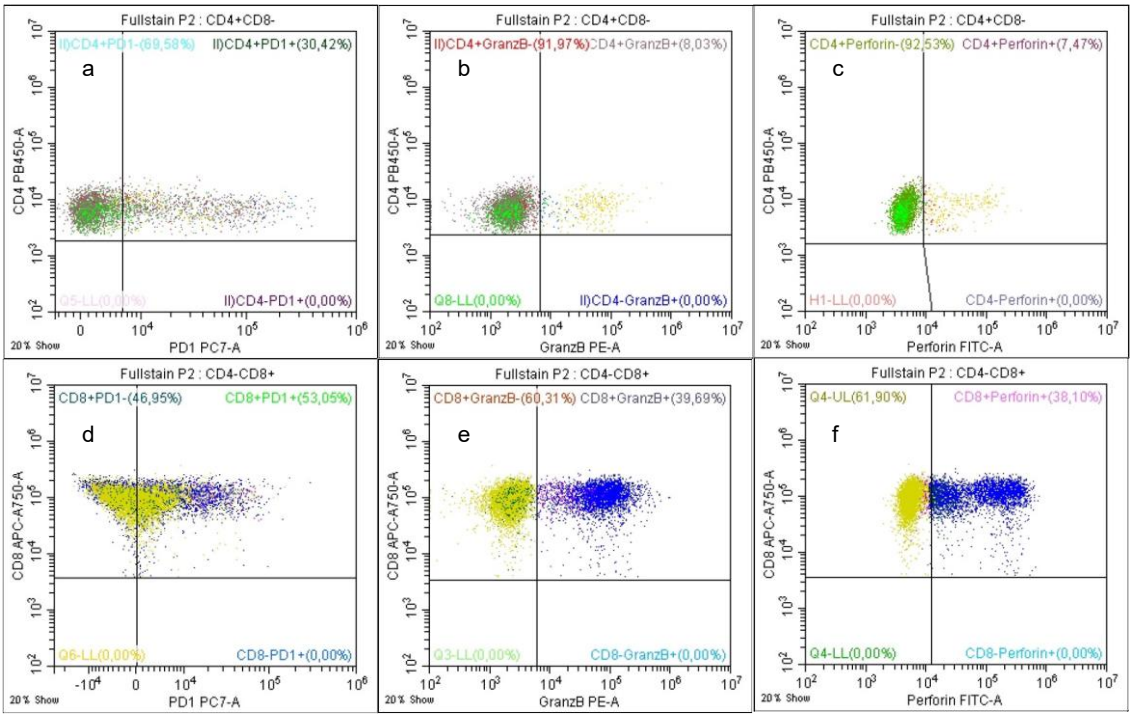

Figure 11 - Exemplary gating strategy: Panel 2

Gating strategy for T cell subsets. a – T helper cells positive for PD1 (CD3+CD4+CD8-PD1+); b – T helper cells carrying intracellular GranzymeB (CD3+CD4+CD8-GranzB+); c – T helper cells carrying intracellular Perforin (CD3+CD4+CD8-Perforin+); d – cytotoxic T cells positive for PD1 (CD3+CD4+CD8-PD1+); e – cytotoxic T cells carrying intracellular GranzymeB (CD3+CD4+CD8-GranzB+); f – cytotoxic T cells carrying intracellular Perforin (CD3+CD4+CD8-Perforin+)

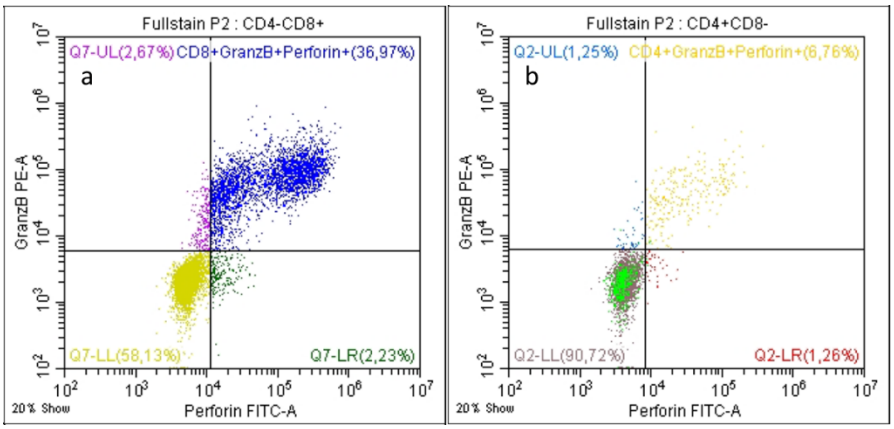

Figure 12 - Exemplary gating strategy: Panel 2

Gating strategy for cytotoxic enzymes in lymphocytes. a – GranzB and Perforin in cytotoxic T cells (CD3+CD8+CD4-GranzB+Perforin+); b – GranzB and Perforin in T helper cells (CD3+CD4+CD8-GranzB+Perforin+)

3.5.4.2.3 Gating Panel 3

In line with the gating strategy of Panel 2, CD3 positive lymphocytes were used as the starting point for further evaluation, followed by plotting the subpopulations T helper cells and cytotoxic T cells (Figure 10).

This panel was further used to portray regulatory T cells (Tregs) hence this panel includes the transcription factor FoxP3. Accordingly, numbers of CD3+CD4+CD25+ positive T helper cells were depicted as well as CD3+CD4+FoxP3+ positive cells (Figure 13a, b). To plot the regulatory T cells, we gated CD25 and FoxP3 in one gate and the resulting double positive cells are considered as regulatory T cells (CD3+CD4+CD25+FoxP3+, Figure 13c). Also, we gated FoxP3 as a marker in CD8 positive cytotoxic T cells (Figure 13d).

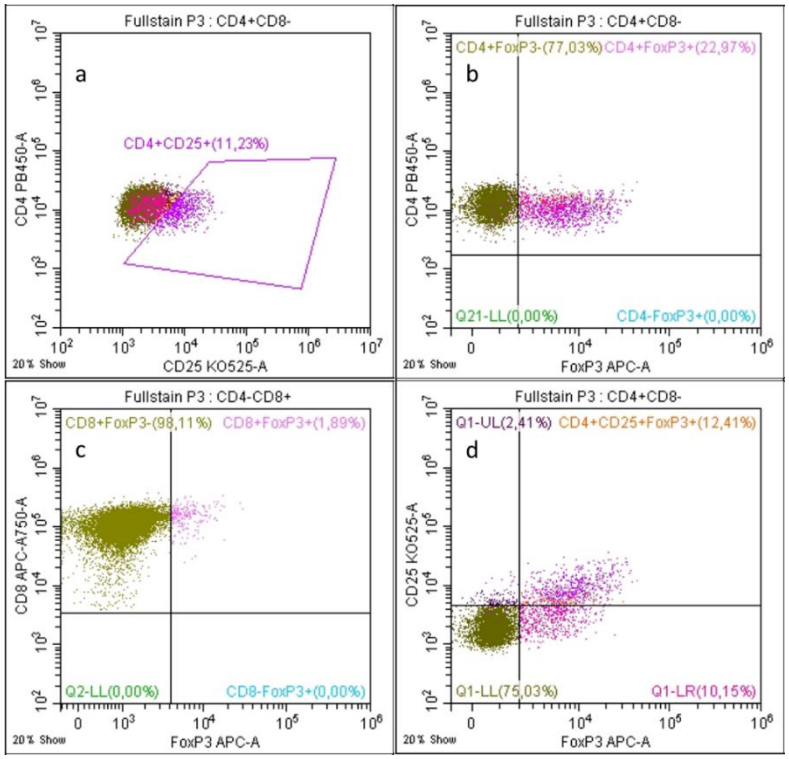

Figure 13 - Exemplary gating strategy: Panel 3

Gating strategy for regulatory T cells. a – CD25 positive T helper cells (CD3+CD4+CD8-CD25+); b – FoxP3 positive T helper cells (CD3+CD4+CD8-FoxP3+); c – regulatory T cells (CD3+CD4+CD8-CD25+FoxP3+); d – FoxP3 positive cytotoxic T cells (CD3+CD8+CD4-FoxP3+).

3.6 Histochemical Staining and Analysis

We also obtained paraffin embedded tumor tissue samples, both from biopsy and surgical resection specimen of all patients included in the study.

3.6.1 Immunohistochemical detection of CD15, CD68 and GranzymeB

The immunohistochemical detection (IHC) of CD15 antigen for neutrophilic granulocytes and CD68 for macrophages and intracellular GranzymeB was performed using an Avidin-Biotin-Alkaline-Phosphatase technique at the Senkenberg Institute of Pathology at the University Hospital Frankfurt am Main. Therefore, the formalin fixed tumor samples were embedded in Paraffin, cut with a rotary microtome (slice thickness 2 µm), applied to an adhesive microscope slide, incubated in Xylol and rehydrated using an alcoholic dilution series. Prior to staining, Trilogy™ (Cell Marque, Rocklin) concentrate was used (according to manufacturer's instruction), which combined removal of paraffin, rehydration and antigen-unmasking necessary prior to staining. Afterwards, the probes were washed in PBS and stained using the AutostainerLink48 (Dako, Santa Clara). Afterwards, to stain the nuclei, the slides were incubated in hematoxylin.

The analysis was performed in our laboratory by two independent persons without knowledge of the clinical characteristics of these patients. The positive cells were scored according to three different locations: in the tumor as well as in the peritumoral and the stromal area. For each location, a score was established: 1 (no or sporadic cells), 2 (moderate number of cells), 3 (abundant occurrence of cells) and 4 (highly abundant occurrence of cells). The numbers for all three locations were added resulting a score with a minimum of 3 points and a maximum of 12 points.

3.6.2 Detection of HLA-DR and HLA-ABC

Histochemical detection of HLA-DR (Human leukocyte antigen) and HLA-ABC was performed in cooperation with the Institute for Neuropathology at the University Hospital Frankfurt am Main (PD Dr. Patrick N. Harter) using a fully automatic immunohistochemistry assay on a Bond-III-tissue stainer (Leica

Biosystems, Wetzlar). Therefore, the tissue samples were heated either in citrate buffer for HLA-I antigens or EDTA buffer for HLA-II antigens.

Analysis was conducted in our laboratory, using a IHC H-score. In this score, staining intensities were determined by 1 (weak), 2 (moderate) and 3 (strong) and the percentage of stained cells within these intensity-areas were estimated over the entire tissue sample. These scores were integrated to a final score from 0-300.[55]

3.6.3 Immunofluorescence staining

To analyze multiple parameters in parallel, staining of the markers CD3, CD8, CD4, CD163 (for monocyte lineage) and PD-1 were performed by the Institute of Biochemistry at the University Hospital Frankfurt am Main by applying immunofluorescence assays (OpalTM 7-Color Manual IHC Kit, PerkinElmer Inc., Waltham, USA). Therefore, the manufacturer's instructions were followed. After preparation of the samples as described above, fluorophore-carrying secondary antibodies were applied to the probes. These could be detected individually or be used to enhance an already detectable signal.

Analysis was done using the Vectra3 automatic quantitative pathology imaging system (Perkin Elmer Inc.) at a 4 x and 20 x magnification and InForm v2.1 software (Perkin Elmer) was used to quantify percentages of positive stained cells.

3.7 Statistical analysis

For statistical analysis, we exported the absolute cell counts from the FACS measurement into Graph Pad Prism 7 (GraphPad Software, San Diego, USA). Those absolute numbers were set in relation with the point of reference for each panel to create percentages. For further statistical testing, including Chi-Square tests and correlation testing, both, Graph Pad Prism 7 and IBM SPSS Statistics software version 25 (IBM Deutschland GmbH, Ehningen) were used. Diagrams were created in Graph Pad Prism and Microsoft Excel (Microsoft Corporation, Redmond, USA). T Tests were used for independent values that followed the Student's t-distribution. This means, that it was used for comparing the mean of specific cell count values from different response groups to CRT and also to

compare specific values of one response group between histological staining and peripheral blood testing. Pearson’s Chi Squared test were applied to determine, weather one and another parameter showed a significant correlation. This was used to compute, whether there was a significant correlation between a marker and the response to nCRT/CT, as well as to prove a possible correlation between tumor tissue samples and peripheral blood testing.

4 Results

4.1 Patients' characteristics and response to nCRT/CT

In total, 22 patients were included in the translational research to the phase II clinical trial CAO-ARO-AIO-12. The median age was 67 years, ranging from 39 to 82 years. In this cohort, 14 patients were male and 8 female; 12 patients were treated in therapy regimen A and 10 in therapy regimen B.

The assessment of clinical and histopathological response to nCRT/CT was built on three different approaches covering downsizing (ypTNM-classificaion), rate of tumor regression (TRG) and development of lymph-node metastases (ypN0 vs. ypN+). Due to different histopathological responses, patients were divided into groups with a good/complete (ypT0ypN0), intermediate (ypT1-4ypN0) and poor response (ypT1-4ypN+) (Table 5). One patient did not undergo surgery but due to a clinical ypT0N0 status was classified in the group of patients with complete response. Instead, a watchful waiting strategy was implied. As depicted in Table 5, five patients presented a complete response (ypT0ypN0), while 13 patients indicated an intermediate response (ypT1 - 4ypN0) and four patients displayed an impaired response to nCRT/CT (ypT1-4ypN+). Considering the patients TRG, 8 patients displayed poor tumor regression (TRG 1+2), whereas 14 patients showed partial or complete tumor regression (TRG 3+4).

Patient	Gender	Therapy arm	cTNM	ypTNM	TRG
P01-023	M	A	cT4cN2cM0	ypT0ypN0	4
P01-029	M	B	cT3cN2cM0	ypT0ypN0	4
P01-031	M	A	cT3cN+cM0	T0N0 „watchful waiting“	(4)
P01-036	F	A	cT3cN+cM0	ypT0ypN0	4
P01-040	M	B	cT3cN+cM0	ypT0ypN0	4

a - ypT0ypN0 (n=5) complete response

Patient	Gender	Therapy arm	cTNM	ypTNM	TRG
P01-025	M	B	cT3cN1cM0	ypT2ypN0	2
P01-026	F	A	cT2cN+cM0	ypT1ypN0	3
P01-027	M	A	cT3cN+cM0	ypT2ypN0	3
P01-028	M	A	cT3cN+cM0	ypT2ypN0	3
P01-030	M	B	cT3cN2cM0	ypT2ypN0	1
P01-032	F	B	cT3cN+cM0	ypT1ypN0	3
P01-034	M	A	cT3cN1cM0	ypT2ypN0	2
P01-035	F	B	cT3cN+cM0	ypT3ypN0	3
P01-037	M	A	cT4cN1cM0	ypT2ypN0	3
P01-038	M	B	cT3cN2cM0	ypT2ypN0	3
P01-039	F	A	cT3cN2cM0	ypT3ypN0	3
P01-041	F	B	cT3cN1cM0	ypTis ypN0	2
P01-043	F	A	cT3cN0cM0	ypT2ypN0	2

b - ypT1-4ypN0 (n=13) intermediate response

Patient	Gender	Therapy arm	cTNM	ypTNM	TRG
P01-022	F	A	cT3cN1cM0	ypT2ypN1a	3
P01-024	M	B	cT3cN1cM0	ypT3ypN1a	2
P01-033	M	B	cT3cN+cM0	ypT3ypN1a	2
P01-042	M	A	cT2cN+cM0	ypT2ypN1b	2

c – ypT1-4ypN+ (n=4) impaired response

Table 5 - Clinical/histopathological characteristics and treatment response following nCRT. Classification of patients with complete (a), intermediate (b), and poor (c) treatment response groups are based in TNM classification. In addition, TRG and lymph node positivity are given. M = male, F = female.

4.2 Assessment of patients' response to nCRT/CT using immune phenotyping from peripheral blood

The major purpose of the study presented here was to monitor the immune contexture in peripheral blood samples of patients and to correlate the contexture with tissue expression and treatment response. By this, three major questions were included: First, does the peripheral blood and/or primary tumor immune contexture predict for response to nCRT/CT? Second, does nCRT/CT modulate the peripheral blood and primary tumor immune profile in preoperative samples compared to baseline samples? Finally, do peripheral blood and primary tumor immune profiles correlate? To address these questions, prospectively collected peripheral blood and paraffine tissue samples were subjected to a detailed FACS-based immune phenotyping of different immune cell subtypes, immunohistochemistry and immunofluorescence analyses and correlated with response to nCRT/CT.

4.2.1 Total T cell count decreases following nCRT/CT

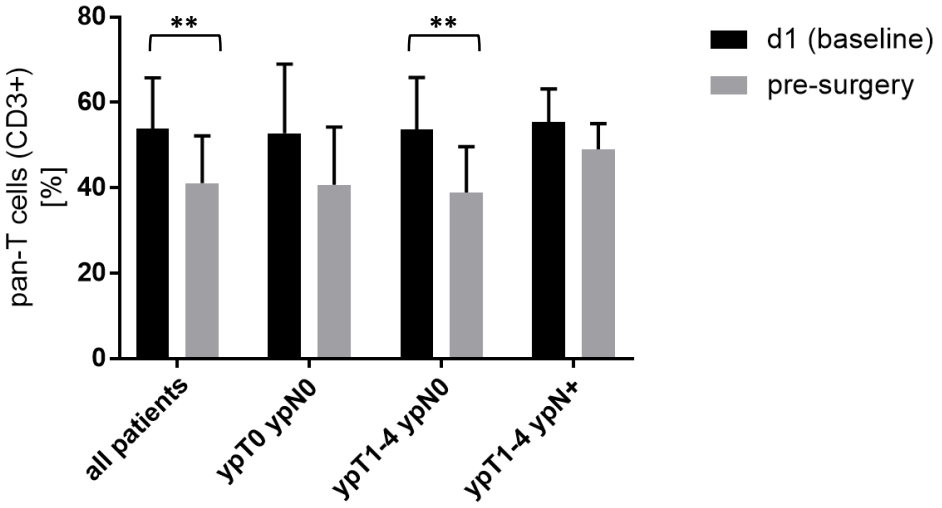

*Figure 14 - Percentage of T lymphocytes (CD3+) based on CD45+ PBMCs at baseline (d1) and before surgical resection as analyzed by FACS phenotyping. Shown are mean values with standard deviation. Significance testing was performed using a two-sided T-test. ** equals $p < 0,005$.*

First, the impact of total T cell count on treatment response was analyzed by correlating cells numbers positive for the pan-specific marker CD3 from pre-treatment (d1) and pre-surgical blood samples. While there was no difference in cell levels concerning treatment response, the average total T cell number

(CD3+) decreases significantly in the entire patient cohort when comparing baseline levels with pre-operative counts (p = 0,0007). Notably, when looking at the different groups separately, in the group of patients with ypT1-4ypN0 category resembling an intermediate response, a significant decrease of total T cell counts was observed (p = 0,0029, Figure 14), whilst good and poor responders lacked a significant decrease in their cell count.

4.2.2 The count of T helper cells correlates with good response to nCRT/CT

Next, the impact of the T helper (CD4+) subpopulation was investigated. Patients with a tumor downsizing in operative specimen (ypT0ypN0) displayed a significantly higher T helper cell count at baseline compared to patients with poor response (ypT1-4ypN+, p = 0,02). In addition, patients with an intermediate response (ypT1-4ypN0) indicated a significantly higher percentage of CD4+ cells compared to patients with poor response (p = 0,012 at baseline, p = 0,036 pre-surgery, Figure 15)

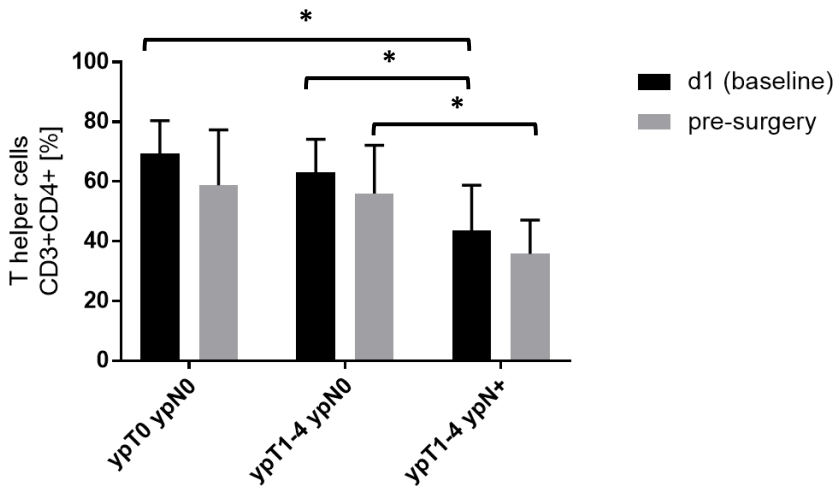

*Figure 15 – Percentage of T helper lymphocytes (CD4+) based on CD45+ PBMCs at baseline (d1) and before surgical resection as analyzed by FACS phenotyping. Shown are mean values with standard deviation. Significance testing was performed using a two-sided T-test. * equals p < 0,05.*

4.2.3 A low count of cytotoxic T cells, expression of PD1 and activation markers GranzymeB and perforin correlate with an improved response to nCRT/CT

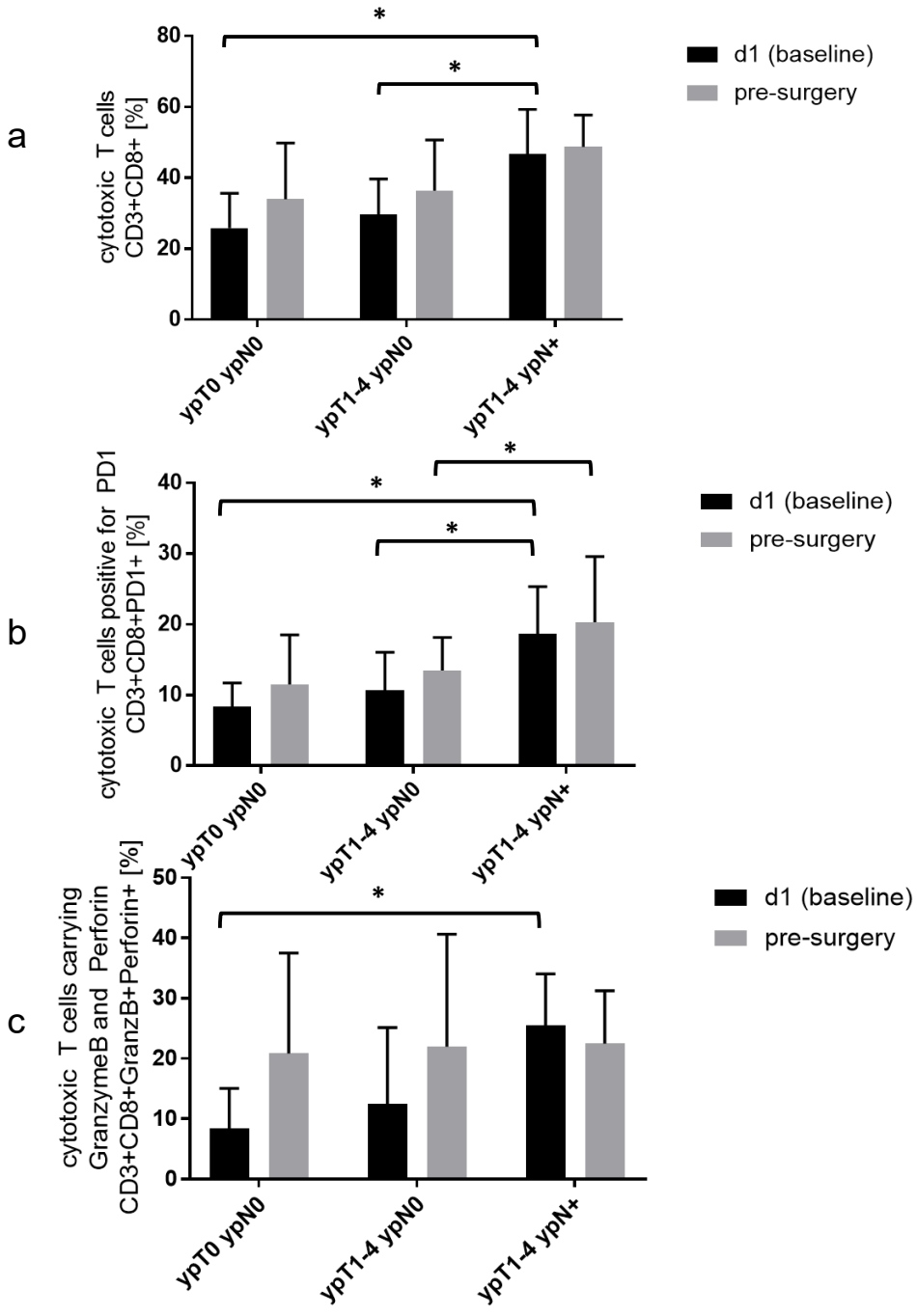

*Figure 16 – Percentages of cytotoxic T lymphocytes (CD8+) (a), cytotoxic T lymphocytes expressing PD1 (b) and CD8+ cells expressing GranzymeB and perforin (c) at baseline (d1) and before surgical resection as analyzed by FACS phenotyping. Shown are mean values with standard deviation. Significance testing was performed using a two-sided T-test- * equals $p < 0,05$.*

Patients with complete response (ypT0ypN0) indicate a significantly lower number of circulating cytotoxic (CD8+) T cells at baseline as compared to patients with poor response to nCRT/CT (ypT1-4ypN+, p = 0,027, Figure 16a). In addition, patients with a partial response (ypT1-4ypN0) showed a significantly lower level of the CD8+ subgroup as compared to patients with poor response at baseline (p = 0,013), whilst the differences disappear when analyzing pre-surgical probes (Figure 16a). Correspondingly, patients with decreasing lymph node burden (ypN0) after nCRT/CT show significantly lower levels of cytotoxic T lymphocytes compared to patients with tumor positive lymph nodes (ypN+, p = 0,0048, Supplementary figure 1).

Further, in order to investigate the PD1/PD-L1 signaling pathway in T cells with relevance for tumor survival,[56] the expression of PD1 was investigated in cytotoxic T lymphocytes. When assessing PD1 expression on CD8+ cells, patients with a ypT0ypN0 and ypT1-4ypN0 response revealed a significantly lower percentage of these cells as compared to patients with a ypT1-4ypN+ situation (p = 0,019 for ypT0ypN0 and p = 0,026 for ypT1-4ypN0, Figure 16b). Also, there is a significantly different expression between partial responders and impaired responders in pre-surgical specimens (p = 0,03, Figure 16b). Same holds true for PD1 positive cytotoxic T cells and the patients' lymph node burden in surgery specimen. Patients with a lymph node free specimen (ypN0) showed significantly lower counts of these cells in peripheral blood at baseline (p=0,007) as well as at pre-surgical testing (p=0,04, Supplementary figure 2**Fehler! Verweisquelle konnte nicht gefunden werden.**). And congruently, patients with a good tumor regression (TRG) in the surgical specimen depicted a significantly lower count of PD1 positive CD8+ T cells than patients with poor tumor regression after nCRT/CT (p = 0,01, Supplementary figure 3*).*

Finally, GranzymeB and perforin covering activation markers for cytotoxic cellular functions were investigated in CD8+ T lymphocytes. In contrast to patients with poor response (ypT1-4ypN+), patients with good response (ypT0ypN0) displayed significantly lower activation marker-positive T cells at baseline (p = 0,011, Figure 16c). Accordingly, comparing lymph node status, patients with an ypN0 situation after nCRT/CT showed significantly lower

GranzymeB and Perforin positive CD8+ T cells at baseline measurement compared to poor responders (ypN+, p=0,03, Supplementary figure 4).

In summary, lower numbers of cytotoxic T cells and elevated levels of T helper cells in pretreatment biopsies predict a higher likelihood of an at least partial response and may be suitable as predictive markers for treatment response to nCRT/CT.

4.2.4 A high CD4/CD8 ratio correlates with good response to nCRT/CT

In line with a differential expression of CD4 and CD8 in T lymphocytes, patients with an intermediate response (ypT1-4ypN0) revealed a higher CD4/CD8 ratio in comparison to patients with a poor response (ypT1-4ypN+) at baseline (p = 0,023) and in pre-surgical specimens (p = 0,025, Figure 17).

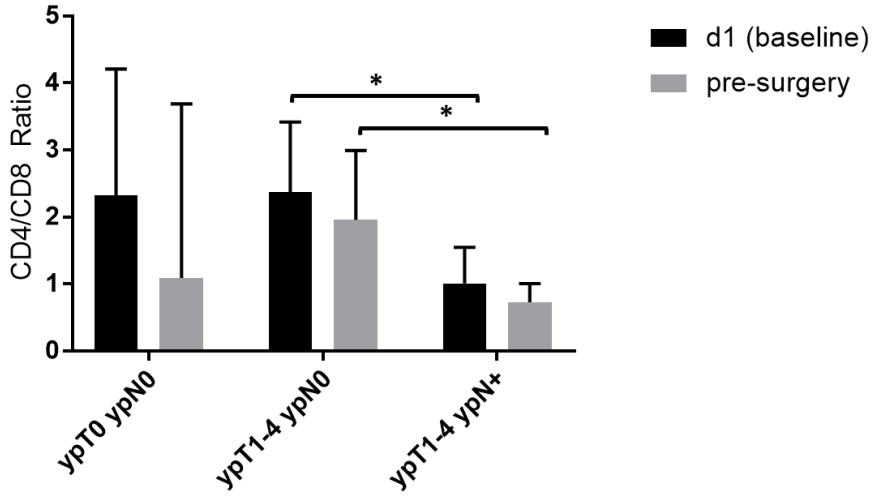

*Figure 17 – Ratio of CD4 and CD8 expressing T lymphocytes (CD4/CD8 ratio) at baseline (d1) and before surgical resection as analyzed by FACS phenotyping. Shown are mean values with standard deviation. Significance testing was performed using a two-sided T-test. * equals p < 0,05.*

Concerning the lymph node burden in surgical specimen, there was a significantly higher CD4/CD8 ratio detectable in patients with tumor free lymph nodes (ypN0) compared to residual tumor positive lymph nodes (ypN+) after nCRT/CT at baseline (p = 0,03, Supplementary figure 5). In conclusion, a high T helper cell count and a low cytotoxic T cell count at baseline, resulting in an elevated CD4/CD8 ratio, is associated with an improved response to nCRT/CT.

4.2.5 A decrease in B cell count correlates with intermediate and impaired response to nCRT/CT

CD19+ B cells cover a second major group of lymphocytes contributing to the adaptive immune response. As depicted in Figure 18, the collective of B cells was decreasing significantly over the course of nCRT/CT (p = 0,0035). Especially patients with intermediate (ypT1-4ypN0) and poor (ypT1-4ypN+) response indicate a significant decrease in the percentage of B lymphocytes (p = 0,026 for ypT1-4ypN0 and p = 0,035 for ypT1-4ypN+, Figure 18), while patients with a complete response (ypT0ypN0) displayed more stable levels.

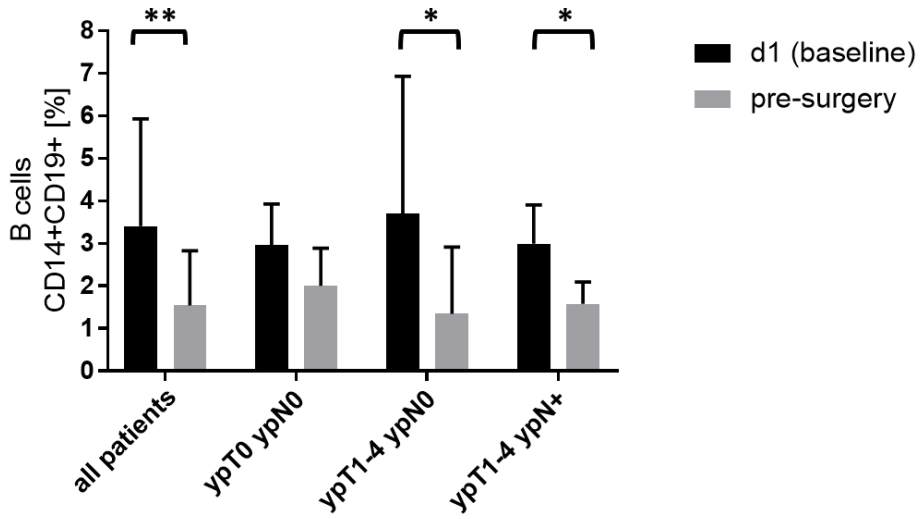

*Figure 18 – Percentage of B lymphocytes (CD19+) based on CD45+ PBMCs at baseline (d1) and before surgical resection as analyzed by FACS phenotyping. Shown are mean values with standard deviation. Significance testing was performed using a two-sided T-test. * equals p < 0,05, ** equals p < 0,005.*

4.2.6 An increase in monocyte count correlates with complete and intermediate response to nCRT/CT

Next, another relevant cell population of the innate immune response, monocytes, characterized as CD45+CD33+CD14+ expressing cells, were investigated for their predictive value. As depicted in Figure 19, when assessing patients with complete (ypT0ypN0) and intermediate response (ypT1-4ypN0), a significant increase of monocyte count was detected (p = 0,015 for ypT0ypN0 and p = 0,0004 for ypT1-4ypN0, Figure 19). The monocytic cell count also increased in patients with a poor response, but the increase did not reach a level of significance.

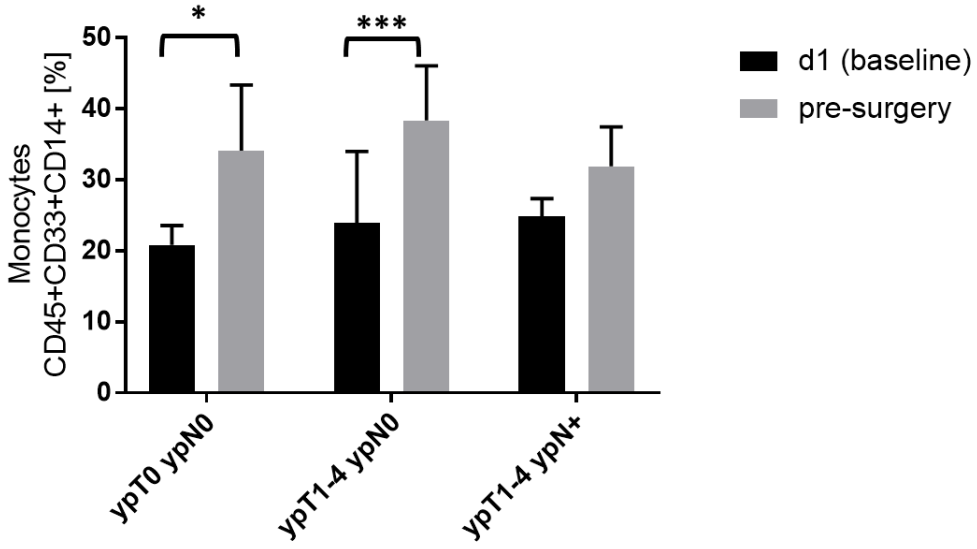

*Figure 19 – Percentage of monocytes (CD33+CD14+) based on CD45+ PBMCs at baseline (d1) and before surgical resection as analyzed by FACS phenotyping. Shown are mean values with standard deviation. Significance testing was performed using a two-sided T-test. * equals p < 0,05, *** equals p < 0,0005.*

4.2.7 HLA molecule expression correlates with treatment response to nCRT/CT

The HLA molecules play an important role in antigen presentation. While HLA-ABC molecules can be detected on all nucleated cells and present antigen-peptides from the cytoplasm to cytotoxic T lymphocytes, HLA-DR molecules, by contrast, are more restricted to antigen-presenting cells and bind to CD4+ T lymphocytes.[57]

Results depicted in Figure 20 indicated an increase in percentage of immune cells (CD45+) carrying surface HLA-DR proteins from pre-treatment to pre-surgical specimens. For all treatment groups, these increased counts also reach a level of significance (p = 2,5E-09 for all patients, p = 0,00021 for ypT0ypN0, p = 5,1E-05 for ypT1-4ypN0 and p = 0,0043 for the ypT1-4ypN+ cohort).

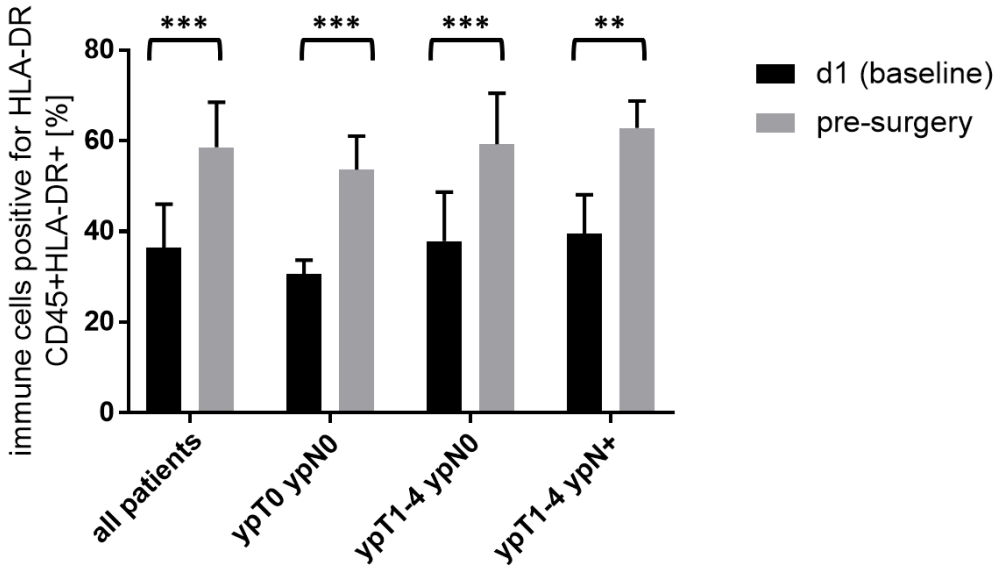

*Figure 20 – Percentage of immune cells (CD45+) expressing HLA-DR molecules at baseline (d1) and before surgical resection as analyzed by FACS phenotyping. Shown are mean values with standard deviation. Significance testing was performed using a two-sided T-test. ** equals p < 0,005, *** equals p < 0,0005.*

Moreover, by analyzing immune subpopulations in more detail, significant values were observed for T lymphocytes, where patients with complete response (ypT0ypN0) to nCRT/CT showed significantly lower counts of HLA-DR positive T cells in pre-surgical blood samples compared to patients with poor response (ypT1-4ypN+, p = 0,026, Figure 21a).

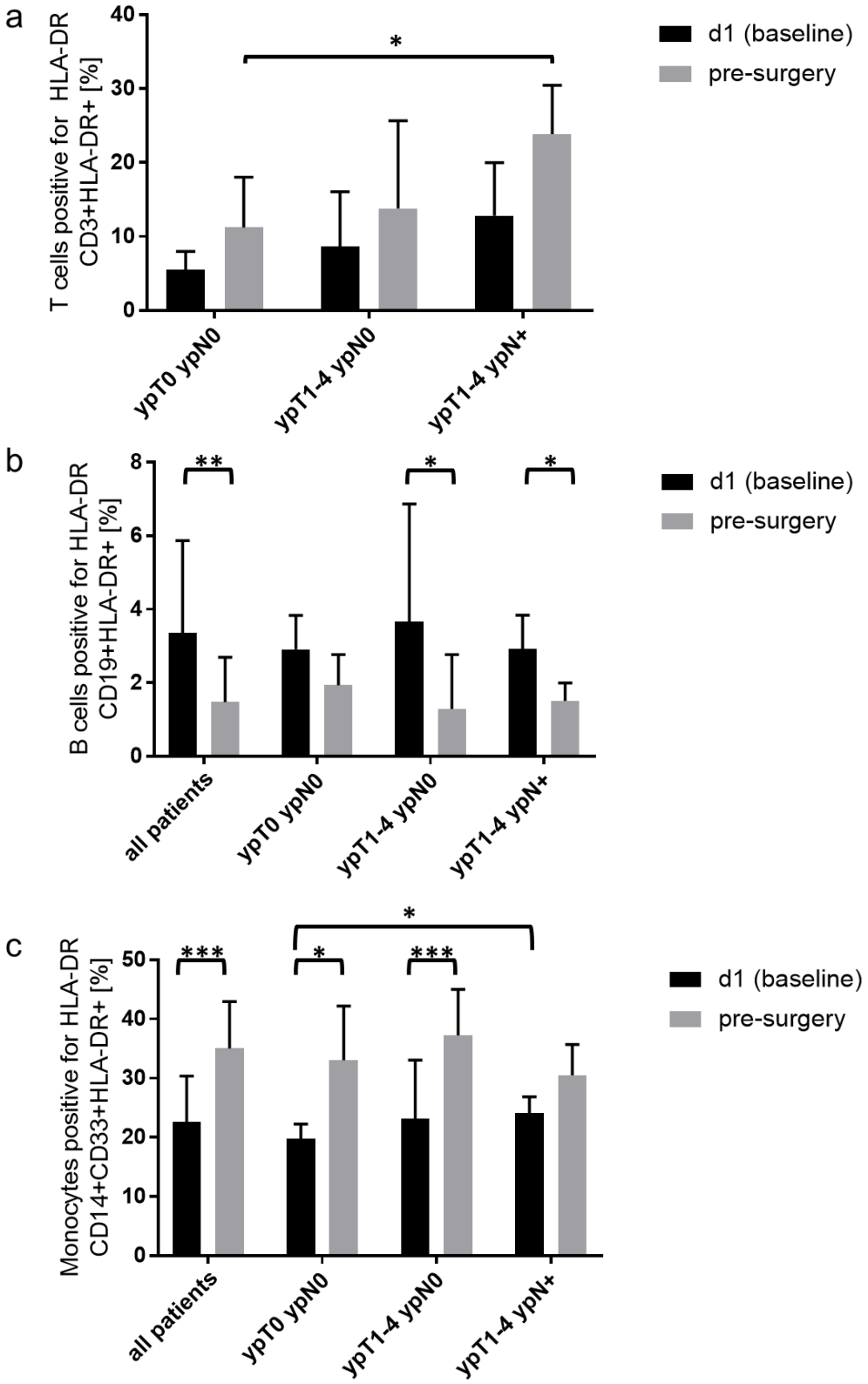

*Figure 21 – Percentages of T lymphocytes (CD3+) (a), B lymphocytes (CD19+) (b) and monocytes (CD14+CD33+) (c) expressing surface HLA-DR molecules at baseline (d1) and before surgical resection as analyzed by FACS phenotyping. Shown are mean values with standard deviation. Significance testing was performed using a two-sided T-test. * equals $p < 0,05$, ** equals $p < 0,005$, *** equals $p < 0,0005$.*

Also, the decrease of HLA-DR expression on B cells was significant in all patients (p = 0,003), intermediate responders (ypT1-4ypN0, p = 0,024) and poor responders (ypT1-4ypN+, p = 0,034) to nCRT/CT (Figure 21b). Finally, for monocytes expressing HLA-DR, a significant increase was demonstrated for all patients (p = 4,4E-06), as well for patients with complete response (ypT0ypN0, p = 0,014) and intermediate response (ypT1-4ypN0, p = 0,0005) to nCRT/CT (Figure 21c). As well, complete responders (ypT0ypN0) depicted significantly lower counts of HLA-DR positive monocytes in baseline blood testing compared to patients with poor response (ypT1-4ypN+, p = 0,04, Figure 21c).

By contrast, additional immune subpopulations (CD11b, CD15, CD25) and intracellular markers (FoxP3) included in FACS analysis did neither reveal significant correlations with patients' therapy response nor significant changes over the course of nCRT/CT. Same holds true for most additional time points of blood testing (d8, d43) with no significant interrelationships with therapy response to be observed.

4.3 Significant correlations and trends between peripheral blood cell count, TNM classification, TRG and lymph node status

In addition to the previously presented statistical values as computed by a student's T-test, Pearson's chi-squared analysis were performed to further determine correlations between immune cells and treatment response. By this, patients were dichotomized into two groups according to a low vs. high cell count. The median was chosen as the cut-off value. Significant findings are given in Table 6, Table 7 and Table 8 for clinical endpoint histopathological response (TNM), tumor regression grading (TRG) and lymph node positivity.

Subpopulation	**Day of testing**	**Significance level ypT0 N0 vs. ypT1-4 N0 vs. ypT1-4 N+**	**Correlation**
cytotoxic T cells (CD3+CD8+)	d1	0,087	low cytotoxic T cells → low TNM
T helper cells (CD3+CD4+)	d1	0,087	high T helper cells → low TNM
	pre-surgery	**0,047**	
cytotoxic T cells positive for PD1 (CD3+CD8+PD1+)	d1	0,087	low PD1+ cytotoxic T cells → low TNM
cytotoxic T cells carrying Granzyme B and Perforin (CD3+CD8+GranzB+Perforin+)	d1	0,087	low GranzymeB+/ Perforin+ cytotoxic T cells → low TNM
CD4/CD8 Ratio	d1	0,087	high CD4/CD8 ratio → low TNM
	pre-surgery	**0,047**	
Monocytes (CD45+CD33+CD14+)	d1	0,053	low monocytes → low TNM

Table 6 – Correlations between TNM status and immune cell populations. Statistical analysis was performed using a Pearson's Chi-Squared test. Significant values (p < 0,05) are marked in bold.

Marker	Day of testing	Significance level TRG 1+2 vs. 3+4	Correlation
cytotoxic T cells (CD3+CD8+)	d1	0,076	low cytotoxic T cells → high TRG
cytotoxic T cells positive for PD1 (CD3+CD8+PD1+)	d1	0,076	low CD3+CD8+PD1+ → high TRG
	d43	**0,049**	
CD4/CD8 Ratio	d1	0,076	low CD4/CD8 ratio → low TRG

Table 7 – Correlations and trends between TRG status and immune cell populations. Statistical analysis was performed using a Pearson's Chi Squared Test. Significant values ($p < 0,05$) are marked in bold.

Marker	Day of testing	Significance level ypN0 vs. ypN+	Correlation
cytotoxic T cells (CD3+CD8+)	**d1**	**0,027**	low cytotoxic T cells → ypN0
T helper cells (CD3+CD4+)	**d1**	**0,027**	high T helper cells → ypN0
	pre-surgery	**0,027**	
T helper cells positive for PD1 (CD3+CD4+PD1+)	d1	0,269	high T helper cells with PD1 → ypN0
	pre-surgery	**0,027**	
cytotoxic T cells positive for PD1 (CD3+CD8+PD1+)	**d1**	**0,027**	low cytotoxic T cells with PD1 → ypN0
cytotoxic T cells carrying Granzyme B and Perforin (CD3+CD8+GranzB+Perforin+)	**d1**	**0,027**	low cytotoxic T cells with GranzB/ Perforin → ypN0
CD4/CD8 Ratio	**d1**	**0,027**	high CD4/CD8 ratio → ypN0
	pre-surgery	**0,027**	
Monocytes (CD45+CD33+CD14+)	**d1**	**0,027**	low monocytes → ypN0

Table 8 – Correlations between lymph node status and immune cell populations. Statistical analysis was performed using a Pearson's Chi Squared Test. Significant values ($p < 0,05$) are marked in bold.

As depicted in the tables above, there are several cellular markers that could, at baseline assessment, predict a patient's response to nCRT/CT. A low amount of cytotoxic T cells (CD8+) is associated with lymph node negativity ($p = 0,027$). The same holds true for PD1 positive CD8+ T cells with a low count to correlate with tumor free lymph nodes ($p = 0,027$). Moreover, at day 43, there is a significant correlation of CD8+PD1+ T lymphocytes and a higher TRG grading

(p = 0,049). Likewise, a low number of activation marker (GranzymeB and perforin) expressing CD8+ T cells at baseline is correlated with a ypN0 situation (p = 0,027). By contrast, an elevated number of T helper cells (CD4+) at baseline significantly correlates with a lymph node negative status (p = 0,027). Also, at pre-operative testing, a low CD4+ T cell count is significantly associated with a lower TNM category (p = 0,047). Further, a high percentage of peripheral blood PD1+ T helper cells (CD4+PD1+) is related to an ypN0 situation at pre-operative testing (p=0,027). Finally, and consistent with the findings for T helper and cytotoxic T cells, a high CD4/CD8 ratio significantly correlates with a complete regression (ypT0ypN0) when being tested at

baseline (p = 0,047) and also lymph node negativity when being tested at baseline (p = 0,027) and in pre-operative samples (p = 0,027).

Finally, a low monocyte count significantly correlates to a ypN0 situation (p = 0,027) and displays a trend (p = 0,053) for a lower TNM category.

Other markers (CD11b, CD15, CD25, FoxP3) did not show any significant correlation with a good or poor response to CRT. Those non-significant values are displayed in Supplementary Table 1, Supplementary Table 2 and Supplementary Table 3.

4.4 Histological assessment of immune markers and correlation with nCRT/CT response

To further unravel a prognostic/predictive relevance of tissue marker expression and a putative correlation with peripheral blood immune cell levels, immunohistochemical and multiparametric immunofluorescence staining were performed from patients' tumor biopsies and surgical resection specimens.

4.4.1 Histochemical assessment of T lymphocytes

For the detection of total T cell (CD3+) count and their subsets, a multiparametric Phenoptics™ immunofluorescence staining approach was applied. Exemplary microphotographs for a high and low expression of CD4 and CD8 fluorescent markers in tumor tissue are given in Figure 22. The evaluation of staining scores was based on a quantitative assessment of the percentage of fluorophore positive cells in tumor tissue as analyzed by Vectra3 automatic quantitative pathology imaging system and InForm v2.1 software.

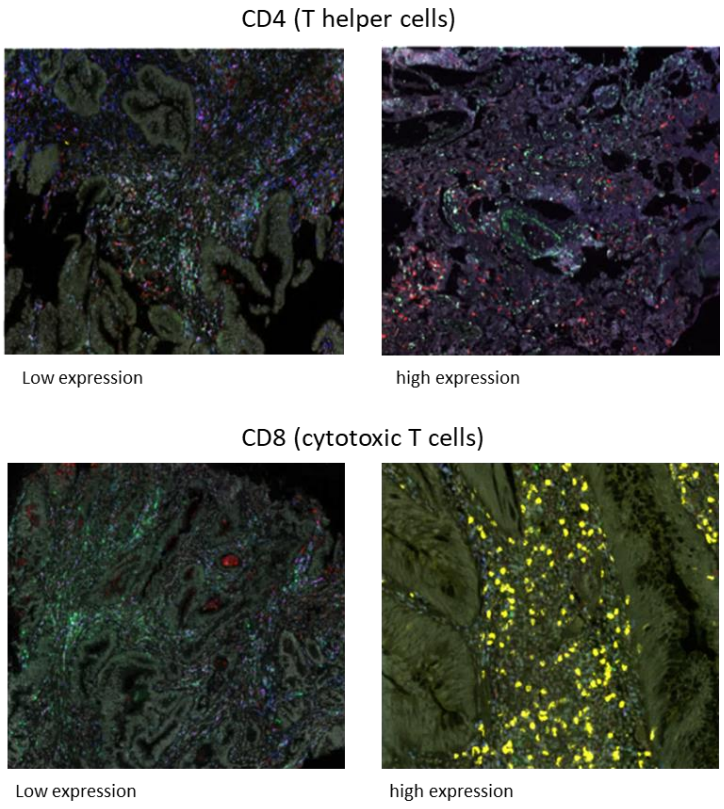

Figure 22 - Examples for multiparametric immunofluorescence staining for CD4 T helper cells (green fluorescence) and CD8 cytotoxic T lymphocytes (yellow fluorescence) showing low and high expression at the tumor site. Magnification x 20.

In contrast to the findings for the peripheral blood testing (Figure 14), tissue expression of total CD3+ T cells did not indicate significant difference in the count of tumor infiltrating T cells (TILs) between the different groups of nCRT/CT responses (Figure 23). Also, there is no significant change of tumor infiltrating T cell levels when comparing pre-therapeutic biopsy and surgical specimen (Figure 23).

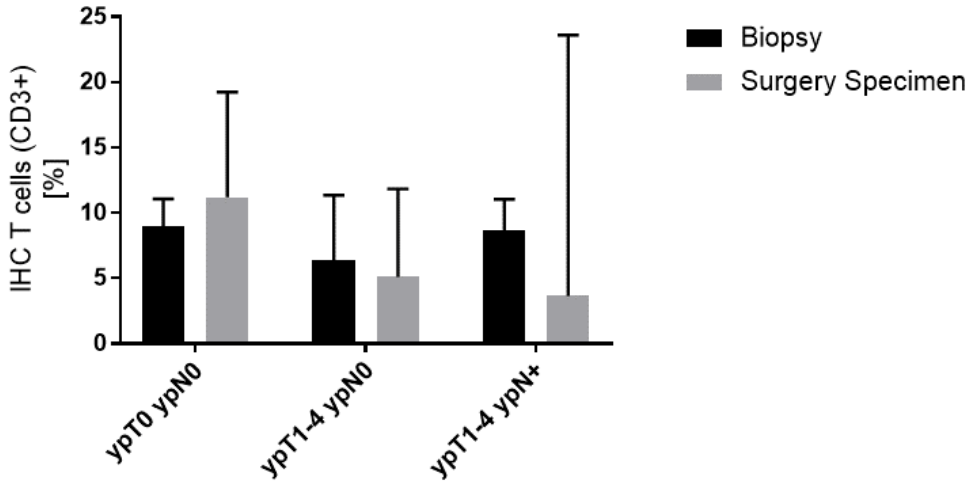

Figure 23 – Percentage of CD3+ tumor infiltrating T lymphocytes in pretreatment biopsies and in surgical resection specimens as analyzed by multiparametric Phenoptics™ immunofluorescence staining. Shown are median values with standard deviation. Significance testing was performed using a two-sided T Test.

When assessing CD4+ T helper and CD8+ cytotoxic T cell subtypes, correlations also lack significances indicating no prognostic value of TILs in the patients' cohort analyzed (Supplementary figure 6). There was, however, a significant impact of PD1+ T cells differentiating patients with complete and intermediate response in post-treatment surgical resection specimen ($p = 0,027$, Figure 24).

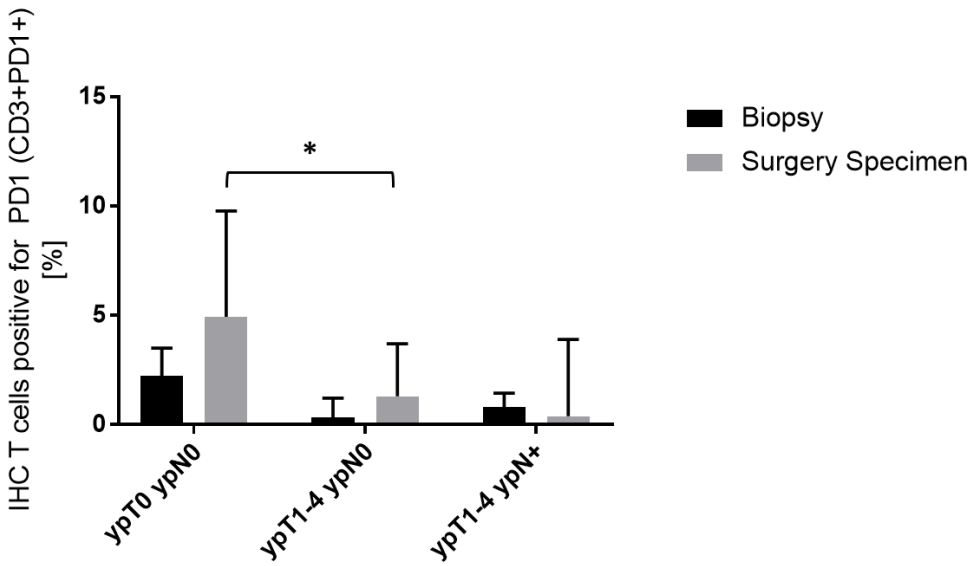

*Figure 24 – Percentage of CD3+ tumor infiltrating T lymphocytes positive for surface PD1 expression in pretreatment biopsies and surgical resection specimens as analyzed by multiparametric Phenoptics™ immunofluorescence staining. Shown are median values with standard deviation. Significance testing was performed using a two-sided T-Test. * equals $p < 0,05$.*

4.4.2 Histochemical assessment of neutrophils, natural killer cells, macrophages and GranzymeB

Next, tissue expression and distribution of additional immune markers were assessed by immunohistochemistry. Examples of tissue expression of neutrophilic granulocytes (CD15 staining) and macrophages (CD68 staining) are presented in Figure 25. For natural killer (NK) cells, CD56 marker expression was analyzed. The evaluation of staining characteristics was based on a quantitative assessment of the amount of marker positive cells and staining intensity resulting in a staining score ranging from 0-12.

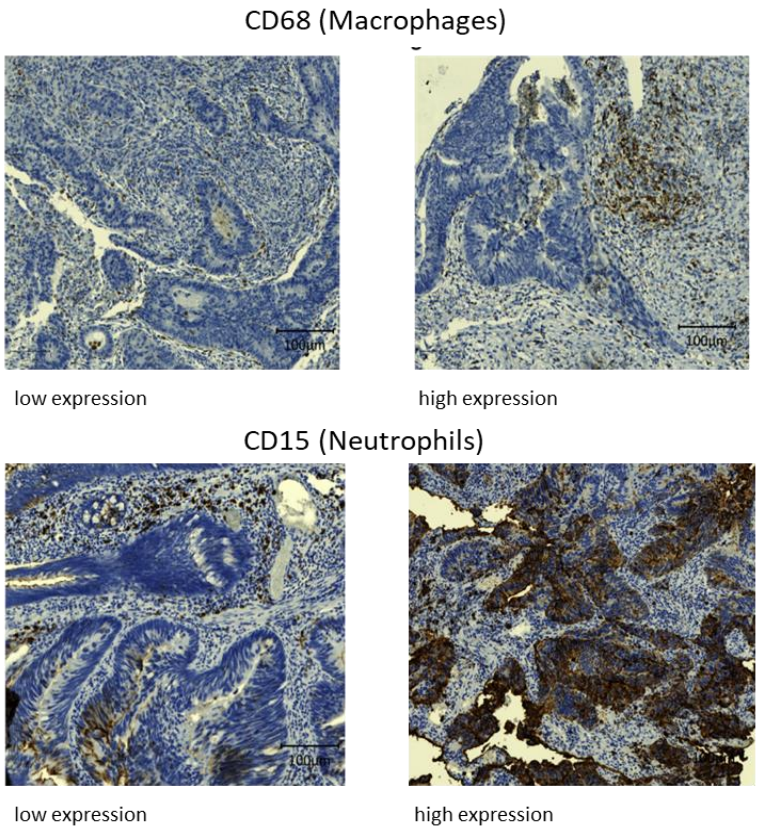

Figure 25 - Examples for immunohistochemical staining of macrophages (CD68) and neutrophils (CD15), showing low expression and high expression of these markers in the tumor. Magnification x 25, scale bars indicate 100 µm.

4.4.2.1 Neutrophilic count decreases significantly in patients with good response to nCRT/CT

As given in Figure 26, patients with a complete response (ypT0ypN0) displayed a decrease in the amount of infiltrating neutrophils as the immunoscore of CD15+ cells was significantly higher in patient's biopsies compared to post-nCRT/CT surgical specimen ($p = 0,003$), while no significant decrease in patients with partial (ypT1-4ypN0) or poor response (ypT1-4ypN+) from pretreatment biopsies and tumor resection specimens was observed. When analyzing the neutrophil density in the surgical specimens, the score for patients with complete response is significantly lower as compared to intermediate and poor responders ($p = 0,048$ for ypT1-4ypN0 and $p = 0,044$ for ypT1-4ypN+, Figure 26).

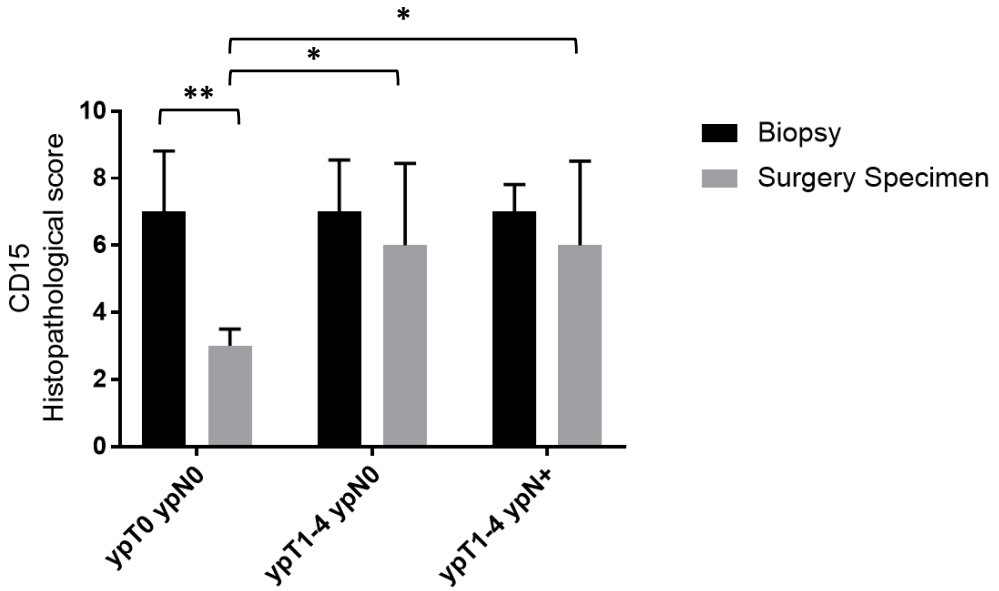

*Figure 26 – Detection (immunoscore) of CD15+ neutrophils in pretreatment biopsies and surgical resection specimens as analyzed by immunohistochemical staining. Shown are median values with standard deviation. Significance testing was performed using a two-sided T-Test. * equals p < 0,05, ** equals p < 0,005.*

4.4.2.2 NK cell counts increase significantly in patients with good and intermediate response to nCRT/CT

NK cells are a group of cytotoxic lymphocytes critical to the innate immune system. The role of NK cells is analogous to that of cytotoxic T cells in the vertebrate adaptive immune response but does not require an antigen specific activation.[58]

In both, patients with complete (ypT0ypN0) and intermediate (ypT1-4ypN0) response to nCRT/CT, an increase of CD56+ cells was observed, reaching levels of significance (p = 0,0088 for ypT0ypN0 and p = 1,7E-05 for ypT1-4ypN0), respectively (Figure 27). This increase was also significant for all patients combined (p = 4E-08, Figure 27).

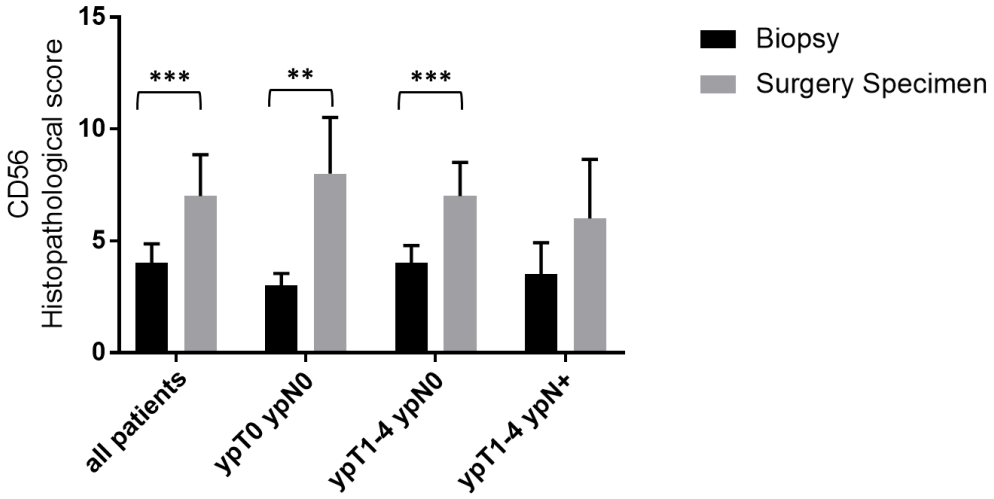

*Figure 27 - Detection (immunoscore) of CD56+ NK cells in pretreatment biopsies and surgical resection specimens as analyzed by immunohistochemical staining. Shown are median values with standard deviation. Significance testing was performed using a two-sided T-Test. ** equals p < 0,005, *** equals p < 0,0005.*

4.4.2.3 Increased macrophage count correlates with an intermediate response to nCRT/CT

Macrophage CD68 cell count increases when being assessed in pre-therapeutic biopsy and post-nCRT/CT surgery specimen of patients with a good and intermediate response, reaching a level of significance in the intermediate (ypT1-4ypN0, p = 0,032) response cohort, when analyzing tissue samples using multiparametric Phenoptics^{TM} immunofluorescence staining (Figure 28).
These findings failed to be reproduced in conventional immunohistochemistry staining using the described immunoscore (Supplementary figure 7).

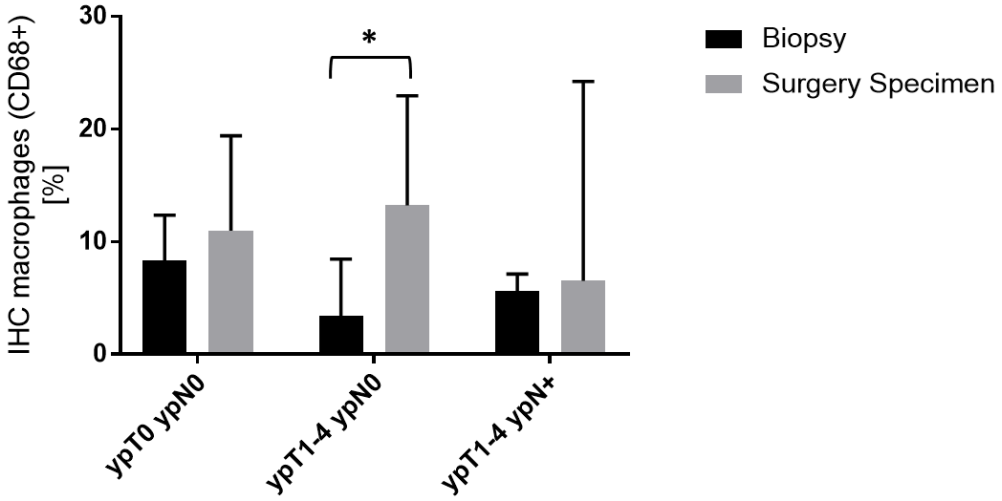

*Figure 28 - Percentage of CD68+ tumor infiltrating macrophages in pretreatment biopsies and surgical resection specimens as analyzed by multiparametric Phenoptics™ immunofluorescence staining. Shown are median values with standard deviation. Significance testing was performed using a two-sided T-Test. * equals p < 0,05.*

4.4.2.4 An increase in GranzymeB detection is associated with improved response to nCRT/CT

When analyzing GranzymeB positive cells in the tumor microenvironment, a significant increase of the staining scores was observed in patients with complete response (ypT0ypN0, p = 0,011) and a trend was visible in patients with intermediate response (ypT1-4ypN0) to nCRT/CT, whereas patients with an impaired response indicate constant low levels in both pre-therapeutic and pre-surgical specimens (Figure 29). In addition, patients with complete response revealed significantly higher GranzymeB scores than poor responders at post-nCRT/CT testing (p = 0,025, Figure 29).

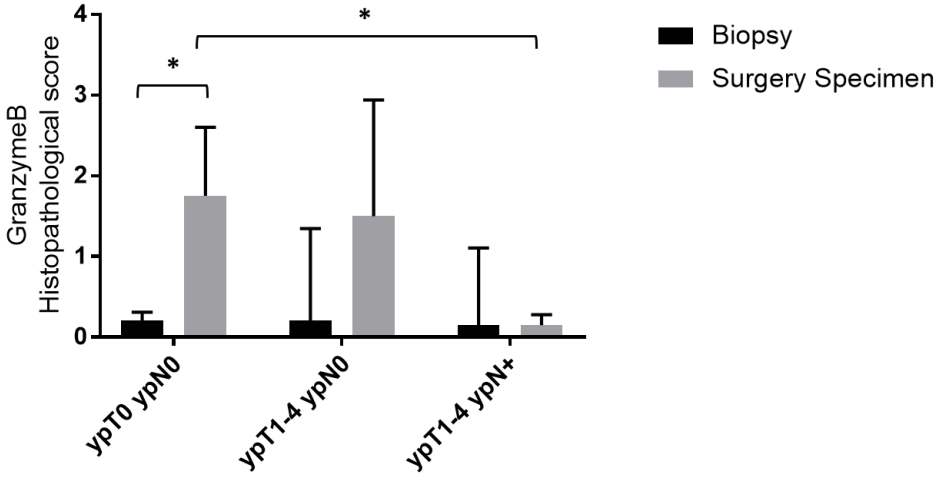

*Figure 29 – Immunodetection (immunoscore) of GranzymeB expression in pre-treatment biopsies and surgical resection specimens as analyzed by immunohistochemical staining. Shown are median values with standard deviation. Significance testing was performed using a two-sided T-Test. * equals p < 0,05.*

4.5 Correlation between immunohistological detection and peripheral blood immune cell count

Finally, the question on an interrelationship of peripheral blood and primary tumor immune profiles was addressed by analyzing a correlation between percentages of subpopulations and their corresponding histochemical score. For all exemplarily plotted cell populations –T cells and their subsets CD4+ T helper cells and CD8+ cytotoxic T cells as well as monocytes/macrophages – the dots were not aligned in any specific manner. This may be interpreted as the lack of a percept for the distribution of immune cells. Thus, elevated levels in peripheral blood do not automatically indicate a high level of tissue expression of the markers. In this case, the calculation of a correlation coefficient did not prove beneficial, as the informative value is low due to the low number of patients included in this trial.

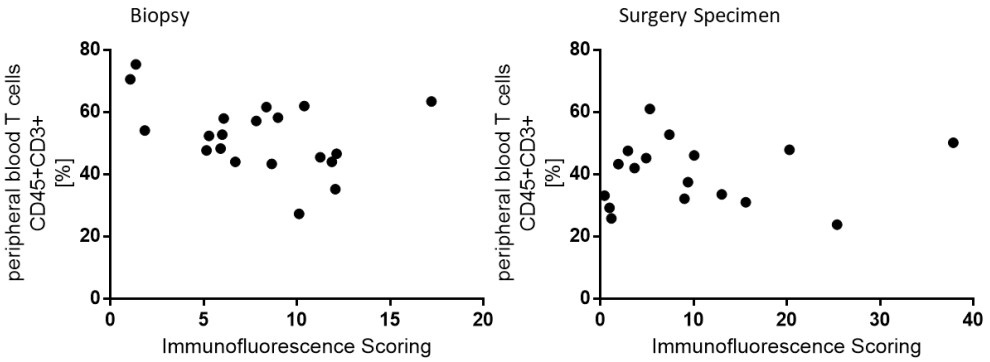

Figure 30 – Correlation between peripheral blood and histological tissue expression of T lymphocytes plotted as percentage of CD45+CD3+ cells and tumor immunoscore in pretreatment blood samples and biopsies (left) and post treatment blood samples and surgical resection specimens (right).

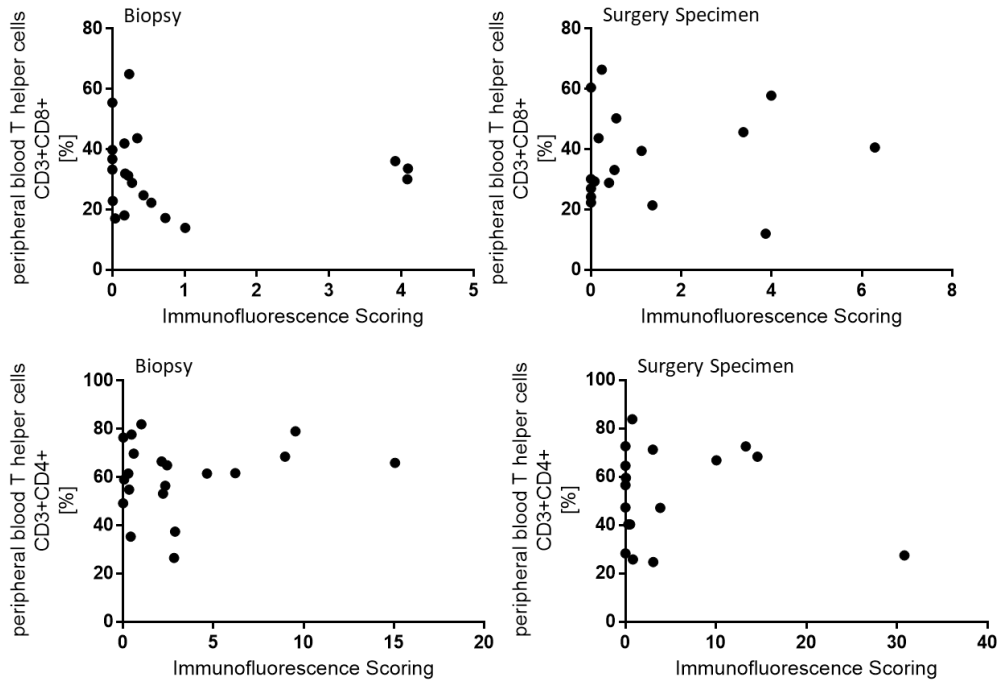

Figure 31 – Correlation between peripheral blood and histological tissue expression of cytotoxic T lymphocytes (upper row) and T helper lymphocytes (lower row) plotted as percentage of CD8+ and CD4+ cells and tumor immunoscore in pretreatment blood samples and biopsies (left) and post treatment blood samples and surgical resection specimens (right).

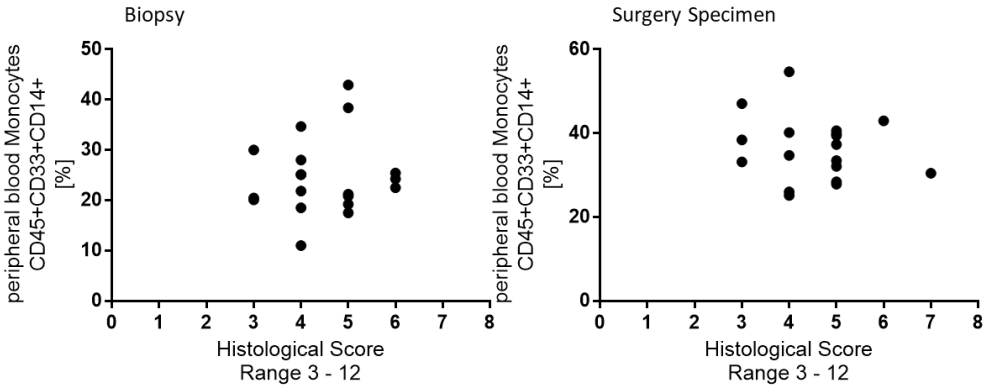

Figure 32 – Correlation between peripheral blood and histological tissue expression of monocytes/macrophages plotted as percentage of CD33+CD14+ cells and tumor immunoscore in pretreatment blood samples and biopsies (left) and post-treatment blood samples and surgical resection specimen (right).

5 Discussion

Treatment response to nCRT varies considerably among individual patients in rectal cancer.[11] Accordingly, there is an urgent need to predict treatment efficacy to optimize patient stratification, personalized treatment and organ sparing approaches. Moreover, it is of great interest to develop easy to handle and non-invasive methods as sources of markers to accomplish a molecular based prediction. In recent years, blood borne biomarkers have become increasingly attractive as predictors because they are easy to collect, relatively inexpensive, reflect information on different aspects of tumor biology and can be accurately measured by standardized methods.[59]

Against this background, the present study was conducted in the context of the DKTK and FCI to investigate a potential predictive value of the peripheral blood immune cell contexture in patients with rectal cancer treated with nCRT/CT. In addition, we prospectively tracked the changes in peripheral immune cell components elicited by nCRT/CT and subsequently assessed whether these parameters could predict the pathologic treatment response.

Recapitulated, the most important findings are:

- Lymphocytes seem to play a crucial role in the nCRT/CT mediated systemic anticancer immunological response.
- Peripheral blood T lymphocytes play a central role in predicting treatment response. A high number of T helper cells (CD4+) at baseline correlates with complete response and tumor free surgical specimens after nCRT/CT. Accordingly, a low number of (CD8+) cytotoxic T cells, as well as PD1 and GranzymeB positive lymphocytes, is associated with good treatment response.
- Over the course of nCRT/CT, an increase in monocyte counts is visible in patients with complete and intermediate response. Also, the HLA-DR expression on monocytes increases significantly in good responders to nCRT/CT.
- Tumor infiltrating T cells did not indicate significant difference between the different groups of nCRT/CT response opposed to peripheral blood T

cells. Also, no significant change over the course of neoadjuvant treatment is visible.

- Tumor infiltrating neutrophils decrease significantly in patients with complete response, leading to a significantly lower tissue based neutrophil count in surgical specimens compared to patients with intermediate and poor response.

5.1 The count of T lymphocytes correlates with response to nCRT/CT

In addition to the direct cytotoxic effect of radiation and chemotherapy, multiple studies have demonstrated the involvement of an immunological host response, which also contributes to a tumor regression induced by nCRT.[60,61] Initially, we evaluated the association between peripheral blood leukocyte counts and the pathologic response as assayed in the surgical resection specimens. By this, findings suggest a potential role of the levels of T helper cells (CD4+) and cytotoxic T lymphocytes (CD8+) as well as monocytes and HLA molecule expression in predicting the response to nCRT/CT in patients with advanced rectal cancer.

Kitayama et al. were among the first to indicate circulating lymphocytes to be valuable determinants of the effectiveness of preoperative RT in rectal cancer. In their report, patients with high lymphocyte percentages in peripheral blood white cells revealed an increased rate of complete responses and a favorable clinical outcome.[62]

By contrast, a recent study indicates an unfavorable role of peripheral blood leukocytosis in the context of inflammation in rectal cancer. Assessing a huge number of patients (n = 1236) within the CAO/ARO/AIO-04 randomized phase 3 trial, Diefenhardt et al. reported the biomarkers baseline leukocytosis (>7,8/nl) and neutrophilia to cover independent adverse prognostic factors for DFS, distant metastasis free-survival and OS in multivariable analysis, while treatment-induced leukopenia correlated with a favorable clinical outcome.[63] Off note, leukocytosis further showed a significant correlation with lower TRG. These analyses, however, are based on differential blood cell count derived from patients records and do not discriminate between immune cell subtypes.

Further, Tada et al. reported that patients with advanced response to 5-FU based nCRT comprised significantly higher numbers of pre-treatment total lymphocytes and (CD4+) T helper lymphocytes compared to cases with an impaired response. In addition, the pre-CRT total number of T lymphocytes and CD4+ T helper cells significantly correlated with the tumor regression, whereas the number of cytotoxic (CD8+) T lymphocytes and post-treatment lymphocyte subsets showed no correlation with tumor response.[64]

Corroborating these findings, in the present study, the average total (CD3+) T cell count decreases in the entire patient cohort when comparing baseline levels with pre-operative counts (Figure 14). These findings may indicate, that the ability of radiation and chemotherapy to deplete sensitive leukocytes[65] and to induce apoptosis[66] may contribute to its therapeutic outcome and support the notion that the efficacy of nCRT is mediated by factors other than its direct cytotoxicity, including inhibition of immunosuppressive circuitries.[67] Conversely, this finding may, at least partially, also reflect, that patients who received sufficient cytotoxic CRT experienced higher incidence of leucopenia, resulting in better clinical outcome.

By collecting five samples from the onset of nCRT to surgery, Lee et al. described a continuous decrease of total lymphocytes during the course of CRT, followed by an increase after treatment. Notably, at the onset of nCRT, total leukocyte count did not significantly differ between patients with and without a complete response. At two weeks after initiating nCRT, however, patients with a complete tumor regression had significantly lower leukocyte, neutrophil and monocyte counts. Also, and in line with the findings of the present study, the proportion of CD4+ T cells among total lymphocytes was relatively higher than the proportion of CD8+ T lymphocytes.[46] Moreover, in the present study, patients with a complete or intermediate tumor regression in operative specimen (ypT0ypN0, ypT1-4ypN0) displayed a significantly higher T helper cell count at baseline as compared to patients with poor response (ypT1- 4ypN+). In addition, patients with an intermediate response (ypT1- 4ypN0) revealed a significantly lower percentage of CD8+ cells compared to patients with poor response (Figure 15, Figure 16).

5.2 A low count of cytotoxic T cells, activation markers GranzymeB/perforin and PD1 expression at baseline correlate with an improved response to nCRT/CT

As stated before, in the present study, patients with a complete (ypT0ypN0) and partial response (ypT1-4ypN0) indicate a significantly lower number of circulating cytotoxic (CD8+) T cells at baseline as compared to patients with poor response (Figure 16). This is somehow unexpected, as CD8+ T lymphocytes are considered the major executing cellular component of the adaptive immune system and major fighters against malignant cells.[68,69] However, the sole number of circulating cells may not reflect their real anti-cancer activity due to the presence of inhibitory markers like checkpoint PD-1 molecule expression or their cytotoxic activation status as displayed by the expression of intracellular markers GranzymeB and perforin. Against this background, we further assayed the intracellular concentration of GranzymeB, the most abundant serine protease in humans[70] in CD8+ T cells. In contrast to patients with poor response (ypT1-4ypN+), patients with a favorable response (ypT0ypN0) displayed significantly decreased activation marker-positive cells at baseline (Figure 16), indicating, although in low numbers, an impaired activation of the cytotoxic T lymphocytes. In contrast to our findings, a recent study reported an increased number of CD8+/GranzymeB+ cytotoxic T cells in rectal cancer tissue to correlate with higher TRG and thus improved tumor response.[71] In addition, Huang et al. indicated the amount of GranzymeB to cover a signature of exhaustion in circulating T cells.[40] T cell exhaustion, a state of dysfunction when being exposed to a persistent antigen or inflammation, was first reported in cytotoxic T cells in chronic infection. It comes along with an upregulation of inhibitory checkpoint receptors, such as PD1.[72] Indeed, when assessing the impact of the PD1/PD-L1 signaling pathway resulting T cell anergy[73] in circulating CD8+ T lymphocytes, patients with a worse (ypT1-4ypN+) response revealed a significantly elevated percentage of this subpopulation as compared to patients with good or intermediate responses (Figure 16). Accordingly, one may speculate that these cells cover an anergic status to, e.g. prevent toxic side effects and anti-checkpoint therapy may increase the therapeutic effect in future clinical applications or treatment

regimens in rectal cancer. Supporting this notion, PD1 inhibition by antibody treatment is shown to result in a reversal into functional T cells.[74] Further, in a mouse model with chronically infected mice, PD1 blockage resulted in a quantitative and qualitative reinvigoration of cytotoxic T cell function with formerly exhausted cells to undergo substantial proliferation and expansion.[75] In conclusion, the detailed and exact impact of peripheral T helper and cytotoxic T lymphocytes remains elusive and has to be clarified in future investigations.

5.3 A decrease in B cell count correlates with intermediate and impaired response to nCRT/CT

As the second major cellular component of the adaptive immune response, B lymphocytes (characterized as CD19+ cells) were examined in the present study. Patients with intermediate (ypT1-4ypN0) and poor (ypT1-4ypN+) response indicated a significant decrease in the percentage of B cells, while patients with a complete response (ypT0ypN0) displayed more stable levels (Figure 18). Data on an involvement of B lymphocytes in colorectal cancer treatment response is rare in literature. Notably, a number of studies have documented the participation of T lymphocytes, but not B lymphocytes, in the radiation-induced antitumor immunity.[76,77] Supporting this statement, Tada et al. indicated the involvement of T helper lymphocytes, but not B cells, in the treatment response in rectal cancer.[64] In contrast to these reports, the findings in the present investigation favor the notion that antibody-dependent cellular cytotoxicity may contribute to advanced treatment response in the present cohort. This hypothesis, however, requires confirmation in an extended number of patients investigated.

5.4 An increase in peripheral blood monocyte count correlates with complete and intermediate response to nCRT/CT

When assessing patients with a complete (ypT0ypN0) and intermediate response (ypT1-4ypN0), a significant increase of monocyte (CD14+CD33+) count was detected from pre-treatment to pre-surgical samples (Figure 19). In contrast to these findings, Lee et al. reported the monocyte count to decrease during the initial two weeks of nCRT but is maintained or increased afterwards.

Moreover, monocyte counts after the initiation of nCRT were significantly lower in patients with pathologic complete response at two weeks after initiation of CRT but not at baseline.[46] Notably, as reported by Li et al., colon cancer patients with a low monocyte count in peripheral blood further showed an increased OS rate with decreased metastatic lesions.[78] In addition, an elevated peripheral blood pre-operative monocyte count was shown to be an independent risk factor for liver metastasis.[79] Finally, based on a meta-analysis, Wen et al. indicated an elevated monocyte count to be associated with worse OS, DFS and PFS in patients with rectal cancer.[80] In contrast to the data described above, our findings indicate a favorable clinical response in patients with higher counts of monocytes that may argue for a differential regulation of monocytes in the setting of the treatment schedule of the present study with a sequential application of induction chemotherapy and chemoradiotherapy.

5.5 Human leukocyte antigen (HLA-DR) molecule expression correlates with treatment response to nCRT/CT

HLA-DR is a major histocompatibility complex (MHC class II) cell surface receptor, which in combination with antigen peptides constitutes a ligand for the T cell receptor (TCR) for antigen-specific activation.[81] Our findings indicate an increase in the percentage of immune cells (CD45+) carrying surface HLA-DR proteins from baseline to pre-surgical specimens. For all treatment groups, these increased counts reached a level of significance (Figure 20). Finally, for monocytes positive for HLA-DR expression, significantly increased counts were demonstrated in complete responders (ypT0ypN0) compared to non-responders in pre-treatment samples, as well as a significant increase over the course of nCRT/CT was found in complete and intermediate (ypT1-4ypN0) responders (Figure 21). HLA-DR molecules present extracellular antigens to CD4+ T lymphocytes whereas CD8+ lymphocytes require HLA-ABC molecule activation.[57] Thus, an elevated HLA-DR expression suggests activation of the adaptive immune response and may be in line with the finding of an increased count of CD4+ T cells in peripheral blood correlating with an improved response and displays a further starting point for continuative clinical and experimental investigations.

In summary, lower numbers of cytotoxic T cells, monocytes and elevated levels of T helper cells in baseline predict a higher likelihood of an at least partial response and may be suitable as predictive markers for treatment response to nCRT/CT.

5.6 Predictive relevance of tissue resident immune cell contextures

Another major purpose of the present study was further to unravel a putative interrelationship between peripheral blood immune contexture and the tumor microenvironment expression. Densities of immune cell populations were investigated in paraffin-embedded tissue samples derived from pre-therapeutic biopsies and surgical tumor resection specimens of the same patients. In a multiparametric (Phenoptics^{TM}) immunohistochemical analysis of the corresponding tumor tissue and its microenvironment, we first observed no significant difference between good responders and poor responders concerning infiltration of total T lymphocyte count (CD3+) or their subsets CD4+ and CD8+ cells (Figure 23, Supplementary figure 6).

These findings differ from the data given in literature. For instance, Galon et al. and Anitei et al. reported CD3+ T cell infiltration to display an independent prognostic marker in colorectal tumors, with high cell counts to be associated with elevated DFS and OS.[37,82] In addition, Yasuda and colleagues demonstrated that the densities of CD3+ and CD8+ TILs were significantly associated with the histological grade after CRT, and the density of CD8+ TILs in tumor biopsies to be an independent prognostic factor for achieving a downstaging of the tumor or complete response after therapy.[83] A prognostic impact for TILs in primary and metastatic colorectal cancer was further confirmed in a meta-analysis showing high CD3+, CD8+ and FoxP3 densities to be associated with improved OS for primary colorectal cancer, and the level of CD8+ cells to display a significant predictor of good tumor regression grade after CRT in locally advanced rectal cancer.[84]

As there is evidence pointing TILs to be crucial in the anti-tumor response,[15] the lack of correlation in the present study may arise from the low number of patients included or from a heterogeneous distribution of T cells in the tumor

tissue resulting in non-representative biopsies. The latter may strongly influence the results when the number of subjects is small. Indeed, in the present study, a trend was observed in favor of a correlation between elevated levels of CD8+ T cells in patients with good response (Supplementary figure 6), indicating a need for including additional patients and multiple tissue samples in future analysis.

Cytotoxic T cells, the major executive compartment of the adaptive immune system, exert their tumor cell killing activity by a variety of mechanisms including the release of cytolytic substances such as GranzymeB from intracellular granula.[85] In the present investigation, comparing biopsy and surgical resection specimen, patients with a complete response to nCRT/CT revealed a significant increase in the GranzymeB+ cell density in tumor tissue, while a trend was observed in patients with intermediate response (Figure 29). As opposed to the data for infiltrating T cells, this finding in our analysis is supported in the literature. Galon et al. also reported a higher GranzymeB infiltration to be associated with improved OS.[37] GranzymeB is a cytolytic protein enabling the cleavage of proteins linked to DNA fragmentation and cell death, conclusively resulting in tumor cell apoptosis.[85] This capability may cover an explanation why patients with an increase in their GranzymeB levels revealed a better tumor response following nCRT/CT. Moreover, as our patient cohort did not indicate an increase in their TILs, it seems reasonable that the favorable response to CRT in the context of GranzymeB expression is mediated by tissue resident activated lymphocytes finally resulting in a tumor destruction and a favorable response to nCRT/CT.

5.7 Tissue neutrophil count decreases in patients with good response to nCRT/CT

Human neutrophils (CD15+), initially recognized as key effectors in the first-line host defense against invading pathogens, are the most abundant subpopulation of leukocytes.[86] While a multitude of reports exist on the relevance of a neutrophil to lymphocyte ratio in peripheral blood parameters for treatment response or prognosis,[87,88] less data is available on the prognostic/predictive impact of tumor-associated neutrophils (TANs). Some reports indicate elevated levels of TANs to associate with improved OS in patients with stage II colorectal

cancer and to display a favorable prognostic factor in early stages of colon cancer.[89,90] On the contrary, other groups report increased intratumoral neutrophils to closely correlate with a malignant phenotype and to predict patients' adverse prognosis in colorectal carcinomas.[91] In favor of the latter reports, in the present study, patients with a complete response (ypT0ypN0) displayed a decrease in the amount of infiltrating neutrophils as the immunoscore of CD15+ cells was significantly higher in patients' biopsies as compared to post-nCRT/CT surgical specimen, while no significant change was observed in patients with a partial (ypT1-4ypN0) or poor response (ypT1-4ypN+, Figure 26). A possible explanation for the differing findings in the literature could be the ability of neutrophils to develop a polarization, leading to different functions in cancer development.[44] To further analyze the findings in this trial, future evaluations of additional polarization markers could be useful.

5.8 Elevated tissue levels of natural killer (NK) cells correlate with good and intermediate response

NK cells cover cytotoxic lymphocytes of the innate immune system and act as the body's first line of defense against tumor cells.[92] In the present patient cohort, an increase of NK cell (CD56+) density was observed between pre-therapeutic biopsies and tumor resection specimens, reaching levels of significance for complete and partial responses (Figure 27). This data is in concordance with a recent report by Alderdice and colleagues. By analyzing therapy related transcriptional alterations applying high-throughput gene expression profiling in 40 pairs of paraffin-embedded rectal cancer biopsies and matched resection specimens, the group reported an NK-like signature observed post therapy. Moreover, a NK cell population as assayed by immunohistochemistry was shown to be significantly higher in patients with TRG grade 3 compared with TRG grade 1-2 and correlated with increased OS.[93] Also, Sconocchia et al. observed that enrichment of both, NK and CD8+ T cells, improved the clinical outcome for colorectal cancer patients.[94]

5.9 Increase in tumor infiltrating macrophages correlates with an intermediate response to nCRT/CT

Macrophage (CD68) percentage increases when being assessed in pre-therapeutic biopsies and corresponding post-nCRT/CT surgery specimens, reaching a level of significance in the intermediate (ypT1-4ypN0) response cohort (Figure 28). In the majority of tumor entities analyzed, a high density of tumor-associated macrophages (TAMs) correlated with a poor prognosis.[95,96] Nevertheless, the role of macrophages in colorectal cancer is discussed controversially.[97] On one hand, there is evidence, that a high macrophage infiltration occurs more often in patients with negative lymph nodes, whereas a low macrophage count is often linked to an advanced tumor invasion.[98] Other reports, on the other hand, revealed an improved survival[99] as well as a TNM downsizing and a reduced number of hepatic metastasis in patients with a high macrophage invasion at the tumor front.[100] One possible explanation for those controversial findings may cover the presence and differentiation in M1 and M2 macrophage subpopulations.[101] The M1 subtype presents a classic subtype

activated by damage-associated molecular patterns (DAMP) mounting an anti-tumor response. M2 macrophages, by contrast, are activated alternatively by proinflammatory cytokines released from cancer cells. This subtype is associated with tumor progression.[102] TAMs show, depending on signals from the tumor and its microenvironment, either a M1 or M2 dominant polarization.[103]

Finally, we aimed to clarify whether circulating lymphocyte densities may reflect local immunological responses and, if so, to identify the subset of lymphocytes mostly involved, that may serve as potential predictors of the pathological nCRT/CT response. For all immune subpopulations, monocytes/macrophages, T cells and their subsets CD4+ T helper cells and CD8+ cytotoxic T cells, we did not observe a 1:1 tumor-blood correlation. Thus, elevated levels in peripheral blood do not reflect a high level of tissue expression of the markers and vice versa. In concordance with the results of the present study, Milne et al. have reported that the lymphocyte count in peripheral blood did not correlate with CD8+ or CD20+ TIL density in patients with ovarian cancer and both, lymphocyte count and TILs, significantly correlated with prognosis, although the correlations were independent from each other.[104]

5.10 Limitations and validity of the study

The significance of the study presented is limited primarily by the small number of 22 patients included. However, the study is considered representative for a broader cohort of patients due to different reasons. First, the clinical/histopathological characteristics of the patient group, with 14 males (63,6%) and 8 females (36,4%) and a median age of 67 years is comparable to the data from the German cancer registry published by the Robert Koch Institute with 55% males and a median age of 72-76 years.[105] Second, therapy response in our relatively small cohort of patients is comparable to the results published from the phase-2-CAO/ARO/AIO-12 trial, including a number of 311 patients. In this study, a complete regression (ypT0ypN0) was reported in 17% of the patients in treatment regimen A and in 25% in treatment regimen B resulting in a total response rate of 20.9%.[8] In the present study, a percentage of 22,7% complete remission was observed, indicating inclusion of a representative sample of patients with good response. Third, histopathological

results are similar to a recent meta-analysis on 28 studies with 3579 patients treated with oxaliplatin-based chemotherapy, radiation doses of 50,4 Gy plus induction chemotherapy. Data given in this analysis indicate a total complete remission in 22,4% of patients,[106] which is comparable to our findings. A further limitation covers the partly manual and subjective assessment of the immunohistochemical staining that may result a bias evaluation. To counteract this constriction, however, two individual observers reaching final common results, performed evaluation. Finally, our prospective analysis focused on early treatment response but due to short follow-up time in the prospective study, does not include analysis in clinical response including local recurrences, metastasis, and patients' survival. Although, tumor regression grading covers an individual level surrogate for DFS in patients with rectal cancer,[10] correlating the peripheral blood and tissue immune contexture with clinical endpoints OS, DFS and metastases-free-survival would further increase the significance and validity of the present study.

5.11 Conclusion

Neoadjuvant CRT has become a standard procedure to treat locally advanced rectal cancer prior to surgery, markers to predict the response to CRT, however, still remain elusive. Our prospective study raises the following issues. First, peripheral lymphocytes seem to play a crucial role in the CRT-mediated systemic anticancer immunological response. Second, among the various lymphocyte subsets, T lymphocytes and monocytes seem to play a central role in the immunological response. By this, baseline blood phenotyping revealed a lymphocyte distribution with high T helper cell levels and low cytotoxic T cell levels to be associated with good response to nCRT/CT in our patient's cohort. To validate and expand these findings, a continuation of the analysis is necessary. Indeed, an expansion of the prospective analysis cohort in a translational program of a current CAO/ARO/AIO-16 trial and validation of immune profile data in primary tumor using two further retrospective patient cohorts is currently ongoing as a follow-up study performed at the Department of Radiotherapy and Oncology, University Hospital in Frankfurt. In addition, a detailed insight on the role of peripheral blood T cells and monocytes and their activation status is desirable. In a follow-up trial, soluble activation

markers/cytokines should be assayed, differencing activated from resting or exhausted lymphocytes.

6 Summary

Treatment response to neoadjuvant chemoradiotherapy (nCRT) varies considerably among individual patients in advanced rectal cancer indicating a clinical need for markers to predict treatment efficacy and to stratify patients for future personalized treatment. In recent years, there is a tremendous evidence on a pivotal impact of immune components on the development/pathogenesis of cancer and on mediating response to radiation and chemotherapy. Moreover, liquid biopsy biomarkers have become increasingly attractive to predict treatment response because they are easy to collect, reflect information on different aspects of tumor biology and can be accurately measured by standardized methods.

This study aimed to investigate the peripheral blood and tumor tissue immune cell contexture in patients with rectal adenocarcinoma treated with nCRT and chemotherapy (CT) within a prospective randomized phase II CAO-ARO-AIO-12 trial, conducted in the context of DKTK (Deutsches Konsortium für translationale Krebsforschung) and FCI (Frankfurt Cancer Institute), to address the questions whether peripheral blood and/or primary tumor immune contexture predict for treatment response, were modulated by nCRT/CT and correlated with each other. By this, immune cell components were assayed by flow cytometry from peripheral blood mononuclear cells (PBMCs) at baseline, day 43, and pre-surgery of 22 patients treated with nCRT/CT and subsequently correlated with pathologic treatment response. Immunophenotyping was performed applying different staining panels covering myeloid immune cells and human leukocyte antigen (HLA) molecules, T lymphocyte subpopulations and programmed cell death (PD)-1 protein expression and regulatory T cells (Tregs). In addition, tumor tissue samples from pre-therapeutic biopsies and surgical specimens were analyzed by immunohistochemistry and multiparametric immunofluorescence.

The present prospective study raised the following issues. First, peripheral lymphocytes seem to play a crucial role in the nCRT/CT mediated systemic anticancer immunological response. Second, among the various lymphocyte subsets, peripheral blood, but not tissue resident T lymphocytes seem to play a

central role in predicting treatment response. By this, baseline blood phenotyping revealed a lymphocyte distribution with high numbers of (CD3+CD4+) T helper cells and low numbers of (CD3+CD8+) cytotoxic T cells expressing PD1, activation markers GranzymeB, perforin and HLA-DR to be associated with an improved response (ypT0ypN0) to nCRT/CT in the patient's cohort investigated. Further, a decrease in B lymphocyte (CD3+CD19+) count correlated with intermediate and impaired response while an elevated monocyte (CD14+CD33+) levels predicted a complete and intermediate (ypT1-4ypN0) response to nCRT/CT. On a tissue level, patients with a complete response displayed a decrease in the amount of infiltrating neutrophils as the immunoscore of CD15+ cells was significantly higher in patients' biopsies compared to post-nCRT/CT surgical specimen, while in both, patients with complete and intermediate response an increase of natural killer (CD56+) cell density and GranzymeB expression was observed. Finally, no significant correlation was observed between peripheral blood and tissue immune marker expression.

To validate and expand these findings, a continuation of the analysis in an extended patient cohort is necessary. In addition, a detailed insight on the role of peripheral blood T cells and monocytes and their activation status is desirable. Further, in a follow-up trial, soluble activation markers/cytokines should be assayed, further distinguishing activated from resting or exhausted lymphocytes.

7 Zusammenfassung

Das Ansprechen auf eine neoadjuvante Chemoradiotherapie (nCRT) variiert erheblich bei Patienten mit fortgeschrittenem Rektumkarzinom. Es ist deshalb von hoher klinischer Relevanz, Marker zu etablieren, welche eine Voraussage der Behandlungseffizienz und eine Stratifizierung von Patienten für eine künftige personalisierte Behandlung ermöglichen. In den letzten Jahren mehren sich dabei die Hinweise auf eine zentrale Bedeutung von Immunkomponenten und des Immunsystems bei der Entwicklung/Pathogenese von Krebs und bei der Vermittlung des Ansprechens auf eine Strahlen- und Chemotherapie. Darüber hinaus werden Biomarker aus Blutproben zur Vorhersage des Behandlungserfolgs immer attraktiver, da sie leicht zu gewinnen sind, Informationen über verschiedene Aspekte der Tumorbiologie widerspiegeln und mit standardisierten Methoden exakt gemessen werden können.

Ziel der Studie war es, die Immunzellkontextur im peripheren Blut sowie im Tumorgewebe von Patienten mit rektalem Adenokarzinomen, welche im Rahmen einer prospektiven, randomisierten Phase-II-Studie (CAO-ARO-AIO-12) in Zusammenarbeit mit dem DKTK (Deutsches Konsortium für translationale Krebsforschung) und dem FCI (Frankfurt Cancer Institute) mit einer nCRT und Chemotherapie (CT) behandelt wurden, zu untersuchen. Dabei wurden analysiert, ob und in welchem Umfang die Immunkontextur im peripheren Blut und/oder im Primärtumor das Ansprechen auf die Behandlung voraussagt, durch nCRT/CT moduliert wird und ob Blut- und Gewebeexpression miteinander korrelieren. Zu diesem Zweck wurden Immunzellkomponenten mittels Durchflusszytometrie von mononukleären Zellen des peripheren Blutes (PBMCs) zu Studienbeginn, am Tag 43 und vor der Operation bei 22 mit nCRT/CT behandelten Patienten untersucht und anschließend mit dem pathologischen Ansprechen auf die Behandlung korreliert. Für die Immunphänotypisierung wurden verschiedene Färbepanels verwendet, die myeloide Immunzellen und humane Leukozytenantigene (HLA), T-Lymphozyten-Subpopulationen und die Expression des Proteins PD-1 sowie regulatorische T-Zellen (Tregs) abdeckten. Darüber hinaus wurden Tumorgewebeproben aus prä- therapeutischen Biopsien und chirurgischen

Präparaten mittels Immunhistochemie und multiparametrischer Immunfluoreszenz analysiert.

Die Ergebnisse der vorliegenden prospektiven Studie lasen sich folgendermaßen zusammenfassen. Erstens scheinen periphere Lymphozyten eine entscheidende Rolle bei der nCRT/CT-vermittelten systemischen immunologischen Reaktion gegen Rektumtumoren zu spielen. Zweitens spielen unter den verschiedenen Lymphozyten-Subpopulationen die T-Lymphozyten im peripheren Blut, nicht aber gewebeständige T-Zellen, eine zentrale Rolle bei der Vorhersage des Ansprechens auf die Behandlung. So ergab die Phänotypisierung von prätherapeutischen Blutproben, dass eine Lymphozytenverteilung mit einem hohen Anteil an (CD3+CD4+) T-Helferzellen und einem geringen Anteil an (CD3+CD8+) zytotoxischen T-Zellen, die PD1, die Aktivierungsmarker GranzymeB, Perforin und HLA-DR exprimierten, in dem untersuchten Patientenkollektiv mit einem verbesserten Ansprechen (ypT0ypN0) auf die nCRT/CT assoziiert waren. Darüber hinaus korreliert eine Abnahme der B-Lymphozytenzahl (CD3+CD19+) mit einem intermediären- und schlechten Ansprechen, während erhöhte Monozyten (CD14+CD33+) ein vollständiges und intermediäres (ypT1-4ypN0) Ansprechen nach nCRT/CT vorhersagten. Auf Gewebeebene zeigte sich bei Patienten mit komplettem Ansprechen eine Abnahme der Dichte an infiltrierenden Neutrophilen, da der Immunoscore von CD15+-Zellen in den Biopsien der Patienten im Vergleich zu den chirurgischen Resektaten signifikant erhöht war. Zudem konnte bei Patienten mit komplettem und intermediärem Ansprechen eine Zunahme der Dichte natürlicher Killerzellen (CD56+) und der Leukozyten GranzymeB-Expression beobachtet werden. Schließlich wurde keine signifikante Korrelation zwischen der Expression von Immunmarkern im peripheren Blut und im Gewebe festgestellt.

Um diese Ergebnisse zu validieren ist eine Fortsetzung der Analyse in einer erweiterten Patientenkohorte erforderlich. Darüber hinaus ist ein detaillierter Einblick in die Rolle der T-Lymphozyten und Monozyten im peripheren Blut und deren Aktivierungsstatus wünschenswert. Außerdem sollten in einer Folgestudie zusätzliche Aktivierungsmarker/Zytokine untersucht werden, um aktivierte von ruhenden oder erschöpften Lymphozyten zu differenzieren.

8 Appendix

8.1 Appendix 1 – Reagents used

Reagent	Company	Reference number
Biocoll Separing Solution	Biochrom	L6115
Phosphate Buffered Saline (PBS)	Gibco	14190250
FCS	Thermo Fischer	
Trypan blue staining	Gibco	15250061
Hu FcR Binding Inhibitor Purified	eBioscience	14-9161-73
Fix & Perm (A&B)	Nordic Mubio	GAS-002A-1 GAS-002B-1
FoxP3 staining set (FoxP3 clone 236A/E7; Fixation/Permeabilization Concentrate and Diulent; Normal Mouse Serum; Permeabilization Buffer)[1]	Affymetrix, Invitrogen	77-5774
Viability Dye Stain 620	BD Horizon	564996
BD FACS Lysing Solution	BD Biosciences	349202
RPMI Med. 1640 (1x)	Gibco	72400-021
Glutamax	Gibco	35050-038
Sodium Pyruvate 100mM (100x)	Gibco	11360-039
Human AB Serum	Gibco	10270-106
DMSO (dimethyl sulfoxide for cell culture)	Applichem	A3672,0250

[1] All components can be ordered separately.

Cyto Flex Daily QC Fluorophores	Beckman Coulter	B53230
VersaComp Antibody Capture Bead Kit	Beckman Coulter	B22840
DNeasy Blood and Tissue Kit (250)	Qiagen	69506
Trilogy™	Cell Marque	920P-06

8.2 Appendix 2 – Antibodies

Antibody	Clone	Company	Flourophore	Reference number
HLA-DR	L243	BD Bioscience	V450	655874
CD45	2D1	BD Bioscience	V500	655873
CD33	P67.6	BD Bioscience	APC	345800
CD19	SJ25C1	BD Bioscience	PeCy7; PC7	341113
CD14	MφP9	BD Bioscience	APC-H7	641394
CD15	MMA	BD Bioscience	FITC	332778
CD11b	D12	BD Bioscience	PE	333142
CD3	SK7	BD Bioscience	PerCP-Cy5,5	332771
CD4	SK3	BD Bioscience	V450	651849
CD8	SK1	BD Bioscience	APC-H7	641400
CD25	2A3	BD Bioscience	BV510	740198
PD1 (CD279)	eBioJ105	eBioscience	PeCy7; PC7	25-2799-42
Perforin	dG9	BD Bioscience	FITC	556577
Granzyme B	GB11	BD Bioscience	PE	561142
FoxP3	236A/E7	eBioscience	APC	17-4777-42
FoxP3[2]	PCH101	eBioscience	APC	17-4776-42

[2] FoxP3 clone PCH101 was only used in the time of 02/13/2017 – 04/12/2017 (13.02.2017 – 12.04.2017). Before and after, FoxP3 clone 236A/E7 was used.

8.3 Appendix 3 – Isotype controls

Isotype control	Replaced antibody	Clone	Company	Flouro-phore	Reference number
Mouse IgG2a, κ Isotype Control	HLA-DR V450	MOPC-173	BD Horizon	V450	560882
Mouse IgG1, κ Isotype Control	CD45 V500	X40	BD Horizon	V500	560787
Mouse IgG1, κ Isotype Control	CD33 APC	MOPC-21	BD Horizon	APC	550854
Mouse IgG2b, κ Isotype Control	CD14 APC-H7	27-35	BD Horizon	APC-H7	560183
Mouse IgG1, κ Isotype Control	CD3 PerCP-Cy5.5	X40	BD Horizon	PerCP-Cy5.5	347202
Mouse IgG1, κ Isotype Control	CD19 PE-Cy7	X40	BD Horizon	PE-Cy7	347202
Mouse IgM, κ Isotype Control	CD15 FITC	G155-228	BD Horizon	FITC	551448
Mouse IgG2a, κ Isotype Control	CD11b PE	G155-178	BD Horizon	PE	554648
Mouse IgG1	CD56 BV650	X40	BD Horizon	BV 650	563231
Mouse IgG1, κ Isotype Control	CD4 V450	X40	BD Horizon	V450	561504
Mouse IgG1, κ Isotype Control	CD8 APC-H7	X40	BD Horizon	APC-H7	561427
Mouse IgG1, κ Isotype Control	CD25 V500	X40	BD Horizon	BV510	562946
Mouse IgG1, κ Isotype Control	PD1 PE-Cy7	P3.6.2.8.1	eBioscience	PE-Cy7	25-4714

Mouse-IgG1, κ Isotype Control	GranzB PE	MOPC 21	BD Horizon	PE	555749
Mouse IgG2b, κ Isotype Control	Perforin FITC	27-35	BD Horizon	FITC	51-66374X-2
Mouse IgG1, κ Isotype Control	FoxP3 clone 236A/E7, APC	P3.6.2.8.1	eBioscience	APC	17-4714
Rat IgG2a, κ Isotype Control	FoxP3 clone PCH101, APC	eBR2a	eBioscience	APC	17-4321

9 Supplementary Tables

9.1 Supplementary Table 1: Cell Types and correlation with TRG Status in surgery specimen

Marker	Day of testing	Significance level TRG 1+2 vs. 3+4
Pan-leukocytes (CD45)	d1	0,375
	pre-surgery	0,076
Monocytes (CD45+CD33+CD14+)	d1	0,375
	pre-surgery	1
T cells (CD45+CD3+)	d1	0,076
	pre-surgery	0,076
B cells (CD45+CD19+)	d1	1
	pre-surgery	0,375
cytotoxic T cells (CD3+CD8+CD4-)	d1	0,076
	pre-surgery	0,375
T helper cells (CD3+CD4+CD8-)	d1	0,375
	pre-surgery	1
T helper cells positive for PD1 (CD3+CD4+PD1+)	d1	1
	pre-surgery	0,076
cytotoxic T cells positive for PD1 (CD3+CD8+PD1+)	d1	0,076
	d43	0,049
	pre-surgery	1
cytotoxic T cells carrying GranzymeB (CD3+CD8+GranzB+)	d1	0,375
	pre-surgery	1
cytotoxic T cells carrying Perforin (CD3+CD8+Perforin+)	d1	0,375
	pre-surgery	1
cytotoxic T cells carrying Granzyme B and Perforin (CD3+CD8+GranzB+Perforin+)	d1	0,375
	pre-surgery	0,375
	d1	1

T helper cells positive for CD25 (CD3+CD4+CD25+)	pre-surgery	0,375
regulatory T cells (CD3+CD4+CD25+FoxP3+)	d1	0,076
	pre-surgery	1
CD4/CD8 Ratio	d1	0,076
	pre-surgery	1
MMDSC	d1	0,375
	pre-surgery	0,375
eMDSC	d1	0,076
	pre-surgery	0,375
PNM MDSC	d1	0,375
	pre-surgery	1

Supplementary Table 1 – Markers from FACS peripheral blood staining correlated with TRG status in surgery specimen. Compared were TRG 1+2 with TRG 3+4. Statistical method was Pearson's Chi Squared Test. P values marked in bold are significant (P<0,05).

9.2 Supplementary Table 2: Cell Types and Correlation with lymph node Status in surgery specimen

Marker	Day of testing	Significance level ypN0 vs. ypN+
Pan-leukocytes (CD45)	d1	1
	pre-surgery	0,269
Monocytes (CD45+CD33+CD14+)	d1	0,027
	pre-surgery	0,269
T cells (CD45+CD3+)	d1	0,269
	pre-surgery	0,269
B cells (CD45+CD19+)	d1	0,269
	pre-surgery	0,269
cytotoxic T cells (CD3+CD8+CD4-)	d1	0,027
	pre-surgery	0,269
T helper cells (CD3+CD4+CD8-)	d1	0,027
	pre-surgery	0,027
T helper cells positive for PD1 (CD3+CD4+PD1+)	d1	0,269
	pre-surgery	0,027
cytotoxic T cells positive for PD1 (CD3+CD8+PD1+)	d1	0,027
	pre-surgery	0,269
cytotoxic T cells carrying GranzymeB (CD3+CD8+GranzB+)	d1	1
	pre-surgery	1
cytotoxic T cells carrying Perforin (CD3+CD8+Perforin+)	d1	1
	pre-surgery	1
cytotoxic T cells carrying Granzyme B and Perforin (CD3+CD8+GranzB+Perforin+)	d1	0,027
	pre-surgery	1
T helper cells positive for CD25 (CD3+CD4+CD25+)	d1	1
	pre-surgery	0,269
	d1	1

regulatory T cells (CD3+CD4+CD25+FoxP3+)	pre-surgery	1
CD4/CD8 Ratio	d1	0,027
	pre-surgery	0,027
MMDSC	d1	0,269
	pre-surgery	0,027
eMDSC	d1	1
	pre-surgery	0,269
PNM MDSC	d1	1
	pre-surgery	0,269

Supplementary Table 2 – Markers from FACS peripheral blood staining correlated with lymph node status in surgery specimen. Compared were ypN0 with ypN+. Statistical method was Pearson's Chi Squared Test. P values marked in bold are significant (P<0,05).

9.3 Supplementary Table 3: Cell Types and correlation with TNM Status in Surgery Specimen

Marker	Day of testing	Significance level ypT0 N0 vs. ypT1-4 N0 vs. ypT1-4 N+
Pan-leukocytes (CD45)	d1	0,871
	pre-surgery	0,388
Monocytes (CD45+CD33+CD14+)	*d1*	*0,053*
	pre-surgery	0,388
T cells (CD45+CD3+)	d1	0,388
	pre-surgery	0,528
B cells (CD45+CD19+)	d1	0,528
	pre-surgery	*0,094*
cytotoxic T cells (CD3+CD8+CD4-)	*d1*	*0,087*
	pre-surgery	0,388
T helper cells (CD3+CD4+CD8-)	*d1*	*0,087*
	pre-surgery	0,047
T helper cells positive for PD1 (CD3+CD4+PD1+)	d1	0,528
	pre-surgery	*0,087*
cytotoxic T cells positive for PD1 (CD3+CD8+PD1+)	*d1*	*0,087*
	pre-surgery	0,528
cytotoxic T cells carrying GranzymeB (CD3+CD8+GranzB+)	d1	0,871
	pre-surgery	0,288
cytotoxic T cells carrying Perforin (CD3+CD8+Perforin+)	d1	0,871
	pre-surgery	0,288
cytotoxic T cells carrying Granzyme B and Perforin (CD3+CD8+GranzB+Perforin+)	*d1*	*0,087*
	pre-surgery	0,871
T helper cells positive for CD25 (CD3+CD4+CD25+)	d1	0,288
	pre-surgery	0,388
	d1	0,288

regulatory T cells (CD3+CD4+CD25+FoxP3+)	pre-surgery	0,871
CD4/CD8 Ratio	*d1*	*0,087*
	pre-surgery	0,047
MMDSC	d1	0,388
	pre-surgery	*0,053*
eMDSC	d1	0,871
	pre-surgery	*0,094*
PNM MDSC	d1	0,871
	pre-surgery	0,388

Supplementary Table 3 - Markers from FACS peripheral blood staining correlated with TNM status in surgery specimen. Compared were ypT0N0 with ypT1-4N0 and ypT1-4N+. Statistical method was Pearson's Chi Squared Test. P values marked in bold are significant (P<0,05).

10 Supplementary figures

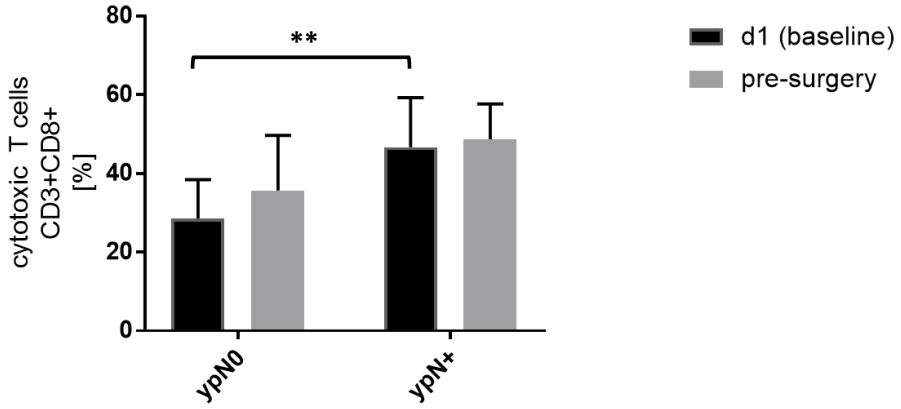

*Supplementary figure 1 - Percentage of cytotoxic T lymphocytes (CD8+) based on CD3+ T cells at baseline (d1) and before surgical resection as analyzed by FACS phenotyping. Shown are mean values with standard deviation. Significance testing was performed using a two-sided T-test. ** equals p < 0,005.*

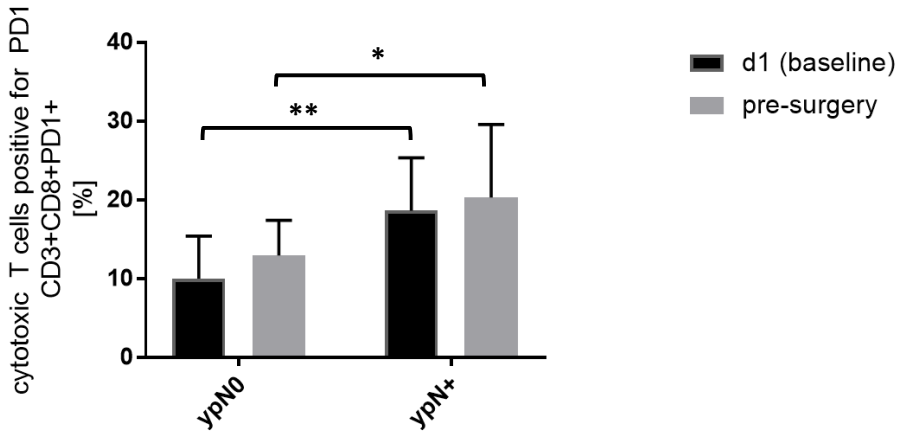

*Supplementary figure 2 - Percentage of cytotoxic T lymphocytes (CD8+) positive for PD1 based on CD3+ T cells at baseline (d1) and before surgical resection as analyzed by FACS phenotyping. Shown are mean values with standard deviation. Significance testing was performed using a two-sided T-test. ** equals p < 0,005.*

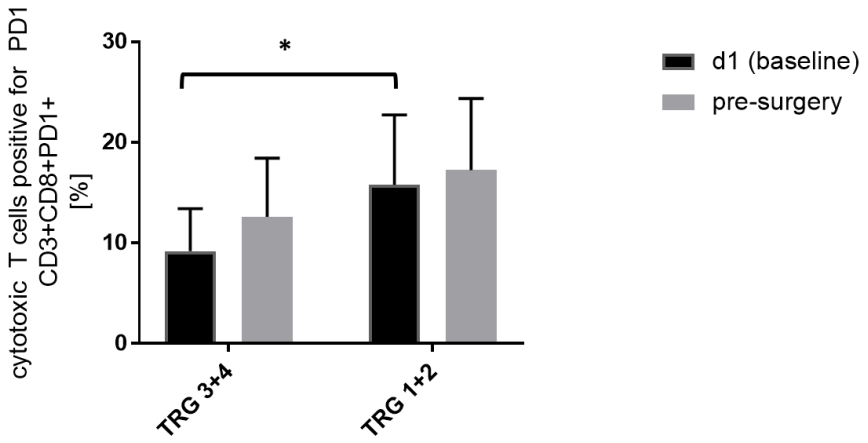

*Supplementary figure 3 - Percentage of cytotoxic T lymphocytes (CD8+) positive for PD1 based on CD3+ T cells at baseline (d1) and before surgical resection as analyzed by FACS phenotyping. Shown are mean values with standard deviation. Significance testing was performed using a two-sided T-test. * equals p < 0,05.*

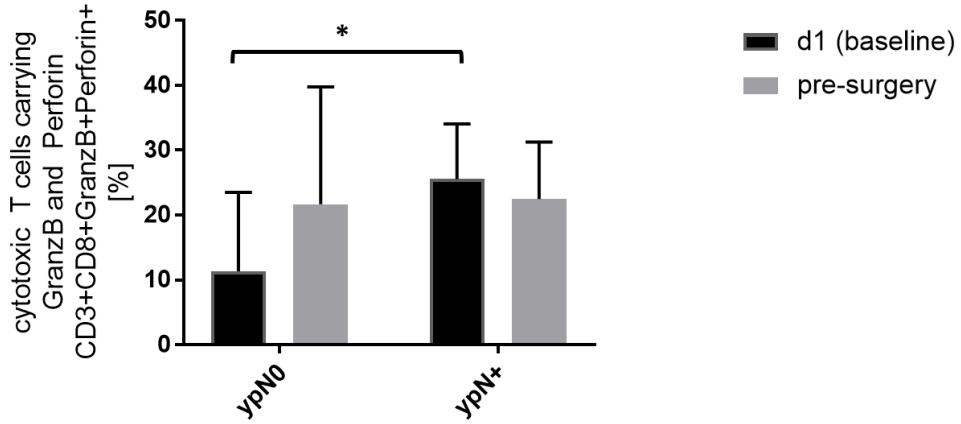

*Supplementary figure 4 - Percentage of cytotoxic T lymphocytes (CD8+) carrying activation markers GranzymeB and perforin based on CD3+ T cells at baseline (d1) and before surgical resection as analyzed by FACS phenotyping. Shown are mean values with standard deviation. Significance testing was performed using a two-sided T-test. * equals p < 0,05.*

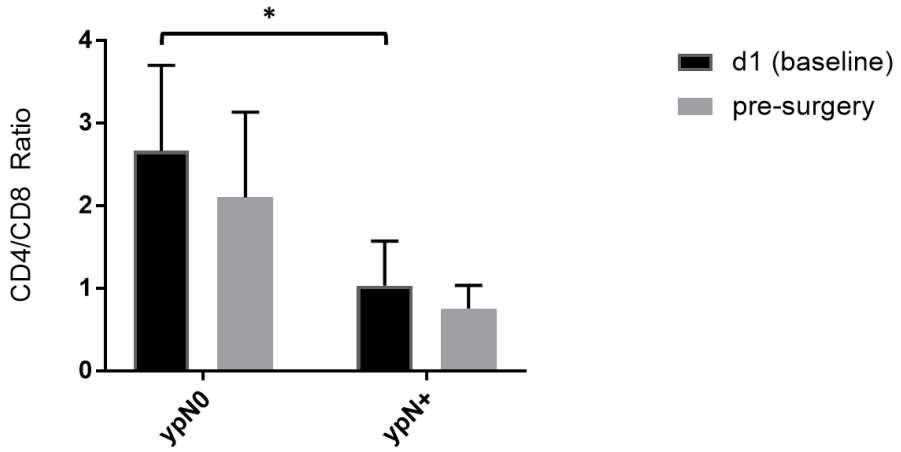

*Supplementary figure 5 – Ratio of CD4 and CD8 expressing T lymphocytes (CD4/CD8 ratio) at baseline (d1) and before surgical resection as analyzed by FACS phenotyping. Shown are mean values with standard deviation. Significance testing was performed using a two-sided T-test. * equals p < 0,05.*

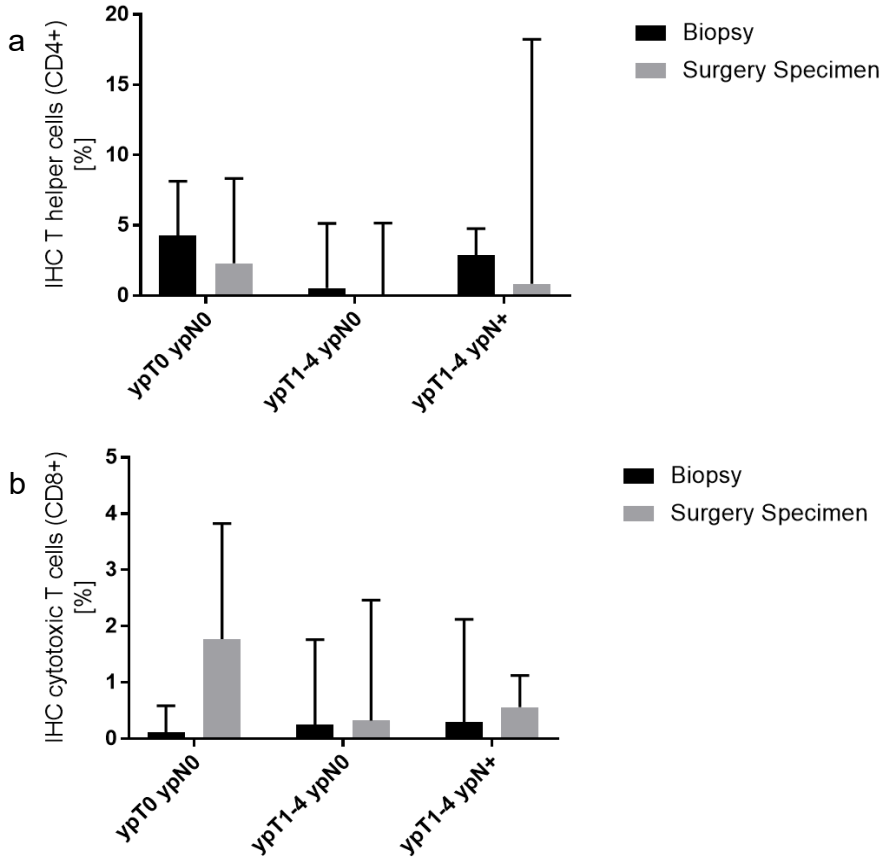

Supplementary figure 6 – Percentage of tumor infiltrating CD4+ T helper cells (a) and CD8+ cytotoxic T cells (b) in pretreatment biopsies and surgical resection specimens as analyzed by multiparametric Phenoptics™ immunofluorescence staining. Shown are median values with standard deviation. Significance testing was performed using a two-sided T-Test.

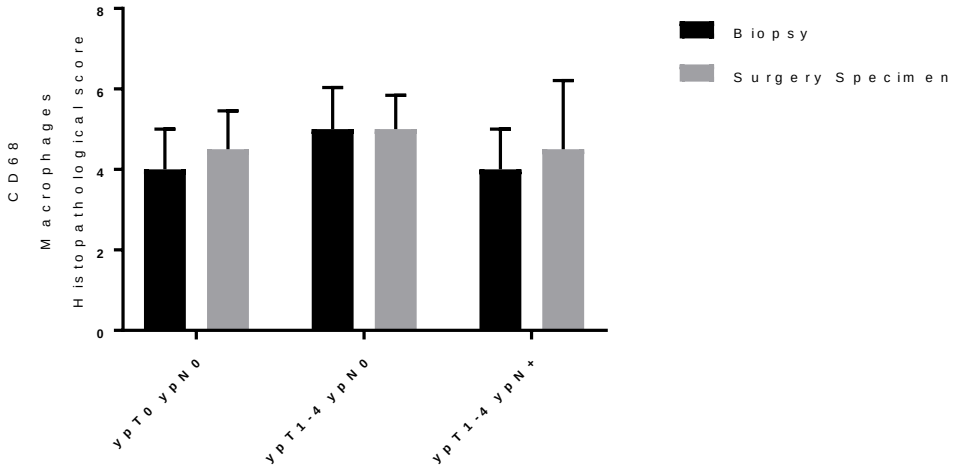

Supplementary figure 7 – Immunodetection (immunoscore) of macrophages (CD68) in pre-treatment biopsies and surgical resection specimens as analyzed by immunohistochemical staining. Shown are median values with standard deviation. Significance testing pas performed using a two-sided T-Test.

11 References

1. Bray F, Ferlay J, Soerjomataram I, Siegel RL, Torre LA, Jemal A. Global cancer statistics 2018: GLOBOCAN estimates of incidence and mortality worldwide for 36 cancers in 185 countries. *CA Cancer J Clin*. 2018;68(6):394-424. doi:10.3322/caac.21492.
2. Magalhães B, Peleteiro B, Lunet N. Dietary patterns and colorectal cancer: systematic review and meta-analysis. *Eur J Cancer Prev*. 2012;21(1):15-23. doi:10.1097/CEJ.0b013e3283472241.
3. Herold G, ed. *Innere Medizin 2018: Eine vorlesungsorientierte Darstellung unter Berücksichtigung des Gegenstandskataloges für die Ärztliche Prüfung mit ICD 10-Schlüssel im Text und Stichwortverzeichnis*. Köln: Gerd Herold; 2018.
4. Wittekind C, Meyer H-J. *TNM-Klassifikation maligner Tumoren.* Weinheim Wiley-Blackwell; 2012. 1. Aufl. s.l.: Wiley-VCH; 2012. https://ebookcentral.proquest.com/lib/senc/detail.action?docID=1162078. Accessed January 1, 2021.
5. European Society for Medical Oncology. Clinical Practice Guidelines Slideset Rectal Cancer. esmo.org/Guidelines/Gastrointestinal-Cancers/Rectal-Cancer. Accessed January 24, 2021.
6. Sauer R, Liersch T, Merkel S, et al. Preoperative versus postoperative chemoradiotherapy for locally advanced rectal cancer: results of the German CAO/ARO/AIO-94 randomized phase III trial after a median follow-up of 11 years. *J Clin Oncol*. 2012;30(16):1926-1933. doi:10.1200/JCO.2011.40.1836.
7. Rödel C, Graeven U, Fietkau R, et al. Oxaliplatin added to fluorouracil-based preoperative chemoradiotherapy and postoperative chemotherapy of locally advanced rectal cancer (the German CAO/ARO/AIO-04 study): final results of the multicentre, open-label, randomised, phase 3 trial. *Lancet Oncol*. 2015;16(8):979-989. doi:10.1016/S1470-2045(15)00159-X.
8. Fokas E, Allgäuer M, Polat B, et al. Randomized Phase II Trial of Chemoradiotherapy Plus Induction or Consolidation Chemotherapy as Total Neoadjuvant Therapy for Locally Advanced Rectal Cancer: CAO/ARO/AIO-12. *J Clin Oncol.* 2019;37(34):3212-3222. doi: 10.1200/JCO.19.00308.

9. Dworak O, Keilholz L, Hoffmann A. Pathological features of rectal cancer after preoperative radiochemotherapy. *Int J Colorectal Dis*. 1997;12(1):19-23. doi:10.1007/s003840050072.
10. Fokas E, Ströbel P, Fietkau R, et al. Tumor Regression Grading After Preoperative Chemoradiotherapy as a Prognostic Factor and Individual-Level Surrogate for Disease-Free Survival in Rectal Cancer. *J Natl Cancer Inst*. 2017;109(12). doi:10.1093/jnci/djx095.
11. Fokas E, Liersch T, Fietkau R, et al. Tumor regression grading after preoperative chemoradiotherapy for locally advanced rectal carcinoma revisited: updated results of the CAO/ARO/AIO-94 trial. *J Clin Oncol*. 2014;32(15):1554-1562. doi:10.1200/JCO.2013.54.3769.
12. Wang J-J, Lei K-F, Han F. Tumor microenvironment: recent advances in various cancer treatments. *Eur Rev Med Pharmacol Sci*. 2018;22(12):3855-3864. doi:10.26355/eurrev_201806_15270.
13. Hanahan D, Weinberg RA. The Hallmarks of Cancer. *Cell*. 2000;100(1):57-70. doi:10.1016/s0092-8674(00)81683-9.
14. Niesel KA. *The influence of radio-immunotherapy on the tumor microenvironment of breast-to-brain metastasis and the investigation of novel adjuvant therapies*. [Dissertation]. Darmstadt: Technische Universität, Deutschland; 2021.
15. Hanahan D, Weinberg RA. Hallmarks of cancer: The next generation. *Cell*. 2011;144(5):646-674. doi:10.1016/j.cell.2011.02.013.
16. Fedi P, Kimmelman A, Aaronson SA. Growth factor Signal Transduction in Cancer. In Holland JF, Frey E, Bast RC, eds. *Cancer medicine.* 5th ed. Hamilton, Ont.: Decker; 2000:33-55.
17. Lowe SW, Cepero E, Evan G. Intrinsic tumour suppression. *Nature*. 2004;432(7015):307-315. doi:10.1038/nature03098.
18. Blasco MA. Telomeres and human disease: ageing, cancer and beyond. *Nat Rev Genet*. 2005;6(8):611-622. doi:10.1038/nrg1656.
19. Hanahan D, Folkman J. Patterns and Emerging Mechanisms of the Angiogenic Switch during Tumorigenesis. *Cell*. 1996;86(3):353-364. doi:10.1016/s0092-8674(00)80108-7.

20. Talmadge JE, Fidler IJ. AACR centennial series: the biology of cancer metastasis: historical perspective. *Cancer Res*. 2010;70(14):5649-5669. doi:10.1158/0008-5472.CAN-10-1040.
21. Schütt C, Bröker B. *Grundwissen Immunologie.* 2. Auflage. Heidelberg: Spektrum Akademischer Verlag; 2009.
22. Chen GY, Nuñez G. Sterile inflammation: sensing and reacting to damage. *Nat Rev Immunol*. 2010;10(12):826-837. doi:10.1038/nri2873.
23. Mantovani A, Allavena P, Sica A, Balkwill F. Cancer-related inflammation. *Nature*. 2008;454(7203):436-444. doi:10.1038/nature07205.
24. Dunn GP, Old LJ, Schreiber RD. The immunobiology of cancer immunosurveillance and immunoediting. *Immunity*. 2004;21(2):137-148. doi:10.1016/j.immuni.2004.07.017.
25. Dvorak HF. Tumors: wounds that do not heal. Similarities between tumor stroma generation and wound healing. *N Engl J Med*. 1986;315(26):1650-1659. doi:10.1056/NEJM198612253152606.
26. Balkwill F, Mantovani A. Inflammation and cancer: back to Virchow? *Lancet*. 2001;357(9255):539-545. doi:10.1016/S0140-6736(00)04046-0.
27. Teng MWL, Swann JB, Koebel CM, Schreiber RD, Smyth MJ. Immune-mediated dormancy: an equilibrium with cancer. *J Leukoc Biol*. 2008;84(4):988-993. doi:10.1189/jlb.1107774.
28. Pagès F, Galon J, Dieu-Nosjean M-C, Tartour E, Sautès-Fridman C, Fridman W-H. Immune infiltration in human tumors: a prognostic factor that should not be ignored. *Oncogene*. 2010;29(8):1093-1102. doi:10.1038/onc.2009.416.
29. Schumacher TN, Schreiber RD. Neoantigens in cancer immunotherapy. *Science*. 2015;348(6230):69-74. doi:10.1126/science.aaa4971.
30. Lippitz BE. Cytokine patterns in patients with cancer: A systematic review. *Lancet Oncol*. 2013;14(6):e218-e228. doi:10.1016/S1470-2045(12)70582-X.
31. Chen DS, Mellman I. Oncology meets immunology: the cancer-immunity cycle. *Immunity*. 2013;39(1):1-10. doi:10.1016/j.immuni.2013.07.012.
32. García-Martínez E, Gil GL, Benito AC, et al. Tumor-infiltrating immune cell profiles and their change after neoadjuvant chemotherapy predict response and prognosis of breast cancer. *Breast Cancer Res*. 2014;16(6):488-505. doi:10.1186/s13058-014-0488-5.

33. Ino Y, Yamazaki-Itoh R, Shimada K, et al. Immune cell infiltration as an indicator of the immune microenvironment of pancreatic cancer. *Br J Cancer*. 2013;108(4):914-923. doi:10.1038/bjc.2013.32.
34. Martin D, Rödel F, Balermpas P, Rödel C, Fokas E. The immune microenvironment and HPV in anal cancer: Rationale to complement chemoradiation with immunotherapy. *Biochim Biophys Acta Rev Cancer*. 2017;1868(1):221-230. doi:10.1016/j.bbcan.2017.05.001.
35. Balermpas P, Martin D, Wieland U, et al. Human papilloma virus load and PD-1/PD-L1, $CD8^+$ and FOXP3 in anal cancer patients treated with chemoradiotherapy: Rationale for immunotherapy. *Oncoimmunology*. 2017;6(3):e1288331. Published 2017 Feb 6. doi:10.1080/2162402X.2017.1288331.
36. Balermpas P, Michel Y, Wagenblast J, et al. Tumour-infiltrating lymphocytes predict response to definitive chemoradiotherapy in head and neck cancer. *Br J Cancer*. 2014;110(2):501-509. doi:10.1038/bjc.2013.640.
37. Galon J, Costes A, Sanchez-Cabo F, et al. Type, Density, and Location of Immune Cells Within Human Colorectal Tumors Predict Clinical Outcome. *Science*. 2006;313(5795):1960-1964. doi:10.1126/science.1129139.
38. Shinto E, Hase K, Hashiguchi Y, et al. CD8+ and FOXP3+ tumor-infiltrating T cells before and after chemoradiotherapy for rectal cancer. *Ann Surg Oncol*. 2014;21 Suppl 3:S414-421. doi:10.1245/s10434-014-3584-y.
39. Mlecnik B, Tosolini M, Kirilovsky A, et al. Histopathologic-based prognostic factors of colorectal cancers are associated with the state of the local immune reaction. *J Clin Oncol*. 2011;29(6):610-618. doi:10.1200/JCO.2010.30.5425.
40. Huang AC, Postow MA, Orlowski RJ, et al. T-cell invigoration to tumour burden ratio associated with anti-PD-1 response. *Nature*. 2017;545(7652):60-65. doi:10.1038/nature22079.
41. Krieg C, Nowicka M, Guglietta S, et al. High-dimensional single-cell analysis predicts response to anti-PD-1 immunotherapy [published correction appears in Nat Med. 2018 Nov;24(11):1773-1775]. *Nat Med*. 2018;24(2):144-153. doi:10.1038/nm.4466.
42. Ichihara F, Kono K, Takahashi A, Kawaida H, Sugai H, Fujii H. Increased populations of regulatory T cells in peripheral blood and tumor-infiltrating

lymphocytes in patients with gastric and esophageal cancers. *Clin Cancer Res*. 2003;9(12):4404-4408.

43. Foulds GA, Vadakekolathu J, Abdel-Fatah TMA, et al. Immune-Phenotyping and Transcriptomic Profiling of Peripheral Blood Mononuclear Cells From Patients With Breast Cancer: Identification of a 3 Gene Signature Which Predicts Relapse of Triple Negative Breast Cancer. *Front Immunol*. 2018;9:2028. Published 2018 Sep 11. doi:10.3389/fimmu.2018.02028.
44. Coffelt SB, Wellenstein MD, Visser KE de. Neutrophils in cancer: neutral no more. *Nat Rev Cancer*. 2016;16(7):431-446. doi:10.1038/nrc.2016.52.
45. Haram A, Boland MR, Kelly ME, Bolger JC, Waldron RM, Kerin MJ. The prognostic value of neutrophil-to-lymphocyte ratio in colorectal cancer: A systematic review. *J Surg Oncol*. 2017;115(4):470-479. doi:10.1002/jso.24523.
46. Lee YJ, Lee SB, Beak SK, et al. Temporal changes in immune cell composition and cytokines in response to chemoradiation in rectal cancer. *Sci Rep*. 2018;8(1):7565. Published 2018 May 15. doi:10.1038/s41598-018-25970-z.
47. Fokas E, Allgäuer M, Polat B, et al. Randomized Phase II Trial of Chemoradiotherapy Plus Induction or Consolidation Chemotherapy as Total Neoadjuvant Therapy for Locally Advanced Rectal Cancer: CAO/ARO/AIO-12. *J Clin Oncol*. 2019;37(34):3212-3222. doi:10.1200/JCO.19.00308.
48. Heald RJ, Husband EM, Ryall RDH. The mesorectum in rectal cancer surgery—the clue to pelvic recurrence? *Br J Surg*. 1982;69(10):613-616. doi:10.1002/bjs.1800691019.
49. Abcam. https://www.abcam.com/protocols/introduction-to-flow-cytometry. Accessed September 23, 2019.
50. Ibrahim SF, van den Engh G. Flow cytometry and cell sorting. *Adv Biochem Eng Biotechnol*. 2007;106:19-39. doi:10.1007/10_2007_073.
51. Szalóki G, Goda K. Compensation in multicolor flow cytometry. *Cytometry A*. 2015;87(11):982-985. doi:10.1002/cyto.a.22736.
52. Hulspas R, O'Gorman MRG, Wood BL, Gratama JW, Sutherland DR. Considerations for the control of background fluorescence in clinical flow cytometry. *Cytometry B Clin Cytom*. 2009;76(6):355-364. doi:10.1002/cyto.b.20485.

53. Bio-Rad. Gating Strategies for Effective Flow Cytometry Data. https://www.bio-rad-antibodies.com/flow-cytometry-gating-strategies.html. Accessed July 20, 2021.
54. Roederer M. Spectral compensation for flow cytometry: visualization artifacts, limitations, and caveats [published correction appears in Cytometry 2002 Jun 1;48(2):113]. *Cytometry*. 2001;45(3):194-205. doi:10.1002/1097-0320(20011101)45:3<194::aid-cyto1163>3.0.co;2-c.
55. Zeiner PS, Zinke J, Kowalewski DJ, et al. CD74 regulates complexity of tumor cell HLA class II peptidome in brain metastasis and is a positive prognostic marker for patient survival. *Acta Neuropathol Commun*. 2018;6(1):18. Published 2018 Mar 1. doi:10.1186/s40478-018-0521-5.
56. Chen DS, Mellman I. Elements of cancer immunity and the cancer-immune set point. *Nature*. 2017;541(7637):321-330. doi:10.1038/nature21349.
57. Murphy K, Weaver C. Wie Antigene den T-Lymphocyten präsentiert werden. In: Murphy KM, Weaver C, Janeway C, eds. *Janeway Immunologie*. 9. Auflage. Berlin: Springer Spektrum; 2018:273-326.
58. Becker PSA, Suck G, Nowakowska P, et al. Selection and expansion of natural killer cells for NK cell-based immunotherapy. *Cancer Immunol Immunother*. 2016;65(4):477-484. doi:10.1007/s00262-016-1792-y.
59 Dayde D, Tanaka I, Jain R, Tai MC, Taguchi A. Predictive and Prognostic Molecular Biomarkers for Response to Neoadjuvant Chemoradiation in Rectal Cancer. *Int J Mol Sci*. 2017;18(3):573. Published 2017 Mar 7. doi:10.3390/ijms18030573.
60. Jarosz-Biej M, Smolarczyk R, Cichoń T, Kułach N. Tumor Microenvironment as A "Game Changer" in Cancer Radiotherapy. *Int J Mol Sci*. 2019;20(13):3212. Published 2019 Jun 29. doi:10.3390/ijms20133212.
61. Demaria S, Bhardwaj N, McBride WH, Formenti SC. Combining radiotherapy and immunotherapy: a revived partnership. *Int J Radiat Oncol Biol Phys*. 2005;63(3):655-666. doi:10.1016/j.ijrobp.2005.06.032.
62. Kitayama J, Yasuda K, Kawai K, Sunami E, Nagawa H. Circulating lymphocyte is an important determinant of the effectiveness of preoperative radiotherapy in advanced rectal cancer. *BMC Cancer*. 2011;11:64. Published 2011 Feb 10. doi:10.1186/1471-2407-11-64.

63. Diefenhardt M, Hofheinz RD, Martin D, et al. Leukocytosis and neutrophilia as independent prognostic immunological biomarkers for clinical outcome in the CAO/ARO/AIO-04 randomized phase 3 rectal cancer trial. *Int J Cancer*. 2019;145(8):2282-2291. doi:10.1002/ijc.32274.
64. Tada N, Kawai K, Tsuno NH, et al. Prediction of the preoperative chemoradiotherapy response for rectal cancer by peripheral blood lymphocyte subsets. *World J Surg Oncol*. 2015;13:30. Published 2015 Feb 7. doi:10.1186/s12957-014-0418-0.
65. Heylmann D, Rödel F, Kindler T, Kaina B. Radiation sensitivity of human and murine peripheral blood lymphocytes, stem and progenitor cells. *Biochim Biophys Acta*. 2014;1846(1):121-129. doi:10.1016/j.bbcan.2014.04.009.
66. Ishihara S, Iinuma H, Fukushima Y, et al. Radiation-induced apoptosis of peripheral blood lymphocytes is correlated with histological regression of rectal cancer in response to preoperative chemoradiotherapy. *Ann Surg Oncol*. 2012;19(4):1192-1198. doi:10.1245/s10434-011-2057-9.
67. Galluzzi L, Buqué A, Kepp O, Zitvogel L, Kroemer G. Immunological Effects of Conventional Chemotherapy and Targeted Anticancer Agents. *Cancer Cell*. 2015;28(6):690-714. doi:10.1016/j.ccell.2015.10.012.
68. Raskov H, Orhan A, Christensen JP, Gögenur I. Cytotoxic CD8+ T cells in cancer and cancer immunotherapy. *Br J Cancer*. 2021;124(2):359-367. doi:10.1038/s41416-020-01048-4.
69. Melief CJ. Tumor eradication by adoptive transfer of cytotoxic T lymphocytes. *Adv Cancer Res*. 1992;58:143-175. doi:10.1016/s0065-230x(08)60294-8.
70. Rousalova I, Krepela E. Granzyme B-induced apoptosis in cancer cells and its regulation (review). *Int J Oncol*. 2010;37(6):1361-1378. doi:10.3892/ijo_00000788.
71. Jarosch A, Sommer U, Bogner A, et al. Neoadjuvant radiochemotherapy decreases the total amount of tumor infiltrating lymphocytes, but increases the number of CD8+/Granzyme B+ (GrzB) cytotoxic T-cells in rectal cancer. *Oncoimmunology*. 2017;7(2):e1393133. Published 2017 Nov 7. doi:10.1080/2162402X.2017.1393133.
72. Pauken KE, Wherry EJ. Overcoming T cell exhaustion in infection and cancer. *Trends Immunol*. 2015;36(4):265-276. doi:10.1016/j.it.2015.02.008.

73. McDermott DF, Atkins MB. PD-1 as a potential target in cancer therapy. *Cancer Med*. 2013;2(5):662-673. doi:10.1002/cam4.106.
74. Wherry EJ. T cell exhaustion. *Nat Immunol*. 2011;12(6):492-499. doi:10.1038/ni.2035.
75. Barber DL, Wherry EJ, Masopust D, et al. Restoring function in exhausted CD8 T cells during chronic viral infection. *Nature*. 2006;439(7077):682-687. doi:10.1038/nature04444.
76 Demaria S, Formenti SC. Role of T lymphocytes in tumor response to radiotherapy. *Front Oncol*. 2012;2:95. Published 2012 Aug 24. doi:10.3389/fonc.2012.00095.
77. Ma Y, Kepp O, Ghiringhelli F, et al. Chemotherapy and radiotherapy: cryptic anticancer vaccines. *Semin Immunol*. 2010;22(3):113-124. doi:10.1016/j.smim.2010.03.001.
78. Li Z, Xu Z, Huang Y, et al. The predictive value and the correlation of peripheral absolute monocyte count, tumor-associated macrophage and microvessel density in patients with colon cancer. *Medicine (Baltimore)*. 2018;97(21):e10759. doi:10.1097/MD.0000000000010759.
79. Hu S, Zou Z, Li H, et al. The Preoperative Peripheral Blood Monocyte Count Is Associated with Liver Metastasis and Overall Survival in Colorectal Cancer Patients. *PLoS One*. 2016;11(6):e0157486. Published 2016 Jun 29. doi:10.1371/journal.pone.0157486.
80. Wen S, Chen N, Peng J, et al. Peripheral monocyte counts predict the clinical outcome for patients with colorectal cancer: a systematic review and meta-analysis. *Eur J Gastroenterol Hepatol*. 2019;31(11):1313-1321. doi:10.1097/MEG.0000000000001553.
81. Hennecke J, Wiley DC. T Cell Receptor–MHC Interactions up Close. *Cell*. 2001;104(1):1-4. doi:10.1016/S0092-8674(01)00185-4.
82. Anitei M-G, Zeitoun G, Mlecnik B, et al. Prognostic and predictive values of the immunoscore in patients with rectal cancer. *Clin Cancer Res*. 2014;20(7):1891-1899. doi:10.1158/1078-0432.CCR-13-2830.
83. Yasuda K, Nirei T, Sunami E, Nagawa H, Kitayama J. Density of CD4(+) and CD8(+) T lymphocytes in biopsy samples can be a predictor of pathological response to chemoradiotherapy (CRT) for rectal cancer. *Radiat Oncol*. 2011;6:49. Published 2011 May 16. doi:10.1186/1748-717X-6-49.

84. Kong JC, Guerra GR, Pham T, et al. Prognostic Impact of Tumor-Infiltrating Lymphocytes in Primary and Metastatic Colorectal Cancer: A Systematic Review and Meta-analysis. *Dis Colon Rectum*. 2019;62(4):498-508. doi:10.1097/DCR.0000000000001332.
85. Russell JH, Ley TJ. Lymphocyte-mediated cytotoxicity. *Annu Rev Immunol*. 2002;20:323-370. doi:10.1146/annurev.immunol.20.100201.131730.
86. Nathan C. Neutrophils and immunity: challenges and opportunities. *Nat Rev Immunol*. 2006;6(3):173-182. doi:10.1038/nri1785.
87. Nagasaki T, Akiyoshi T, Fujimoto Y, et al. Prognostic Impact of Neutrophil-to-Lymphocyte Ratio in Patients with Advanced Low Rectal Cancer Treated with Preoperative Chemoradiotherapy. *Dig Surg*. 2015;32(6):496-503. doi:10.1159/000441396.
88. Sung S, Son SH, Park EY, Kay CS. Prognosis of locally advanced rectal cancer can be predicted more accurately using pre- and post-chemoradiotherapy neutrophil-lymphocyte ratios in patients who received preoperative chemoradiotherapy. *PLoS One*. 2017;12(3):e0173955. Published 2017 Mar 14. doi:10.1371/journal.pone.0173955.
89. Berry RS, Xiong MJ, Greenbaum A, et al. High levels of tumor-associated neutrophils are associated with improved overall survival in patients with stage II colorectal cancer. *PLoS One*. 2017;12(12):e0188799. Published 2017 Dec 6. doi:10.1371/journal.pone.0188799.
90. Wikberg ML, Ling A, Li X, Öberg Å, Edin S, Palmqvist R. Neutrophil infiltration is a favorable prognostic factor in early stages of colon cancer. *Hum Pathol*. 2017;68:193-202. doi:10.1016/j.humpath.2017.08.028.
91. Rao H-L, Chen J-W, Li M, et al. Increased intratumoral neutrophil in colorectal carcinomas correlates closely with malignant phenotype and predicts patients' adverse prognosis. *PLoS One*. 2012;7(1):e30806. doi:10.1371/journal.pone.0030806.
92. Chiossone L, Dumas PY, Vienne M, Vivier E. Natural killer cells and other innate lymphoid cells in cancer [published correction appears in Nat Rev Immunol. 2018 Oct 12]. *Nat Rev Immunol*. 2018;18(11):671-688. doi:10.1038/s41577-018-0061-z.
93. Alderdice M, Dunne PD, Cole AJ, et al. Natural killer-like signature observed post therapy in locally advanced rectal cancer is a determinant of

pathological response and improved survival. *Mod Pathol*. 2017;30(9):1287-1298. doi:10.1038/modpathol.2017.47.

94. Sconocchia G, Eppenberger S, Spagnoli GC, et al. NK cells and T cells cooperate during the clinical course of colorectal cancer. *Oncoimmunology*. 2014;3(8):e952197. Published 2014 Aug 3. doi:10.4161/21624011.2014.952197.

95. Li C, Xu X, Wei S, et al. Tumor-associated macrophages: potential therapeutic strategies and future prospects in cancer. *J Immunother Cancer*. 2021;9(1):e001341. doi:10.1136/jitc-2020-001341.

96. Hwang I, Kim JW, Ylaya K, et al. Tumor-associated macrophage, angiogenesis and lymphangiogenesis markers predict prognosis of non-small cell lung cancer patients. *J Transl Med*. 2020;18(1):443. Published 2020 Nov 23. doi:10.1186/s12967-020-02618-z.

97. Erreni M, Mantovani A, Allavena P. Tumor-associated Macrophages (TAM) and Inflammation in Colorectal Cancer. *Cancer Microenviron*. 2011;4(2):141-154. doi:10.1007/s12307-010-0052-5.

98. Funada Y, Noguchi T, Kikuchi R, Takeno S, Uchida Y, Gabbert HE. Prognostic significance of CD8+ T cell and macrophage peritumoral infiltration in colorectal cancer. *Oncol Rep*. 2003;10(2):309-313.

99. Forssell J, Oberg A, Henriksson ML, Stenling R, Jung A, Palmqvist R. High macrophage infiltration along the tumor front correlates with improved survival in colon cancer. *Clin Cancer Res*. 2007;13(5):1472-1479. doi:10.1158/1078-0432.CCR-06-2073.

100. Zhou Q, Peng RQ, Wu XJ, et al. The density of macrophages in the invasive front is inversely correlated to liver metastasis in colon cancer. *J Transl Med*. 2010;8:13. Published 2010 Feb 8. doi:10.1186/1479-5876-8-13.

101. Italiani P, Boraschi D. From Monocytes to M1/M2 Macrophages: Phenotypical vs. Functional Differentiation. *Front Immunol*. 2014;5:514. Published 2014 Oct 17. doi:10.3389/fimmu.2014.00514.

102. Dehne N, Mora J, Namgaladze D, Weigert A, Brüne B. Cancer cell and macrophage cross-talk in the tumor microenvironment. *Curr Opin Pharmacol*. 2017;35:12-19. doi:10.1016/j.coph.2017.04.007.

103. Mantovani A, Marchesi F, Malesci A, Laghi L, Allavena P. Tumour-associated macrophages as treatment targets in oncology. *Nat Rev Clin Oncol*. 2017;14(7):399-416. doi:10.1038/nrclinonc.2016.217.

104. Milne K, Alexander C, Webb JR, et al. Absolute lymphocyte count is associated with survival in ovarian cancer independent of tumor-infiltrating lymphocytes. *J Transl Med*. 2012;10:33. Published 2012 Feb 27. doi:10.1186/1479-5876-10-33.

105. Robert Koch-Institut, Gesellschaft der epidemiologischen Krebsregister in Deutschland e.V., ed. Krebs in Deutschland 2015/2016. Berlin: Robert Koch Institut, 2019. doi:10.25646/5977.

106. Petrelli F, Trevisan F, Cabiddu M, et al. Total Neoadjuvant Therapy in Rectal Cancer: A Systematic Review and Meta-analysis of Treatment Outcomes. *Ann Surg*. 2020;271(3):440-448. doi:10.1097/SLA.0000000000003471.

12 Schriftliche Erklärung

Schriftliche Erklärung

Ich erkläre ehrenwörtlich, dass ich die dem Fachbereich Medizin der Johann Wolfgang Goethe-Universität Frankfurt am Main zur Promotionsprüfung eingereichte Dissertation mit dem Titel

Dissecting the immune contexture to monitor and predict chemoradiotherapy response in patients with rectal cancer

in der Klinik für Strahlentherapie und Onkologie des Universitätsklinikums Frankfurt unter Betreuung und Anleitung von Prof. Dr. Dr. Emmanouil Fokas mit Unterstützung durch Prof. Dr. rer. Franz Rödel ohne sonstige Hilfe selbst durchgeführt und bei der Abfassung der Arbeit keine anderen als die in der Dissertation angeführten Hilfsmittel benutzt habe. Darüber hinaus versichere ich, nicht die Hilfe einer kommerziellen Promotionsvermittlung in Anspruch genommen zu haben.

Ich habe bisher an keiner in- oder ausländischen Universität ein Gesuch um Zulassung zur Promotion eingereicht. Die vorliegende Arbeit wurde bisher nicht als Dissertation eingereicht.

Vorliegende Ergebnisse der Arbeit wurden (oder werden) in folgendem Publikationsorgan veröffentlicht:

Frankfurt, den 27.09.2021

(Ort, Datum) (Unterschrift)

13 Danksagung

Mein Dank geht an Prof. Dr. med. Dr. Emmanouil Fokas und Prof. Dr. rer. nat. Franz Rödel für die Überlassung des Themas für diese Arbeit sowie die Unterstützung bei der Durchführung der Untersuchungen als auch beim Schreiben der Dissertation.

Zudem danke ich Prof. Dr. Michael Rieger für seine Fachkompetenz und Hilfe während der Etablierung der Immunphenotypisierung.

Bei Prof. Dr. Claus Rödel bedanke ich mich für die Möglichkeit, meine Doktorarbeit in seinem Institut durchführen zu können.

Mein Dank geht auch an die Frankfurter Promotionsförderung für die finanzielle Unterstützung mit einem Stipendium.

Zudem bedanke ich mich sehr herzlich bei dem gesamten restlichen Team der Strahlenbiologie PD Dr. Stephanie Hehlgans, Jeannie Peifer, Julius Oppermann, Melanie Hoffmann und Ömer Güllülü für die konstruktive Unterstützung. Ein großes Dankeschön geht dabei an Jeannie für ihre Hilfe bei der Durchführung der Experimente sowie der Einarbeitung im Labor.

Außerdem gilt mein Dank Dr. Markus Diefenhardt für die Hilfe bei den Berechnungen und der Erstellung der Graphen sowie an Anton Burkhard-Meier für die Hilfe bei den Experimenten und den Berechnungen.

Ein großes Danke geht auch an Larissa Neidert für ihr offenes Ohr und ihre guten Ratschläge.

Zuletzt möchte ich mich bei meinen Eltern und meinen Freunden für die Unterstützung und Ermutigung während des gesamten Prozesses bedanken.